Imperial College London

Institute of Clinical Sciences

Computational analysis of firing regularity and burst firing in midbrain dopamine neurons

Rajeshwari Iyer

Submitted in part fulfillment of the requirements for the degree of

Doctor of Philosophy

Declaration

I herewith certify that all material in this dissertation, which is not my own work, has been properly acknowledged. The copyright of this thesis rests with the author and is made available under a Creative Commons Attribution Non-Commercial No Derivatives license. Researchers are free to copy, distribute or transmit the thesis on the condition that they attribute it, that they do not use it for commercial purposes and that they do not alter, transform or build upon it. For any reuse or redistribution, researchers must make clear to others the licence terms of this work.

Rajeshwari Iyer

Abstract

Dopamine neurons in the substantia nigra pars compacta (SNc) and ventral tegmental area (VTA) regulate day-to-day activities such as reward-related learning, and motor control. Dysfunction of these neurons is implicated in disorders like Schizophrenia, addiction to drugs, and Parkinson's disease. Dopamine neurons fire action potentials with variability in inter-spike intervals (ISI) interspersed with bursts of spikes, both firing patterns being a result of co-ordinated action of synaptic inputs and ion channels. Pharmacological inhibition of calcium-activated potassium (SK) channels increases the variability in their firing pattern, sometimes also increasing the number of spikes fired in bursts, indicating that SK channels play an important role in maintaining dopamine neuron firing regularity and burst firing. However, the exact mechanisms underlying these effects are still unclear. We hypothesized that the post-spike after hyperpolarisation (AHP) provided by the SK current controls and standardises the availability of other voltage-gated ion channels, thus timing successive action potentials at regular intervals. Here, I develop a biophysical model of a dopamine neuron incorporating ion channel stochasticity that enabled me to analyse availability of ion channels in multiple states during spiking. Decreased firing regularity is primarily due to a significant decrease in the AHP that in turn resulted in a reduction in the fraction of available voltage-gated sodium channels. Insufficient AHP causes a failure of sodium channels to recover from inactivation and, due to ion channel stochasticity, a variable number of sodium channels are available to fire a spike, in the absence of AHP, thus resulting in an irregular spike train. My model further predicts that inhibition of SK channels results in a depolarisation of action potential threshold along with an increase in its variability, thus suggesting that SK channels regulate spike threshold in midbrain dopamine neurons.

Moreover, a quantitative description of action potential features during endogenous burst firing in midbrain dopamine neurons has not been reported, perhaps due to a lack of *in vivo* whole-cell

recordings that can shed light on membrane dynamics. Because we had available *in vivo* whole-cell recordings from immuno-histochemically identified dopamine neurons in the VTA, I analysed these using mathematical techniques like Principal Components Analysis (PCA) and the stochastic model mentioned above, in order to provide quantitative descriptions of action potential features during the course of endogenous burst firing. I found that the first detectable change in membrane dynamics that perhaps leads to burst firing is a reduction in the AHP mediated by SK channels. This was accompanied by progressive depolarisation of action potential threshold with each spike within the burst due to reduced availability of sodium channels as a result of progressive decrease in recovery from inactivation. This also resulted in a decrease in rate of change of membrane voltage for each successive spike in a burst. Reduction in action potential height that is commonly observed during burst firing can also be explained by the reduced availability of sodium channels. My model predicts that a reduction in A-type potassium channel current during burst firing could facilitate the transient increase in instantaneous firing rate during bursts and the progressive reduction in sodium channel availability results in the cessation of firing, facilitating burst termination in these neurons.

Acknowledgments

I am eternally grateful to my advisors Mark and Aldo who kept me going through all the ups and downs during the course of my PhD, especially for giving me the opportunity to change to part-time due to various illnesses. I thank them for all the flexibility they provided me with, such that I could be there for my family during our hard times. They have been a constant source of encouragement and support and needless to say, my knowledge bank, to help me shape my research throughout my PhD. They always encouraged me to be proactive with my work and think out of the box and never failed to remind me to think of the bigger picture. I really appreciate all the time they took for each and every meeting so that I left the room feeling confident and knowing what needed to be done and how. It has been an invaluable experience to have the opportunity to work in collaboration with both their labs and gain the perfect mix of computational and biological expertise that I am confident will take me a long way in my career.

I also want to thank Frederic Brischoux who closely supervised me at the beginning of my PhD. He was the one who taught me the tricks and trades of neurophysiology, the art of immunohistochemistry and everything in between – from being organised in the lab to parenting secrets!

My research would not have been possible without the MRC studentship and I am very grateful to the MRC-CSC for giving me the opportunity to train under the guidance of experts in the field, including my mentors Vincenzo De Paola and Alex Sardini, who provided me with timely suggestions and guidance when required. I also want to thank Anne Soutar, our post-graduate director, for all the support and pep talks she provided during the tough times.

My colleagues and mates Ali and Andreas have been most helpful in getting me to grips with some of the programming and the mathematical concepts used in my thesis and I am very thankful to them for all their effort and the time spent in discussions. I also want to thank my lab mates at the CSC, Judith, Matt, Gillian, Jess, Kyoko, Eleanor, Eliza, Rebecca and Azhar for all the help in lab and the wonderful lunch break conversations that I will miss ever so much. I would also like to thank members of my other lab in Bioengineering, Alessandro, Ali, Anastasia, Andreas, Ariadne, Chin-Hsuan, Constantinos, Ekaterina, Feryal, Scott, and William who never failed to make me laugh and made my PhD an unforgettable experience. I consider myself lucky to have met all these

very talented and interesting people and have had some of the most intellectually stimulating, funny and sometimes the most bizarre conversations that I will cherish forever.

My journey in Bioengineering started with my father's interest in this emerging field in the early 2000s back in India and I am eternally gratefully to him for introducing me to this fascinating world. I hope today I can make him proud. I could not have come this far, had it not been for his encouragement to read mathematics at university. My mother has been a constant source of support, encouragement and inspiration throughout my life. Thanks to all those sleepless nights during exam time that she spent staying up with me and making hot drinks for me just so I could study! I can really appreciate today how she so effortlessly managed her own professional life and made my childhood the most rewarding. Both my parents put my needs, both educational and personal, at the forefront of their own lives, and have brought me up to become an independent woman and I hope I can do the same for my children.

I am also extremely thankful to my parents-in-law who always believed in me and supported me throughout, from my Cambridge days, and especially after our son was born and even spent time apart to help me take care of him so I could concentrate on my PhD. No words can describe how grateful I am to them. Thank you also to my sister in law and her family for their support and encouragement especially during the tough times that have kept me going.

Special mention to our friends here in London, especially Sunil and Kavitha, who have also been extremely patient, helpful, and kept the support system going all these years!

Finally, I would like to dedicate my thesis to my loving husband Krishna and our little boy Ashrith. I am sure I will spend the next ten years making up for all the weekends that should have been family time but I was working! I could not have done this without Krishna's support, his nagging, his questions, and above all his belief in me that made me believe in myself. He has always been extremely encouraging and engaging in my work and his own curiosity and knowledge never ceases to amaze me! And every little cuddle, smile and the recurrent innocent question, "when will you finish your PhD, mumma?" from Ashrith has brought me to this stage of completion today. Thank you will never be enough.

TABLE OF CONTENTS

CHAPTER 1 INTRODUCTION 10

1.1 MIDBRAIN DOPAMINE NEURONS – ANATOMICAL LOCATION AND PROJECTION TARGETS 10
1.2 MIDBRAIN DOPAMINE NEURONS - FIRING PATTERNS 13
1.2.1 SINGLE SPIKE FIRING 15
1.2.2 BURST FIRING 19
1.2.3 EXISTING HYPOTHESES FOR BURST FIRING IN DOPAMINE NEURONS 25
1.2.4 THE ROLE OF SK CHANNELS IN REGULATING SINGLE SPIKE AND BURST FIRING IN MIDBRAIN DOPAMINE NEURONS 27
1.3 HYPOTHESES AND AIMS 29
1.3.1 HYPOTHESIS 1 – SK CHANNELS CONTROL THE RECOVERY FROM INACTIVATION OF OTHER VOLTAGE-GATED ION CHANNELS 30
1.3.2 HYPOTHESIS 2 – DATA DRIVEN ANALYSIS OF *IN VIVO* MEMBRANE VOLTAGE CAN PREDICT ION CHANNEL MECHANISMS 31

CHAPTER 2 COMPUTATIONAL MODELLING OF ION CHANNELS AND THE *IN SILICO* DOPAMINE NEURON 33

2.1 INTRODUCTION 33
2.1.1 ION CHANNELS AND ACTION POTENTIALS 33
2.1.2 CHANNEL NOISE – STOCHASTICITY IN VOLTAGE-GATED ION CHANNELS 35
2.1.3 SIMULATING NEURONS AND STOCHASTIC ACTION POTENTIALS 39
2.1.4 THE DOPAMINE NEURON MODEL 42
2.1.5 VOLTAGE-GATED ION CHANNELS AND THEIR ROLES IN DOPAMINE NEURON ELECTROPHYSIOLOGY 42
2.2 METHODS 47
2.2.1 THE STOCHASTIC DOPAMINE NEURON MODEL 47
2.2.2 MODEL PARAMETERS AND RATE FUNCTIONS 51
2.2.3 CALIBRATION OF *IN SILICO* ION CHANNEL CURRENTS 53
2.3 RESULTS 54
2.3.1 SPONTANEOUS SPIKE TRAIN CHARACTERISTICS AND RESPONSE TO SIMULATED PHARMACOLOGICAL MANIPULATIONS 54
2.3.2 ION CHANNEL CURRENTS REGULATING THE CHARACTERISTICS OF SPONTANEOUS FIRING 58
2.4 DISCUSSION 63

CHAPTER 3 SK CHANNELS CONTROL FIRING PRECISION IN MIDBRAIN DOPAMINE NEURONS BY REGULATING THE AVAILABILITY OF SODIUM AND POTASSIUM CHANNELS 65

3.1 INTRODUCTION 65
3.1.1 CALCIUM-ACTIVATED POTASSIUM CHANNELS AND THEIR ROLE IN DOPAMINE NEURON FIRING 65
3.1.2 HYPOTHESIS AND AIM OF THE PROJECT 70
3.2 METHODS 72
3.2.1 DATA ANALYSIS 72
3.3 RESULTS 74
3.3.1 A SIMULATED INHIBITION OF SK CHANNELS DECREASES FIRING REGULARITY AND INCREASES FIRING RATE 74
3.3.2 SK CHANNELS DETERMINE ACTION POTENTIAL THRESHOLD AND MINIMISE ITS VARIABILITY 76
3.3.3 SK CHANNEL INHIBITION CAUSES INSUFFICIENT RECOVERY FROM INACTIVATION OF SODIUM CHANNELS 79
3.3.4 SK CHANNEL INHIBITION CAUSES REDUCTION IN A-TYPE SUB-THRESHOLD POTASSIUM CURRENT 83
3.4 DISCUSSION 85

CHAPTER 4 QUANTITATIVE ANALYSIS OF BURST WAVEFORMS FROM VTA DOPAMINE NEURONS 88

4.1 INTRODUCTION 88
4.1.1 CHARACTERISTICS OF BURST FIRING IN MIDBRAIN DOPAMINE NEURONS *IN VIVO* 88
4.1.2 HYPOTHESIS AND AIM OF THE PROJECT 90
4.2 METHODS 93
4.2.1 WAVEFORM ANALYSIS AND SPIKE STATISTICS 93
4.2.2 PRINCIPAL COMPONENTS ANALYSIS (PCA) 95
4.2.3 SPIKE TRAIN CLAMP USING PC-RECONSTRUCTED AND RAW WAVEFORMS 96
4.3 RESULTS 97
4.3.1 SPIKE TRAIN AND ACTION POTENTIAL CHARACTERISTICS 97
4.3.2 REDUCED POST-SPIKE AHP IS THE FIRST DETECTABLE CHANGE IN MEMBRANE DYNAMICS DURING A BURST 101
4.3.3 SK CHANNELS MAY NOT CONTRIBUTE TO BURST TERMINATION IN VTA DOPAMINE NEURONS 106
4.3.4 PROGRESSIVE DECREASE IN RECOVERY FROM INACTIVATION OF SODIUM CHANNELS RESULTS IN SLOW MEMBRANE DYNAMICS AND DEPOLARISATION IN ACTION POTENTIAL THRESHOLD DURING BURST FIRING 109
4.3.5 SODIUM CHANNEL INACTIVATION UNDERLIES BURST TERMINATION 113
4.3.6 OTHER CHANGES IN ACTION POTENTIAL CHARACTERISTICS DURING BURST FIRING 115
4.3.7 PCA OF ACTION POTENTIAL WAVEFORMS, AS A NOVEL METHOD FOR STUDYING NEURONAL MEMBRANE DYNAMICS, IDENTIFIES KEY ION CHANNELS IMPLICATED IN BURST FIRING 117
4.3.8 BURST CLAMP – VOLTAGE CLAMP SIMULATION USING THE RAW *IN VIVO* SPIKE TRAIN OBTAINED FROM RECORDING IN THE VTA 127
4.4 DISCUSSION 130

CHAPTER 5 CONCLUSIONS AND DISCUSSION 134

5.1 SUMMARY OF FINDINGS 134
5.2 SIGNIFICANCE OF COMPUTATIONAL MODELLING 139
5.3 NOVEL METHODOLOGY FOR DATA-DRIVEN ANALYSIS OF MEMBRANE VOLTAGE WAVEFORMS AND UNDERLYING ION CHANNEL CURRENTS 140
5.4 PREDICTIONS FROM OUR STUDY THAT COULD BE TESTED EXPERIMENTALLY 142

REFERENCES 147

List of figures

Figure 1.1 Location and projection targets of midbrain dopamine neurons 12
Figure 1.2: Firing patterns seen in dopamine neurons in vivo 14
Figure 1.3: Afferent control of midbrain dopamine neurons 23
Figure 2.1: A variety of ion channels participate during the unique phases of the action potential 34
Figure 2.2: Ion channels and stochasticity 37
Figure 2.3: Modelling ion channels 40
Figure 2.4: Dopamine neuron model schematic and equivalent electrical circuit 49
Figure 2.5: Markov gating schemes for sodium and delayed rectifier potassium channels 50
Figure 2.6: Spontaneous spike train and action potential characteristics obtained from simulations 57
Figure 2.7: Effects of simulated inhibition of ion channels regulating spontaneous firing in the model dopamine neuron 60
Figure 3.1: SK channels control firing precision in physiological midbrain dopamine neurons 69
Figure 3.2: Method for calculation of action potential threshold 73
Figure 3.3: Simulated inhibition of SK channels decreases firing regularity and increases firing rate 75
Figure 3.4: SK channel inhibition causes a decrease in rate of change in membrane voltage 77
Figure 3.5: Action potential threshold depolarises and becomes more variable with simulated SK channel inhibition 78
Figure 3.6: Failure of recovery from inactivation of sodium channels underlies decrease in firing regularity with SK channel inhibition 82
Figure 3.7: Simulated inhibition of SK channels results in a significant decrease in the peak sub-threshold activated A-type potassium current 84
Figure 4.1: Spike train characterisitcs of in vivo whole-cell recordings from dopamine neurons in the VTA 99
Figure 4.2: Burst statistics 100
Figure 4.3: Reduction in endogenous is the first detectable change in membrane dynamics during burst firing 104
Figure 4.4: VTA dopamine neuron bursts are not terminated by prolonged AHP due to greater SK channel activation 108
Figure 4.5: Action potential threshold progressively depolarises during burst firing in VTA dopamine neurons 110
Figure 4.6: Rate of rise in membrane voltage is reduced during burst firing in dopamine neurons 112
Figure 4.7: Progressive inactivation of sodium channels during a burst 114
Figure 4.8: Action potential height and width are significantly reduced during burst firing in VTA dopamine neurons 116
Figure 4.9: Schematic explanation for PCA 119
Figure 4.10: Principal components analysis of burst and non-burst waveforms 122
Figure 4.11: Temporal profile of the first four PCs during the different phases of the action potential 124
Figure 4.12: Peak currents obtained from spike train clamp after increasing PCs by 50% 126
Figure 4.13: Burst clamp 129
Figure 5.1: Schematic representation of firing regularity in midbrain dopamine neurons 136
Figure 5.2: Schematic for the novel and complementary methods used in the analysis of endogenous burst firing data obtained from dopamine neurons in the VTA 138
Figure 5.3: Schematic to demonstrate our prediction that NMDAR-dependent SK channel inhibition triggers endogenous burst firing in VTA dopamine neurons 144
Figure 5.4: Schematic for endogenous burst generation and termination in VTA dopamine neurons 146

Chapter 1 Introduction

1.1 Midbrain dopamine neurons – anatomical location and projection targets

Dopamine neurons are found in ten regions within the brain denoted A8-A17 with the most extensively characterised groups located in the midbrain within the substantia nigra pars compacta (SNc, A9) and the ventral tegmental area (VTA, A10) (Figure 1.1) (Dahlstrom and Fuxe 1964; Ungerstedt 1971; Fallon and Moore 1978). Although these regions appear to be small, dopamine neurons send long axonal projections terminating as dense and complex arbours in the target regions (Matsuda, Furuta et al. 2009). Moreover, such projections are sent to a number of different regions within the brain including the striatum (caudate-putamen), nucleus accumbens, amygdala, and medial prefrontal cortex (Fallon, Koziell et al. 1978; Fallon and Moore 1978; Fallon and Moore 1978). Therefore, dopamine neurons from the midbrain have a significant influence on target neurons and regulate important day-to-day functions like fine motor control (Cousins and Salamone 1996; Nieoullon 2002), learning and memory (Wise 2004; Grace, Floresco et al. 2007; Matsumoto and Takada 2013), reward-related and motivational behaviour (Schultz 1998; Wise 2004; Salamone and Correa 2012), and response to stress and noxious stimuli (Ungless, Magill et al. 2004; Brischoux, Chakraborty et al. 2009; Ungless, Argilli et al. 2010).

Based on the location and projection targets of midbrain dopamine neurons (Figure 1.1), the network they form has historically been referred to as nigro-striatal (dopamine neurons from SNc projecting to striatum) and meso-cortico-limbic pathways (dopamine neurons from the VTA projecting to cortical and limbic areas). However this is an oversimplification because actually these pathways are quite overlapping; projections originating in the SNc also target cortical and limbic areas and neurons that project to the striatum also arise from the VTA (Bjorklund and Dunnett 2007; Ikemoto 2007). Moreover, neurons within the SNc and VTA can also be separated into dorsal

and ventral tiers based on their connectivity and calbindin expression. Ventral tier neurons are calbindin negative and project primarily to the patch compartment of the striatum, while dorsal tier neurons express calbindin and project in a heterogeneous manner to cortical, and limbic areas as well as to the matrix compartment of the striatum (Gerfen, Herkenham et al. 1987; Lavoie and Parent 1991; Bjorklund and Dunnett 2007). Interestingly, calbindin positive dopamine neurons in the SNc are selectively spared from degeneration in Parkinson's disease (PD) (Yamada, McGeer et al. 1990) and this has further been attributed to increased intracellular calcium homeostasis by calbindin, which is a calcium-binding protein.

A dysfunction in these neurons has been linked to several disorders. For example, the positive and negative symptoms of schizophrenia are thought to be due primarily to hyper- and hypo-function of midbrain dopamine neurons projecting to cortical and limbic areas in the brain respectively (Finlay 2001; Liss and Roeper 2008; Howes and Kapur 2009). The rewarding effects of alcohol and drugs of abuse are also mediated by dopamine neurons especially in the VTA (Hyman, Malenka et al. 2006; Di Chiara and Bassareo 2007; Grace, Floresco et al. 2007), and the selective degeneration of SNc dopamine neurons is hallmark in PD, resulting in loss of fine motor control and other cognitive deficits (Dauer and Przedborski 2003).

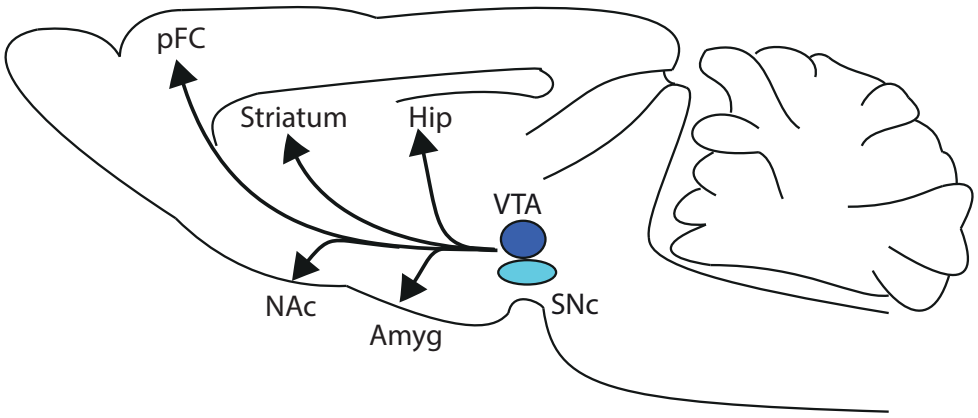


Figure 1.1 Location and projection targets of midbrain dopamine neurons

The cell bodies of the most widely studied subsets of dopamine neurons are located in the midbrain regions of subsantia nigra pars compacta (SNc) and the ventral tegmental area (VTA). Neurons from the SNc and VTA send out long axonal projections to a number of different regions of the brain, some of which are illustrated in this figure, thereby having a significant post-synaptic influence. pFC: pre-frontal cortex; Hip: hippocampus; NAc: nucleus accumbens; Amyg: amygdala.

1.2 Midbrain dopamine neurons - Firing patterns

Dopamine neurons display two principal types of spontaneous firing patterns *in vivo* – single spike firing (Figure 1.2 A) and burst firing (Figure 1.2 B) – both of which are tightly regulated by the co-ordinated action of a variety of ion channels expressed in these neurons alongside the diversity of afferent control received by them. Single spike firing is characterised by single action potentials fired at irregular (or regular) intervals while burst firing is composed of two to ten spikes fired in close succession interspersed with irregular single spikes (Grace and Bunney 1984; Grace and Bunney 1984).

Irregular single spike and burst firing are more predominantly observed in the VTA when compared to the SNc (Grenhoff, Ugedo et al. 1988; Wolfart, Neuhoff et al. 2001). This perhaps is due, in part, to the lower expression of SK channels in VTA dopamine neurons compared to SNc (Wolfart, Neuhoff et al. 2001) - because we know from experiments that SK channels are required to maintain a regular firing pattern, not only in dopamine neurons (Ji and Shepard 2006) but also in many other neuronal types such as globus pallidus, and purkinje neurons (Faber and Sah 2007).

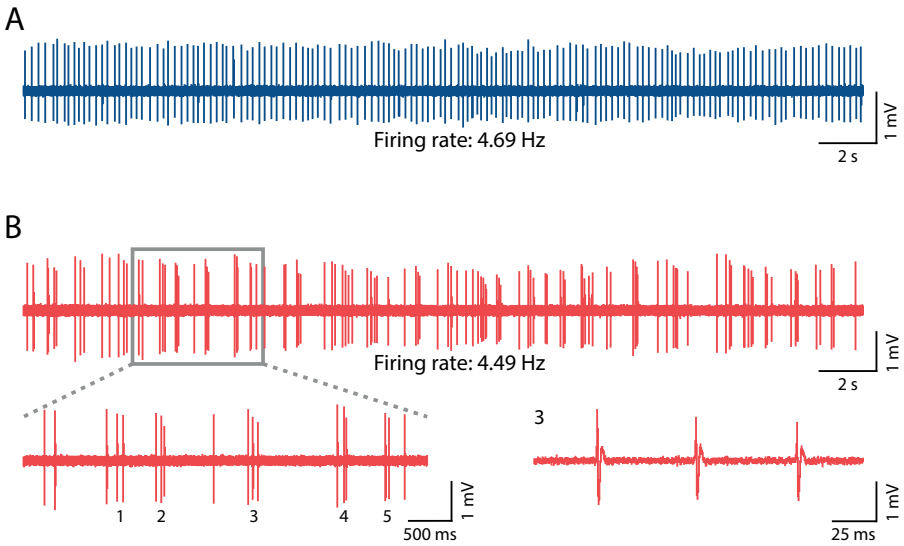


Figure 1.2: Firing patterns seen in dopamine neurons in vivo

A. Tonic single spike firing with fairly regular inter spike intervals (ISI). **B.** Burst firing; five bursts have been expanded (*left*) to observe more clearly the classic properties of bursts such as reducing amplitude of consecutive spikes within a burst in the third burst with three spikes (*right*). Figure reproduced from (Brischoux, Chakraborty et al. 2009).

The spatio-temporal profile of dopamine release in target regions can be modulated by small changes in dopamine neuron firing patterns such as a transient increase in firing rate and/or burst firing, that is associated with two to three times the amount of dopamine released for an equivalent number of spikes fired in tonic mode (Gonon 1988; Floresco, West et al. 2003). This is in part due to accumulation of released dopamine as a result of saturation of dopamine transporters because of a difference in time scales between release and uptake (Gonon 1988; Chergui, Suaud-Chagny et al. 1994; Prasad and Amara 2001). Such an increase in dopamine in target regions is associated with synaptic plasticity and consolidation of behaviour (Schultz, Apicella et al. 1993; Reynolds and Wickens 2002; Calabresi, Picconi et al. 2007). *In vitro*, however, the mode of firing is strikingly tonic single spikes, presumably due to loss of synaptic inputs, with bursts being induced only under special circumstances like in the presence of SK channel inhibitors (Shepard and Bunney 1988; Shepard and Bunney 1991), glutamatergic agonists like N-methyl-D-aspartate (NMDA) (Johnson and Wu 2004), and somatic current injection (Blythe, Wokosin et al. 2009) all of which I will discuss in greater detail in Section 1.2.2.

1.2.1 Single spike firing

In vivo, while some dopamine neurons in the midbrain fire spontaneously due to synaptic drive in conjunction with intrinsic membrane dynamics, others remain silent perhaps due to the prominent inhibitory GABA (gamma-aminobutyric acid)-ergic influence they are under (Grace 1988; Tepper and Lee 2007). For example, stimulating the ventral subiculum indirectly inhibits GABAergic neurons in the ventral pallidum via the activation of GABAergic neurons in the accumbens that results in a disinhibition of VTA dopamine neurons thus regulating number of active dopamine neurons in the VTA (Floresco, Todd et al. 2001). Dopamine neurons also control their own activity by auto-inhibition via dopamine D1/D2 receptors present on them both in the SNc and VTA (Shi, Smith et al. 1997). It has therefore been suggested that extra-synaptic dopamine levels depend on

population activity and is proportional to the number of actively firing dopamine neurons (Grace 1991; Floresco, West et al. 2003).

Single spike firing, with varying degrees of regularity in inter spike intervals (ISI), is the more commonly observed firing pattern in dopamine neurons especially in the SNc and has been hypothesised to help maintain 'tonic' dopamine levels in target regions like the striatum (Grace, Floresco et al. 2007; Rice, Patel et al. 2011). The tonic firing frequency as well as the balance between single spike firing and burst firing modulate the intensity of the phasic response of dopamine neurons and a disruption in this balance might result in the symptoms seen in psychosis and anhedonia (Grace 1991). Tonic dopamine in the striatum is also thought to modulate the trade-off between exploration and exploitation that ultimately guides action selection (Beeler, Daw et al. 2010; Humphries, Khamassi et al. 2012). It is therefore interesting to uncover the physiology and regulatory mechanisms behind this mode of firing in midbrain dopamine neurons.

Single spike firing in the SNc is characterised by single action potentials separated by a significant after hyperpolarisation (AHP) followed by a slow depolarising drive that brings the neuron to action potential threshold (Grace and Bunney 1984; Grace 1988). Firing rate is typically slow, at an average of 4Hz and coefficient of variation (CV) of ISI is generally below 20% (Wolfart, Neuhoff et al. 2001; Herrik, Christophersen et al. 2010; Tateno 2010) for tonic pacemaker-like firing pattern. This is also the type of firing observed typically in midbrain slices, and dissociated neuronal preparations, where synaptic transmission has been severed (Silva, Pechura et al. 1990; Hainsworth, Roper et al. 1991), suggesting that tonic single spike firing is generated and regulated by intrinsic ion channels expressed in the neuron (Amini, Clark et al. 1999). A number of experimental and computational studies have confirmed that the depolarising drive underlying this autonomous firing is mediated by calcium current through L-type channels in the majority of these neurons (Fujimura

and Matsuda 1989; Nedergaard, Flatman et al. 1993; Amini, Clark et al. 1999; Kuznetsova, Huertas et al. 2010).

When action potentials are silenced using tetrodotoxin (TTX), some neurons also exhibit a slow oscillatory potential (SOP) at a rate near the firing frequency, however this is not always the case as explained below. The amplitude of these oscillations is typically between -60mV and -40mV. These SOPs are abolished by L-type calcium channel blockers, suggesting that these channels play a crucial role in maintaining spontaneous firing. (Fujimura and Matsuda 1989; Grace and Onn 1989; Kang and Kitai 1993). The depolarising phase of this sub-threshold potential recruits sufficient intracellular calcium ions to activate SK channels that repolarise it (Wilson and Callaway 2000), thus giving rise to an oscillation in membrane potential. In fact, it has been hypothesised that this kind of L-type calcium channel mediated spontaneous firing in SNc dopamine neurons could result in excessive calcium influx that renders the neuron susceptible to stressors such as environmental toxins or genetic defects contributing to their selective degeneration in PD (Chan, Guzman et al. 2007). Some neurons continue to spike (after TTX has been washed off), even after the sub-threshold oscillations have been abolished by L-type calcium channel blockers. This indicates that in these neurons, sub-threshold oscillations and L-type calcium channels are not essential for spontaneous firing (Guzman, Sanchez-Padilla et al. 2009).

It is possible that in this case, other currents such as hyperpolarisation-activated cation currents (I_h) and sodium currents (I_{Na}) drive pacemaking, as in juvenile dopamine neurons (Chan, Guzman et al. 2007), dopamine neurons in the VTA (Khaliq and Bean 2010) and other spontaneously firing neuronal types (Chan, Shigemoto et al. 2004). Nevertheless, it is generally believed that spontaneous firing in the SNc is due to subthreshold membrane oscillations driven by calcium currents through L-type calcium channels depolarise the neuronal membrane to action potential

threshold to give rise to the traditional sodium spike, and potassium currents through SK channels repolarise the oscillation and subsequently hyperpolarise the membrane to delay the next spike.

While dopamine neurons in the SNc and VTA broadly share similar characteristics, there are subtle differences in firing pattern in the VTA. To start with, single spike firing is more irregular in the VTA compared to the SNc (Wolfart, Neuhoff et al. 2001). Secondly, autonomous firing in VTA dopamine neurons appears to be generated and sustained by sub-threshold sodium channels (Khaliq and Bean 2010) rather than being dependent on calcium channels and subsequent calcium influx, which is the case in the SNc. Voltage dependent calcium currents during the ISI are much smaller than sub-threshold TTX-sensitive sodium current. Moreover, when action potentials are blocked using TTX, there is no sub-threshold membrane oscillation, such as those seen in the SNc. This could perhaps also be the reason why VTA dopamine neurons are spared from degeneration in PD. Calcium currents during the ISI, however, did seem to regulate firing rate to some extent in these neurons, because removal of calcium from the external medium increased firing frequency in their experiments, which they hypothesised was, perhaps in part, due to a reduction in SK current as a result of decreased calcium inflow (Khaliq and Bean 2010).

Firing regularity in midbrain dopamine neurons

The regularity of single spike firing, both *in vivo* and *in vitro*, appears to be controlled by SK channels, because when these channels are inhibited by apamin, firing regularity is decreased as quantified by an increase in the CV of ISI (Waroux, Massotte et al. 2005; Ji and Shepard 2006). This effect is due to a reduction in the post-spike AHP mediated by SK currents. While this effect of SK channel inhibition has been replicated in many experiments, a hypothesis for what the underlying mechanism mediating this effect could be has not yet been proposed for dopamine neurons. Although the physiological importance of maintaining firing regularity in dopamine

neurons has not specifically been explored in behavioural experiments, we can perhaps relate some of the differences between SNc and VTA dopamine neuron firing properties and connectivity to some behavioural functions that could perhaps be in turn related to firing regularity.

From experiments, it has been demonstrated that a reduced expression of SK channels in VTA neurons results in these neurons firing more irregularly along with greater number of spikes in bursts when compared to their SNc counterparts (Wolfart, Neuhoff et al. 2001), which also corroborates well with observing increased burst firing in the presence of apamin *in vitro* (Shepard and Bunney 1988; Gu, Blatz et al. 1992). Decreased firing regularity in cerebellar Purkinje neurons, as a result of insufficient SK channel function, has been linked to decreased motor co-ordination in an ataxia mouse model (Walter, Alvina et al. 2006). Decreased firing regularity associated with increased burst firing due to reduced SK channel function has also been reported in SNc dopamine neurons in mice models of PD (Bishop, Chakraborty et al. 2010). It is therefore important to uncover mechanisms of firing regularity in midbrain dopamine neurons.

1.2.2 Burst firing

Burst firing in midbrain dopamine neurons results in significant increases in dopamine levels in target regions, as a result of accumulation of extracellular dopamine due to the saturation of dopamine transporters (Gonon 1988; Chergui, Suaud-Chagny et al. 1994; Prasad and Amara 2001), in turn influencing a number of post-synaptic neurons. Moreover, *in vivo*, dopamine neurons fire phasic bursts of action potentials in response to unexpected rewards (Schultz 1998) and play a major role in reinforcement learning by encoding a reward prediction error (Glimcher 2011). Burst firing also seems to be important for motivational behaviour (Salamone and Correa 2012), habit learning (Wang, Li et al. 2011), and sleep (Dahan, Astier et al. 2007).

Abnormalities in burst firing appear to be implicated in several disorders. For instance, in models of schizophrenia, increased burst-firing results in higher transients of dopamine in target regions, which manifests as behavioural and motor abnormalities (Dragicevic, Schiemann et al. 2015; Krabbe, Duda et al. 2015). We have also learnt that in rodent models of PD there is a disruption in normal firing of SNc dopamine neurons that is accompanied by an increase in burst firing (Bishop, Chakraborty et al. 2010). Impaired burst firing, for example such as those created by genetically inactivating NMDA-type glutamate receptors, also leads to learning deficits specifically in associative learning tasks (Zweifel, Parker et al. 2009). Increased burst firing is also observed in VTA dopamine neurons under the influence of nicotine that facilitates the reinforcing effects of this drug (Grenhoff, Aston-Jones et al. 1986; Bonci, Bernardi et al. 2003).

Burst firing in vivo

A combination of excitatory and inhibitory inputs from diverse regions of the brain induce burst firing by excitation and dis-inhibition respectively. Excitatory amino acids seem to play a primary role in the production of bursts in dopamine neurons because electrical stimulation of glutamatergic afferents (Grace and Bunney 1984; Chergui, Akaoka et al. 1994; Floresco, West et al. 2003) or direct micro-iontophoretic injection of glutamate (Grace and Bunney 1984; Blythe, Wokosin et al. 2009) robustly induce burst firing in these neurons. The majority of excitatory glutamatergic inputs come from sensory and motor areas such as the pre frontal cortex (Murase, Grenhoff et al. 1993), the subthalamic nucleus in the basal ganglia (Smith and Grace 1992) and the pedunculopontine nucleus in the brain stem (Mena-Segovia, Winn et al. 2008). Glutamate acts on two types of receptors, ionotropic (α-amino-3-hydroxy-5-methyl-4-isoxazolepropionic acid (AMPA), NMDA and kainate) and metabotropic receptors (Group I metabotropic glutamate receptor, mGluR). In midbrain dopamine neurons, glutamate receptor activation of the NMDA type, but not AMPA appears to exert a preferential role in the induction of burst firing (Chergui, Charlety et al. 1993;

Christoffersen and Meltzer 1995; Tong, Overton et al. 1996). This has been attributed to the distinct nonlinear voltage dependence and slope provided by the magnesium block and unblock of the NMDA receptor (NMDAR) (Deister, Teagarden et al. 2009; Ha and Kuznetsov 2013). Conversely, inactivating glutamatergic afferents synapsing onto midbrain dopamine neurons (Svensson and Tung 1989; Smith and Grace 1992) or using glutamate receptor antagonists such as kynurenic acid or NMDA antagonists (Overton and Clark 1992; Chergui, Charlety et al. 1993) switch the firing pattern of these neurons to single spiking. However, there is also some evidence to support the roles of AMPA, kainate and mGlu receptors in burst firing in dopamine neurons *in vivo* (Zhang, Chiodo et al. 1994; Christoffersen and Meltzer 1995; Meltzer, Christoffersen et al. 1997; Prisco, Natoli et al. 2002).

Some of the other regions controlling excitatory inputs to dopamine neurons and in turn regulating burst firing include the laterodorsal tegmental nucleus (LDTg) (Lodge and Grace 2006), tonic activation of which is required for glutamate-elicited burst firing in dopamine neurons of the VTA whereas suppressing the LDTg results in these very same neurons firing only in tonic pacemaker-like single spikes. Similarly, lesions of excitatory afferents from the sub-thalamic nucleus results in a substantial decrease in burst firing of SNc dopamine neurons (Smith and Grace 1992). On the other hand, inhibitory GABAergic inputs arising primarily from the striatum, substantia nigra pars reticulate (SNr), and globus pallidus also regulate burst firing via disinhibition (Tepper and Lee 2007). Using computational modelling and dynamic clamp, Lobb and colleagues show that disinhibition of the GABAergic influence mediated by striatal activation can generate robust bursts in SNc dopamine neurons (Lobb, Wilson et al. 2010; Lobb, Troyer et al. 2011). GABAergic influence is exerted via activation of $GABA_A$ and $GABA_B$ receptors on dopamine neurons and antagonising either of these receptor types enhances burst firing (Erhardt, Nissbrandt et al. 1999;

Paladini and Tepper 1999). A schematic overview of afferent control of midbrain dopamine neurons is illustrated in Figure 1.3.

Other forms of pharmacological manipulations such as iontophoresis by calcium ions, intracellular application of tetraethylammonium (TEA), a potassium channel blocker, and extracellular application of barium (that enter the neuron via calcium channels and block potassium channels) also result in burst firing *in vivo* suggesting a role for calcium in burst generation (Grace and Bunney 1984).

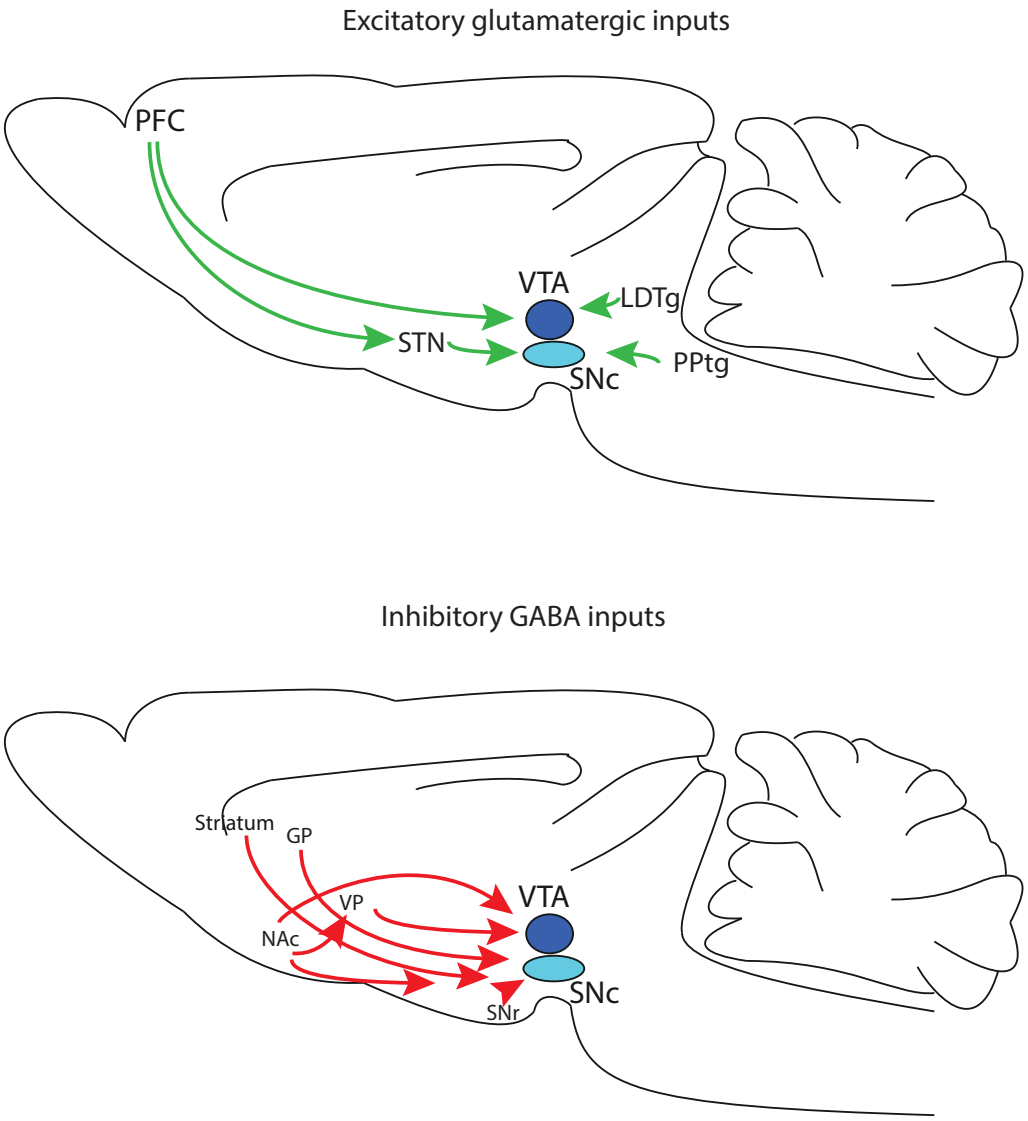


Figure 1.3: Afferent control of midbrain dopamine neurons

Some of the important glutamatergic (top) and GABAergic (bottom) afferent inputs to midbrain dopamine neurons. Abbreviations: PFC: pre-frontal cortex; STN: subthalamic nucleus; LDTg: laterodorsal tegmental nucleus; PPTg: pedunculopontine tegmental nucleus; GP: globus pallidus; NAc: nucleus accumbens; VP: ventral pallidum; SNr: substantia nigra pars reticulate.

Burst firing in vitro

As mentioned earlier, dopamine neurons in brain slices and in isolation fire only single spikes in a regular pacemaker like fashion and bursts can typically only be evoked by specific pharmacological manipulations such as NMDAR activation and/or SK channel block. Spontaneous burst firing in dopamine neurons in the slice preparation has only been observed in immature animals, also dependent on NMDAR activation (Mereu, Lilliu et al. 1997). Depolarising drive in the form of current injection can induce burst firing in many types of neurons *in vitro* including cerebellar Purkinje neurons (Swensen and Bean 2003), and subicular pyramidal neurons in the hippocampus (Staff, Jung et al. 2000) to name a few. In midbrain dopamine neurons, while some studies report not being able to evoke bursts with somatic current injection alone (Grace and Bunney 1983; Kuznetsov, Kopell et al. 2006), when there is sufficient depolarisation, *in vivo*-like bursts can be evoked by somatic current injection (Blythe, Wokosin et al. 2009) *in vitro*. In the majority of these neurons, though, somatic current injection results in cessation of firing termed depolarisation block. This has been attributed to inability of sodium channels to recover from inactivation (Kuznetsova, Huertas et al. 2010). Because spiking fails with excessive depolarisation, a long duration EPSP is therefore not well suited to generate bursts.

Stimulation of glutamatergic afferents and specifically NMDAR activation evokes bursts in dopamine neurons *in vitro* (Johnson, Seutin et al. 1992; Seutin, Johnson et al. 1993; Johnson and Wu 2004). Bath application of NMDA in midbrain slices changes single spike firing to burst firing in majority of dopamine neurons (Johnson, Seutin et al. 1992; Paladini, Iribe et al. 1999; Paladini and Tepper 1999), and this effect is greatly enhanced in the presence of apamin, a selective blocker of calcium activated SK channels (Seutin, Johnson et al. 1993). In fact apamin alone has also been shown to generate bursts in these neurons in brain slices (Shepard and Bunney 1988; Gu, Blatz et

al. 1992). However this is not always the case (Seutin, Johnson et al. 1993; Johnson and Seutin 1997; Wolfart and Roeper 2002).

Moreover, sometimes apamin induced burst firing is absent at low concentrations of apamin (Brodie, McElvain et al. 1999). These data suggest that perhaps SK channels suppress endogenous burst firing in these neurons under basal conditions (Wolfart and Roeper 2002). While NMDAR activation seems sufficient to elicit bursts *in vitro*, there have been instances where additional manipulations were essential to generate robust bursting; for example, a constant hyperpolarising current (Johnson, Seutin et al. 1992).

1.2.3 Existing hypotheses for burst firing in dopamine neurons

Preferential role for NMDAR in burst firing

Some modelling studies have tried to postulate why NMDAR activation appears to have a preferential role in burst firing, allowing for transient high firing frequencies such as those observed *in vivo* without inducing depolarisation block, such as those seen under AMPAR stimulation *in vitro*. As mentioned briefly earlier, this has been attributed to the unique whole-cell I-V characteristics of NMDAR activation endowed by its propensity to a voltage-dependent magnesium block. NMDARs remain closed and blocked with magnesium at resting membrane potentials and become activated only when bound with excitatory molecules such as glutamate and are simultaneously depolarised to remove the magnesium (VanDongen 2009). This gives rise to a negative slope region at hyperpolarised membrane voltages. Below this region, NMDA channels are inactive due to magnesium block but when depolarised beyond this region they allow for a switch to high frequency firing. Therefore with transient depolarisation, NMDAR current supports spiking that is soon blocked by magnesium when the membrane begins to get hyperpolarised perhaps due to intrinsic mechanisms, thus preventing depolarisation block. Whereas when AMPA mediated

depolarisation is present, the hyperpolarised region is short-lived thus promoting depolarisation block (Deister, Teagarden et al. 2009). Moreover, as mentioned earlier, if a simple depolarising synaptic input were sufficient to generate bursts, depolarisation of somatic membrane with current injection would also always give rise to bursts, however this is not always the case (Grace and Bunney 1983; Kuznetsov, Kopell et al. 2006).

Intrinsic (ion channel) mechanisms

It was observed in experiments that dopamine neurons fired bursts when SK channels were blocked with apamin, however spiking often failed due to depolarisation block, subsequently uncovering sub-threshold plateaux-like oscillations (Johnson and Wu 2004). It was hypothesised that a burst rides on the depolarising phase of the subthreshold plateaux potentials that are driven by L-type calcium currents and repolarised by calcium-mediated inactivation of those calcium currents (Amini, Clark et al. 1999). However, more recently, it was suggested that the activation of voltage dependent delayed rectifier-type ether-a-go-go (ERG) potassium currents mediate the repolarisation of plateaux potentials and thus facilitate termination of burst firing (Canavier, Oprisan et al. 2007).

Hypotheses for in vivo mechanisms: co-ordination between synaptic inputs and ion channels

One of the first theories explaining NMDAR-activation induced burst firing in dopamine neurons *in vitro* was based on sodium dynamics and hypothesised that oscillation in sodium concentration in distal dendrites due to incoming sodium current via NMDA receptor activation and sodium extrusion via the sodium pump drives burst firing in dopamine neurons (Johnson, Seutin et al. 1992; Li, Bertram et al. 1996; Canavier 1999). Another hypothesis for NMDAR-activation dependent *in vivo* burst firing is the coupled oscillator model in which the somatic and dendritic 'compartments' exhibit oscillations that are driven by the depolarising L-type calcium currents, repolarised by SK currents and exhibit spontaneous firing at their own natural frequencies depending on the surface-

to-volume ratio (Wilson and Callaway 2000). However transient disruptions in this coupling due to NMDAR activation by excitatory inputs onto dendrites could result in burst firing because of the amplification of the already elevated dendritic oscillations (Kuznetsov, Kopell et al. 2006). This model therefore assigns NMDARs as current amplifiers and predicts a dominant role for dendrites rather than the soma for generating bursts. However this appears to be controversial because NMDAR activation induces bursts in soma as well as in dendrites due to the presence of a high-frequency sub-threshold oscillation that seems to drive bursts that are different from the oscillations driving spiking (Deister, Teagarden et al. 2009). An alternative suggestion, based on electrical coupling between two neurons, predicted that bursts can be generated by an interaction between NMDAR activation and sodium pump in each of the coupled neurons based on the amount of NMDAR activation in each neuron and the strength of coupling (Komendantov and Canavier 2002).

How concurrent action of multiple mechanisms can modulate *in vivo* burst firing has also been explored in a morphologically realistic *in silico* dopamine neuron (Komendantov, Komendantova et al. 2004). In this study, the authors demonstrated that excessive depolarisation, that can be achieved by increased NMDAR activation, can be dampened by a concurrent increase in $GABA_A$ receptor activation. Moreover, while activating AMPA receptors elevates firing rate, as well as changes the firing pattern from single spike firing to burst firing, inhibition of SK channels preferentially only regulates firing pattern independently of rate (Canavier and Landry 2006).

1.2.4 The role of SK channels in regulating single spike and burst firing in midbrain dopamine neurons

While multiple hypotheses have been put forth for each firing mode, some aspects, specifically the role of SK channels in firing regularity and burst firing are still unclear. SK channels are expressed on neuronal membranes of many types of neurons including midbrain dopamine neurons (Stocker and Pedarzani 2000; Faber and Sah 2007). The potassium current that flows through SK channels

hyperpolarises the neuronal membrane after the spike has peaked. This hyperpolarisation helps other voltage-gated ion channels such as sodium to recover from inactivation and increase the number of available channels for activation (Patlak 1991) when the next wave of depolarisation occurs resulting in the next spike. SK channels have been shown to maintain firing rate and more importantly firing precision (Shepard and Bunney 1988; Deignan, Lujan et al. 2012) because when SK channels are pharmacologically blocked using antagonists such as apamin, firing regularity is decreased as quantified by an increase in the CV of ISI, both *in vivo* (Waroux, Massotte et al. 2005; Ji and Shepard 2006) as well as *in vitro* (Shepard and Bunney 1988; Ping and Shepard 1996). When SK channels are inhibited, it is intuitive that the firing rate would increase due to the reduction in post-spike AHP however, why should this result in a decrease in firing regularity? A computational modelling study recently demonstrated a reduced availability of sub-threshold activated sodium and potassium channels in the presence of SK channel blockade due to reduced AHP, resulting in a decrease in firing regularity in globus pallidus neurons (Deister, Chan et al. 2009). Therefore we hypothesised that, similarly in dopamine neurons, due to the reduction in post-spike AHP after SK channel inhibition, sometimes enough sodium channels recover from inactivation and in turn the neuron fires a spike but sometimes majority may still remain inactivated and therefore no spikes will be fired, thus resulting in an irregular spike train.

SK channel inhibition also facilitates a transition of firing pattern from tonic single spikes to burst firing (Shepard and Bunney 1988; Gu, Blatz et al. 1992), and even more so in the presence of excitatory glutamatergic agonists like NMDA (Seutin, Johnson et al. 1993). Because apamin induced bursts *in vitro* appear sensitive to L-type calcium channel blockers (Shepard and Stump 1999; Johnson and Wu 2004), it has been suggested that bursts are generated by the sub-threshold plateaux potentials revealed under the influence of TTX and apamin (Amini, Clark et al. 1999). Increased burst firing is also naturally observed *in vivo* in the VTA (Grenhoff, Ugedo et al. 1988)

that has been attributed to a lower expression of SK channels in this region (Wolfart, Neuhoff et al. 2001). Therefore evidence from the literature suggests that SK channels work towards suppressing burst firing in midbrain dopamine neurons and in some cases SK channel inhibition is sufficient for a transition from single spike mode to bursting (Prisco, Natoli et al. 2002).

1.3 Hypotheses and Aims

In summary, both external synaptic as well as intrinsic cellular mechanisms, including modulation of voltage- and ligand-gated ion channels, play a crucial role in maintaining the firing precision of midbrain dopamine neurons (Fujimura and Matsuda 1989; Overton and Clark 1997; Wilson and Callaway 2000; Floresco, West et al. 2003; Blythe, Wokosin et al. 2009; Oster and Gutkin 2011; Tucker, Huertas et al. 2012). In particular, SK channels maintain the firing precision of these neurons, because a reduction in SK channel current reduces firing regularity and in some cases facilitates the transition to bursting (Seutin, Johnson et al. 1993; Ping and Shepard 1996; Wolfart, Neuhoff et al. 2001; Canavier and Landry 2006; Ji, Hougaard et al. 2009; Herrik, Christophersen et al. 2010; Drion, Massotte et al. 2011; Deignan, Lujan et al. 2012). Pharmacological modulation of SK channels *in vivo* using apamin injections, either systemic (Messier, Mourre et al. 1991) or directly into brain regions such as the VTA (Steketee and Kalivas 1990), show behavioural changes indicative of cognitive and motor function enhancement in rodents (van der Staay, Fanelli et al. 1999). Decreased firing regularity in cerebellar Purkinje neurons, as a result of insufficient SK channel function, has also been linked to decreased motor co-ordination in an ataxia mouse model (Walter, Alvina et al. 2006). Furthermore, recent work in our lab demonstrated that a deletion of PD-associated genes, *PINK1* or *HtrA2/Omi*, leads to a decrease in SK channel function in the dopamine neurons of the SNc that in turn causes an increase in firing irregularity and bursts in these neurons (Bishop, Chakraborty et al. 2010). It is therefore important to understand the role of, and

mechanism(s) by which, SK channels regulate firing precision and transition to burst firing in midbrain dopamine neurons.

Although existing computational studies have helped uncover ion channel mechanisms underlying spontaneous firing and hypothesised about burst firing, none have managed to elucidate how SK channels regulate firing precision in midbrain dopamine neurons. This could be in part because these studies have modelled ion channels as being deterministic, i.e. single lumped conductances representing the entire population of ion channels that do not capture ion channel stochasticity. In other words, current deterministic models of midbrain dopamine neurons are unable to replicate the different transitions between the multiple states ion channels are capable of existing in, such as open, closed, inactivated, to name a few. We therefore sought to build a Markov model based dopamine neuron with ion channel densities similar to that seen in physiology in order to elucidate how SK channels mediate their influence on firing regularity.

1.3.1 Hypothesis 1 – SK channels control the recovery from inactivation of other voltage-gated ion channels

The post-spike AHP provided by the current through SK channels standardises the recovery from inactivation of other voltage-gated ion channels such as sodium and potassium channels in order to time each action potential. With SK channel inhibition, reduced AHP results in a variable amount of sodium channels remaining in the inactivated state, due to ion channel stochasticity, thereby resulting in an irregular spike train.

Ion channels can exist in one of many states such as open, closed, or inactivated depending on the membrane potential and the probability of finding an ion channel in a particular state follows a Markovian scheme. Our aim was therefore to create a computational model representative of a midbrain dopamine neuron with ion channels that were capable of transitioning between multiple

states such as open, inactivated, and closed. This allowed us to determine how the AHP mediated by SK channel current controls the availability of ion channels leading up to action potential threshold. This is in contrast to several other computational models already existing in the field that are deterministic in nature and do not capture this biologically realistic probabilistic nature of ion channel gating and have therefore been unable to explain *how* SK channels regulate firing precision. This project is discussed in detail in Chapter 3.

1.3.2 Hypothesis 2 – data driven analysis of *in vivo* membrane voltage can predict ion channel mechanisms

A quantitative analysis of endogenous burst waveforms gave rise to the hypothesises that:

i) SK channel current is significantly reduced during burst firing

ii) There is a progressive depolarisation in action potential threshold during a burst

iii) The depolarisation in action potential threshold is due to accumulation of sodium channel inactivation

Due to the difficult nature of performing such experiments, *in vivo* intracellular recording from midbrain dopamine neurons has been limited. However, our lab had recently successfully recorded from seven histochemically identified VTA dopamine neurons from anesthetised rats in the intracellular configuration (*Brischoux et. al. manuscript in preparation*) and made it possible to gain an insight into the membrane dynamics during endogenous burst firing in dopamine neurons. We therefore wanted to analyse the membrane voltage trajectories in order to provide a quantitative description of some of the commonly observed features during bursts in dopamine neurons. We also wanted to compare average spike waveforms to detect changes, if any, between non-burst spikes and spikes from within a burst in order to hypothesise mechanisms that produce and terminate bursts.

We wanted to use principal components analysis (PCA) as a complementary approach to identify membrane voltage epochs that were different for burst and non-burst waveforms in order to subsequently relate those changes to ion channels driving these differences if any. If PCA would identify regions in the action potentials that were significantly different between non-burst single spikes and spikes from a bursts, I wanted to then use PCA-modified reconstructed waveforms as voltage commands to my computational dopamine neuron model in order to elucidate those ion channel currents that are also modified as a result of the PCA-modified reconstruction of the spikes. This would in turn help in relating differences between burst and non-burst waveforms to underlying ion channel currents. This is a novel technique that extracts membrane voltage features using PCA that drives maximal variance between spikes of different kinds and in turn relates those differences to ion channel currents.

Moreover, because I built the dopamine neuron model for the firing regularity study, I also wanted to use this model to study currents underlying bursts and select ion channel candidates mediating burst firing. I wanted to use the *in vivo* intracellular spike trains obtained from the VTA as voltage commands to the computational model in order to analyse individual ion channel currents. This method can be considered as the reverse of dynamic clamp, where virtual currents are introduced into the physiological neuron in order to study its effects on the firing properties of that neuron. These methods and results from this analysis are detailed in Chapter 4.

Chapter 2 Computational modelling of ion channels and the *in silico* dopamine neuron

2.1 Introduction

2.1.1 Ion channels and action potentials

Neuroscience today is a multidisciplinary branch of medicine with computational neuroscience also at its forefront. A classic example follows from the inspiring and ground-breaking work of Hodgkin and Huxley who elegantly described the action potential in terms of mathematical equations (Hodgkin and Huxley 1952) and established a framework for simulating neurons and axons that is widely used till date. One of their hypotheses at the time "the distribution of charged particles which…allow sodium to pass…when they occupy particular sites in the membrane" was a prediction that later on led to the discovery of membrane spanning ion channels and the modern day pore theory version of the Hodgkin-Huxley formalism. Therefore, mathematical modelling of neuronal physiology can serve as a first step towards testing hypotheses and developing theoretical ideas before designing future experiments.

Although action potentials share some common features across neuronal types, each population of neurons has hallmark features that give it an electrophysiological identity making it possible, to a certain degree, to identify neurons based on their action potential shape. Since it is the co-ordinated activity of ion channels that gives rise to the action potential, different parts of the action potential are driven by the activity of a combination of one or more ion channels as depicted in Figure 2.1

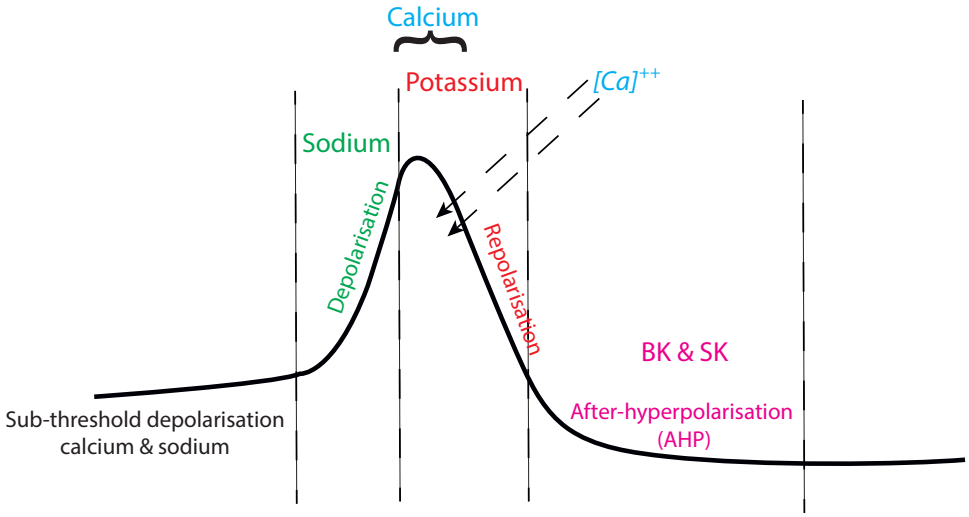


Figure 2.1: A variety of ion channels participate during the unique phases of the action potential

Sub-threshold activated sodium and calcium channels drive the neuronal membrane towards action potential threshold. As the membrane gets depolarised, more and more sodium channels begin to open until enough are open to fire an action potential. As the action potential reaches its peak, sodium channels begin to inactivate and potassium channels open to repolarise the membrane. Calcium channels also open during the positive phase of the action potential bringing into the neuron an influx of calcium ions. The rise in intracellular calcium in turn activates calcium-dependent potassium channels like the BK and SK channels that provide the fast and long lasting post-spike AHP respectively.

2.1.2 Channel noise – stochasticity in voltage-gated ion channels

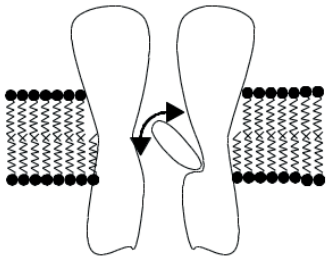
Ion channels are pore-forming protein complexes embedded in the lipid bilayer of the neuronal membrane (Figure 2.2 A). Although on average ion channels open and close (gate) in response to changes in membrane voltage, neurotransmitter release, or intracellular ion concentrations, they are constantly under the influence of thermo-dynamic fluctuations, that impart an element of randomness to their gating characteristics (Neher and Sakmann 1976; Sigworth and Neher 1980; Hille 1992). Sakmann and Neher were the first to record currents from single ion channels in the late 1970s (Neher and Sakmann 1976) such as the one illustrated in Figure 2.2 B. Their recordings provided direct evidence of the existence of ion channels in the neuronal membrane (as predicted by the theoretical work by Hodgkin and Huxley) and it also shed light on the stochastic nature of gating (transition between open and closed states) in ion channels.

Ion channel stochasticity refers to the independent and random transitions between multiple configurationally distinct states, such as *open*, *closed*, *inactivated*, of single ion channels due to thermo-dynamic fluctuations inherent in the neuron. In terms of computational modelling, for a finite number of channels of a particular type, this can be described as a continuous-time Markov chain with voltage-dependent transition probabilities (Goldwyn and Shea-Brown 2011). In other words, the probability that an ion channel will transition from one state to the other depends on the membrane voltage. Ion channels are considered memory-less, which means that the amount of time spent in a particular state does not affect the future state (Hille 1992) and therefore the transitions are modelled as instantaneous. The gating behaviour of ion channels is described as a Markov process because a Markov process is a probabilistic system with a number of discrete set of states. There exist a number of possible transitions from the current state to another state, associated with a specific probability of occurring. These transition rates are the same linear chemical kinetic schemes used in the HH model to determine transition probabilities between discrete channel states.

Each transition corresponds to the binding or unbinding of a gating particle. The Markov states and the associated transition probability rate functions together form a Markovian kinetic gating scheme. The transition rates are sometimes multiplied by a factor k that equals the number of particles of a particular type bound to the previous state before the transition (Faisal, 2007). This is explained in more detail in terms of the model used in this study in Section 2.2.1. This procedure thus helps to configure a stochastic Markov gating particle model from any HH-like deterministic conductance model.

This randomness, or stochasticity, results in channel noise that contributes to electrical noise observed in single neurons (Faisal, Selen et al. 2008; Faisal 2013). The variability we observe in action potential shape (de Polavieja, Harsch et al. 2005) and spike train dynamics (Skaugen and Walloe 1979) even within the same neuron have been attributed to ion channel noise. Trial-to-trial variability in neuronal responses to the same stimuli (White, Rubinstein et al. 2000; Faisal and Laughlin 2007), leading ultimately to variability in behaviour can also be accounted for, in part, by electrical noise due to ion channel stochasticity (Schneidman, Freedman et al. 1998). It was historically believed that the contribution of ion channel stochasticity to neuronal noise was limited because of the large numbers of ion channels involved (Hille 1992; Schneidman, Freedman et al. 1998; Faisal and Laughlin 2007). However recent theoretical and experimental studies have demonstrated otherwise as detailed below.

A



B

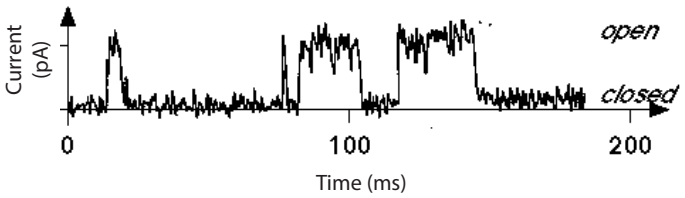


Figure 2.2: Ion channels and stochasticity

A. Schematic of a single ion channel illustrating the concept of gates that open and close to allow selective ions to pass through, giving rise to ion channel currents. Figure adapted from Faisal *et al.* 2005. **B.** Single channel currents recorded from a single potassium channel shows that along with long duration voltage-dependent openings, the ion channel briefly opens for very short durations primarily due to thermo-dynamic fluctuations within the neuron, giving rise to electrical noise due to ion channel stochasticity. Figure adapted from (Krekora 1992).

Channel noise has indeed been shown to be a useful and sometimes an essential component of spiking activity in neurons. For example, ion channel noise can account for changes in action potential shape that depends, on a large extent, on the number of available or *open* sodium and potassium channels during the course of the action potential (de Polavieja, Harsch et al. 2005; Faisal, White et al. 2005). The small number of *open* ion channels (as opposed to the total number of ion channels) is also critical when it comes to firing action potentials in very small diameter patches of neuron where even a single open sodium channel can give rise to spontaneous or 'random' action potentials if it stays open for long enough, which in fact places a lower limit to how small an axon can be (Faisal, White et al. 2005).

The variability in action potential threshold is also in part due to the small number of *open* ion channels around action potential threshold that determines the reliability in action potential initiation and precision (Skaugen and Walloe 1979; Schneidman, Freedman et al. 1998; van Rossum, O'Brien et al. 2003), reinforcing the idea that ion channel noise is important for firing precision. Ion channel noise also seems essential for characteristics like the peri-threshold oscillations observed in entorhinal stellate neurons (Dorval and White 2005) and also plays a key role in amplifying weak, sub-threshold signals coming into the neuron thus enhancing its signal detection capabilities via a process termed 'stochastic resonance' (Moss, Ward et al. 2004; Faisal, Selen et al. 2008).

Another important downstream effect of stochastic gating of voltage-gated ion channels is the noisy changes in intracellular concentrations of important second messenger ions such as calcium. SK channels are known to be spatially co-localised with voltage-gated calcium channels in many neurons (Marrion and Tavalin 1998) including dopamine neurons (Wolfart and Roeper 2002) thus making these channels sensitive to even small changes in intracellular calcium concentration $[Ca^{2+}]_i$

since we know that they have a half activation in the nano-molar (nM) range (Sah 1996; Ji, Hougaard et al. 2009). Therefore, even a small number of ions within the vicinity of SK channels are enough to activate them. For instance, a $[Ca^{2+}]_i$ of 100 nM translates to 60 calcium ions in a $1mm^3$ volume (von Wegner, Wieder et al. 2012). Indeed, Stanley et al. show that calcium transients within calcium micro-domains amplify sub-threshold SK currents by increasing the mean open probability of SK channels, transforming the sub-threshold calcium oscillation into membrane level fluctuations especially at low frequencies (Stanley, Bardakjian et al. 2011).

2.1.3 Simulating neurons and stochastic action potentials

In computational neuroscience, the cell membrane of a neuron is considered as an electrical circuit where important cellular components are analogous to electrical elements (Figure 2.3 A, B) (Hodgkin and Huxley 1952). The main component in the circuit is the somatic membrane itself that is compared to a capacitor (due to its phospho-lipid bilayer) that stores ionic charge (arising from the ions passing through ion channels in the membrane) as the electrical voltage across the membrane. Since ion channels are embedded across the membrane, they are considered as resistors in parallel to one another. In the resting state, the neuronal membrane naturally creates a potential difference across itself due to the charge separation resulting from differences in the types of ions present inside and outside the neuron. At rest, the inside of the neuron is more negative than the outside, which creates a concentration gradient. Movement of charge across this concentration gradient in turn results in an electromotive force in the opposite direction until the two forces balance each other to reach the Nernst or equilibrium potential for that ion. The battery in series with the resistors in the membrane equivalent circuit represents this potential.

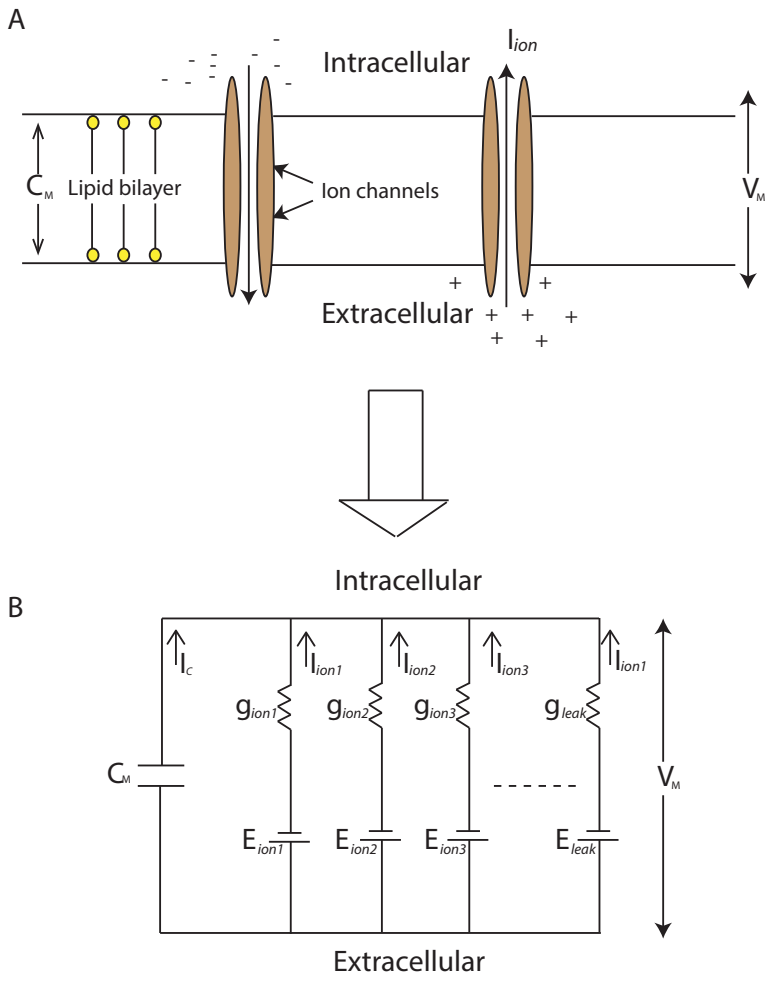


Figure 2.3: Modelling ion channels

A. The phospho-lipid bilayer of the neuronal membrane with ion channels spanning across it. There is a difference in the charge of ions found on either side of the membrane at rest that gives rise to the concentration gradient across the membrane. Movement of ions through selective ion channels leads to an electromotive force in the opposite direction. **B.** The equivalent electrical circuit for the membrane schematic shown in A. The lipid bilayer is the membrane capacitance while all the ion channels are thought of as resistors in parallel to each other along the membrane. The reversal potentials are represented as the battery. V_M is the membrane voltage; C_M is the membrane capacitance; I_{ion} stands for the current passing through the respective ion channel; E_{ion} is the reversal potential for that ion; Ca is the intra-cellular calcium concentration.

Therefore from Ohm's law, current through each of the ion channels can be calculated from the equation

$$I_{ion} = g_{ion} (V_m - E_{ion}), \quad (1)$$

where g_{ion} is the instantaneous ion channel conductance, V_m is the membrane voltage and E_{ion} is the reversal potential for that ion.

In the case of *stochastic* ion channel gating, g_{ion} is the product of maximal ionic membrane conductance $\overline{g}_{ion}$ and $p_{ioni}(V_m)$, the voltage-dependent probability of a single channel being open,

$$g_{ion} = \overline{g}_{ion}\, p_{ioni}(V_m), \quad (2)$$

where $\overline{g}_{ion}$ is the product of single channel conductance γ_i and ρ_i, the number of channels in unit membrane area or channel density. Therefore we can write

$$g_{ion} = \gamma_i \rho_i\, p_{ioni}(V_m) \quad (3)$$

Stochasticity in ion channel gating can be modeled mathematically as a continuous time Markov chain. The probability $p_{ioni}(V_m)$ that an ion channel is open is a product of the individual probabilities that each gate of the channel is in the bound or activated state in a Markovian gating scheme because each gate is considered independent of each other. If q_j is the probability that a single gating particle j is in the bound state then,

$$p_{ioni}(V_m) = q_j(V_m)^l \quad (4)$$

where l is the number of gates of type j. q_j is governed by linear differential equation of the form:

$$q_j = \alpha_j(V_m)(1 - q_j) - \beta_j(V_m)\, q_j \quad (5)$$

where α and β are rate functions that describe the rate of change of q_j. For each Hodgkin-Huxley (HH) sodium channel, p_{Nai} is m^3h and for each delayed rectifier potassium channel p_{Kdri} is n^4. Deterministic currents on the other hand have the general form

$$I_{ion} = \overline{g}_{ion}\, a^k b^l (V_m - E_{ion}), \quad (6)$$

where I_{ion} is the current flowing through the channel, $\overline{g}_{ion}$ is the total maximal ionic conductance, a^k and b^l are activation and inactivation variables raised to the number of gates for that ion channel respectively, V_m is membrane voltage and E_{ion} is the reversal potential for that ion.

2.1.4 The dopamine neuron model

Neurons can be broadly divided into three morphologically and functionally distinct regions: the cell body or soma, the dendritic tree, and the axon. While it is important and might seem practical to take into consideration the full morphology of a neuron to precisely reproduce its physiology *in silico*, modelling only the soma can be sufficient, as a first step, in cases like ours where there is enough evidence to suggest that the soma contains all the ion channels necessary to produce the electrophysiological features of interest; i.e even a dissociated preparation containing only the soma is capable of spontaneous single spike firing (Silva, Pechura et al. 1990; Amini, Clark et al. 1999; Puopolo, Raviola et al. 2007; Kuznetsova, Huertas et al. 2010). Because we were investigating ionic conductances underlying regulation of firing precision in midbrain dopamine neurons, we have used the HH formalism to simulate ion channel dynamics. In particular, our hypothesis (Hypothesis 1, Section 1.3.1) required that we model conductances as individual ion channels that are independent stochastic entities capable of existing in many voltage-dependent states like *open*, *inactivated*, and *closed*, instead of simulating the average gating behaviour of each conductance as is usually seen in deterministic neuronal models (Amini, Clark et al. 1999; Canavier and Landry 2006; Canavier, Oprisan et al. 2007; Kuznetsova, Huertas et al. 2010; Drion, Massotte et al. 2011).

2.1.5 Voltage-gated ion channels and their roles in dopamine neuron electrophysiology

Before going into the details of the model, it is useful to have an understanding of the variety and functions of ion channels that are found in midbrain dopamine neurons. A number of voltage and

ligand gated ion channels, each having a unique role in shaping the action potential and spike train dynamics have been reported in midbrain dopamine neurons. Several experimental studies have revealed that a large repertoire of voltage-gated ion channels is found in dopamine neurons and those relevant to my model are reviewed here, followed by a more detailed review of SK channels and their role in dopamine neuron physiology. Although I provide here a brief overview of many of these channels, for my work I chose to include only those ion channels that are directly involved in generating and maintaining the spontaneous and regular firing pattern observed experimentally to. This enabled me to keep my model simple and answer specifically the questions of interest.

Depolarising currents

Depolarising currents are essential to drive the neuron to action potential threshold and generate the spike itself. Dopamine neurons express both the tetradotoxin (TTX) sensitive, fast inactivating sodium channels as well as TTX-insensitive persistent sodium channels (Grace 1990; Puopolo, Raviola et al. 2007; Khaliq and Bean 2010). While the fast sodium current plays a major role in action potential initiation and propagation (Grace 1990), the background sodium currents contribute to the slow depolarisation that drives the neuron to action potential threshold in a subset of midbrain dopamine neurons, especially in the VTA (Grace and Onn 1989; Puopolo, Raviola et al. 2007; Khaliq and Bean 2010).

A number of voltage-gated calcium channels have been identified in midbrain dopamine neurons including high-voltage activated L-type, N-type, P-type channels (Cardozo and Bean 1995; Durante, Cardenas et al. 2004; Guzman, Sanchez-Padilla et al. 2010), and low-voltage activated T-type channels (Wolfart and Roeper 2002; Cui, Okamoto et al. 2004). Calcium channels play a crucial role in dopamine neuron physiology, not only as an important source of intra-cellular calcium ($[Ca^{2+}]_i$), but also by actively contributing to the shape of the action potential (Yung,

Hausser et al. 1991; Kang and Kitai 1993). Calcium currents are also believed to underlie the rhythmic sub-threshold membrane oscillations (in the presence of TTX) observed in some dopaminergic neurons of the SNc that is thought to drive pacemaking (Llinas, Greenfield et al. 1984; Kang and Kitai 1993; Mercuri, Bonci et al. 1994).

L-type calcium currents provide the depolarising drive to these membrane oscillations and in particular, their voltage-dependence supports pacemaker-like spontaneous firing in SNc dopamine neurons (Nedergaard, Flatman et al. 1993; Mercuri, Bonci et al. 1994; Amini, Clark et al. 1999; Puopolo, Raviola et al. 2007; Guzman, Sanchez-Padilla et al. 2009). While they are not thought to be essential for autonomous firing, in some of these neurons, blocking L-type channels abolishes spontaneous firing (Nedergaard, Flatman et al. 1993). L-type channels also provide the bulk of accumulation of $[Ca^{2+}]_i$ (Durante, Cardenas et al. 2004) that in turn activates SK channels (Wilson and Callaway 2000) which in turn hyperpolarises the neuronal membrane and standardises the time to next action potential, thus contributing to pacemaker-like firing, but see (Putzier, Kullmann et al. 2009).

The hyperpolarisation-activated cyclic nucleotide gated current (I_h) is known to underlie spontaneous firing in cardiac and some neuronal cells (Luthi and McCormick 1998; Robinson and Siegelbaum 2003) because of its sub-threshold activation to provide an excitatory inward drive towards action potential threshold. However, in dopamine neurons, the role of I_h in spontaneous firing is limited. Only in a subset of SNc dopamine neurons that are calbindin negative, I_h is involved in regulating spontaneous firing, where an inhibition of I_h reduces firing frequency (Neuhoff, Neu et al. 2002). Some depolarising currents are particularly active during high frequency firing. For example, additional depolarisation resulting from non-selective cations entering through transient receptor potential (TRP) channels that are activated by the rise in intracellular calcium due

to calcium entry through NMDAR activation is believed to give a boost to burst firing (Mrejeru, Wei et al. 2011) in these neurons.

Hyperpolarising currents

Many types of voltage-gated potassium channels have been described in midbrain dopamine neurons including the tetra-ethyl-ammonium (TEA) sensitive delayed-rectifier (K_{dr})-like slow and non-inactivating potassium current (Grace 1990; Silva, Pechura et al. 1990), and the 4-aminopyridine (4-AP) sensitive A-type fast activating, slowly inactivating potassium current (Silva, Pechura et al. 1990; Koyama and Appel 2006; Khaliq and Bean 2008). K_{dr} is mainly responsible for repolarising the action potential while the A-type current provides a sub-threshold hyper-polarising drive to delay the subsequent depolarisation of the neuron to reach the next action potential threshold (Bunney 2000), thus regulating the firing frequency (Silva, Pechura et al. 1990; Chiodo and Kapatos 1992; Khaliq and Bean 2008). It has also been hypothesised that the A-type current also regulates the height and width of the action potential itself (Segev and Korngreen 2007).

Several other types of potassium channels have recently been described in dopamine neurons and more importantly been associated with modulating burst firing. The M-type voltage-gated potassium channel (Hansen, Ebbesen et al. 2006) preferentially regulates burst firing by activating only during the prolonged plateau potential that is typically believed to underlie a burst and modulates the number of short ISIs within the burst (Drion, Bonjean et al. 2010). ATP-sensitive potassium channels are widely expressed in midbrain dopamine neurons and their role in burst firing appears to be population-specific; in medial-SNc dopamine neurons they are burst-promoting when co-activated with NMDARs (Schiemann, Schlaudraff et al. 2012). ERG (ether-a-go-go related gene) potassium channels seem to terminate bursts in dopamine neurons and limit cessation of

firing by depolarisation block (Canavier, Oprisan et al. 2007; Ji, Tucker et al. 2012) by repolarising the plateaux potentials.

While a number of these ion channels play important roles in shaping the firing properties of midbrain dopamine neurons, I have chosen only a few of them most relevant to my study to be included in my model. My model includes the fast sodium and delayed rectifier potassium channels owing to their roles in generating and maintaining the action potential. While the A-type potassium channel regulates firing frequency, the L-type calcium channel provides the necessary calcium influx to activate the SK channel. In my view, these ion channels are sufficient to reproduce key electrophysiological properties of midbrain dopamine neurons, and specifically allows me to create a simple reduced model to easily test my hypotheses outlined in Chapter 1.

2.2 Methods

2.2.1 The stochastic dopamine neuron model

I developed a hybrid biophysical dopamine neuron model driven by a combination of stochastic and deterministic ion channels. A single spherical compartment of diameter 10μm and capacitance 1μF/cm^2 represents the dopamine neuron soma and holds some of the ionic conductances known to be present in midbrain dopamine neurons (Figure 2.4 A) and more importantly those that are sufficient to reproduce the basic electrophysiological features associated with these neurons as described in detail Section 2.1.5. The model follows HH formalism (Hodgkin and Huxley 1952) that considers the neuronal membrane as an electrical circuit where ionic conductances are in parallel with the membrane capacitance representing the phospholipid bilayer of the neuronal membrane (Figure 2.4 B). The membrane is considered as an iso-potential patch with ion channels distributed uniformly across the membrane. Ion channel activation-inactivation parameters have been adapted from existing deterministic models and modified to fit the dynamics of our model (See section 2.4.2 for equations describing the rate functions for all the ion channels included in our model). While most of the ion channels in the model are *deterministic* (i.e., their gating describes the behaviour of a population of ion channels as a single lumped conductance), each individual fast sodium and delayed rectifier potassium channel in our model has been described as a *stochastic* Markov process (Hille 1992). This means that each sodium and potassium channel can be in one of many states such as *open*, *closed*, *inactivated*, the transitions between which are determined by associated voltage-dependent probability rate functions (Faisal 2013). This gives rise to Markovian gating schemes like the 8-state scheme for a sodium channel and 5-state scheme for a potassium channel (Figure 2.5 A&B). In the case of the sodium channel, the transition rate from the third closed state to the open state is α_m, the inverse transition has a rate $3\beta_m$, and the transition away from the open state would have rate $3\beta_m + \beta_h$ (Figure 2.5 A). The stochastic channel gating is modelled using continuous-time, discreet-state Markov chains, implemented using the Binomial

algorithm (Faisal et al, 2009). There are many algorithms that have been used to implement ion channel stochasticity, broadly classed as synchronous or asynchronous. Synchronous algorithms such as the Langevin for example, update the model's state at a common time interval. It makes a stochastic approximation of the underlying gating Markovian scheme in terms of channel kinetics reduced to Focker-Planck-type equations, adding a Gaussian noise term to the deterministic ODE that solves the transition rate. However, the white noise term does not capture all the properties of channel noise. Moreover the continuous approximation of conductance by the algorithm breaks down due to the discrete nature of the ion channel states.

The single channel and binomial algorithms on the other hand model each channel separately, accounting for the transition probabilities of each channel to transit from one state to another during a fixed time step. The binomial algorithm that is used in my model assumes that ion channels of the same type belong to a binomial population and a binomially distributed number of channels transition from one state to another at a given time. This means that a single binomially distributed random number determines how many channels switch state at each iteration of the simulation. The binomial algorithm is faster than the single channel algorithm due to the fewer random numbers involved.

The Gillespie algorithm is one of the most commonly used asynchronous algorithms where channel kinetics are described by Markov processes and the probability of time a channel spends in a particular state decreases exponentially with time. Two random numbers, one to determine when a particular state ends, and another to determine which transitions occur are used to determine the transition rates for all transitions in a single population of channels.

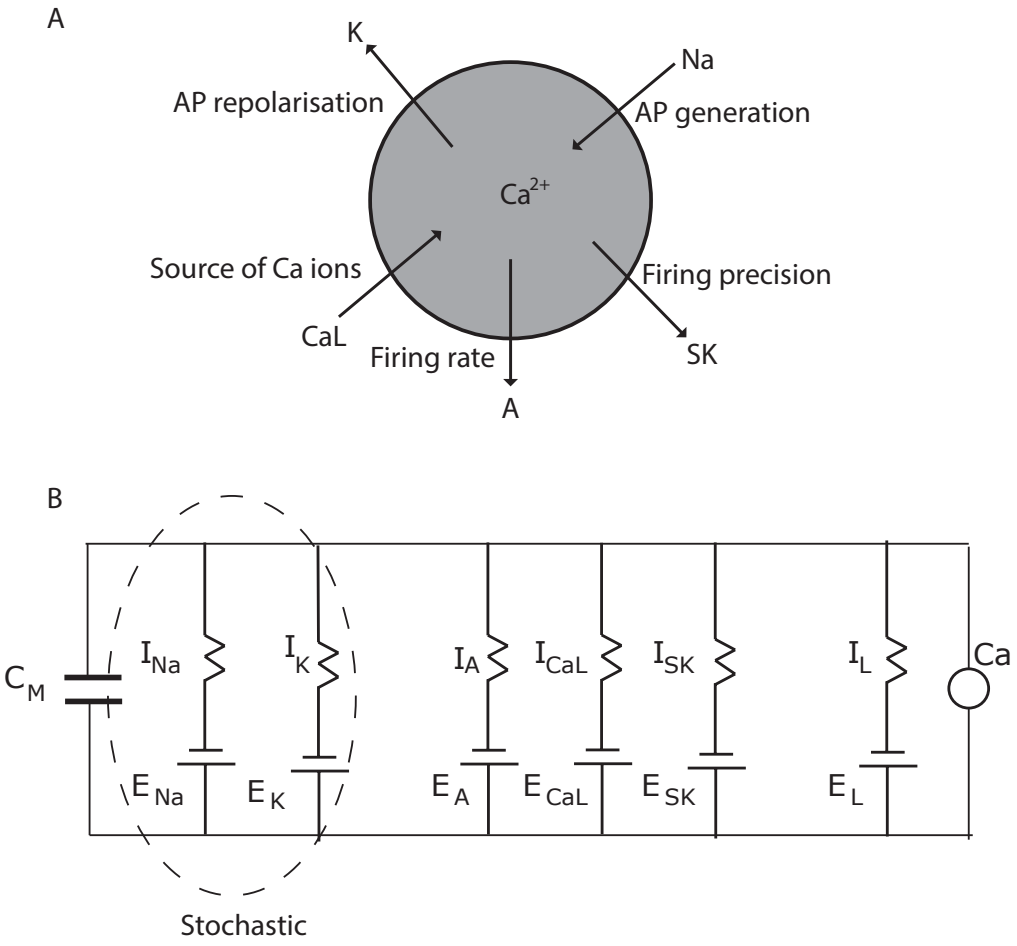


Figure 2.4: Dopamine neuron model schematic and equivalent electrical circuit

A. The schematic is a single compartment representative of the dopaminergic soma consisting of five ion channels namely, Na: sodium and K: delayed rectifier potassium, responsible for action potential generation and repolarisation respectively; A: A-type potassium, responsible for firing rate and spike rate adaptation; CaL: L-type calcium, that is the only source of calcium ions in the model; SK: calcium-activated potassium, that regulates firing precision. **B.** Equivalent electrical circuit for the model in A, where $C_{M:}$ membrane capacitance; E: reversal potential for respective ion; I: current through respective channel. Note that the sodium and potassium channels have been modelled as stochastic while the remaining ion channels are deterministic.

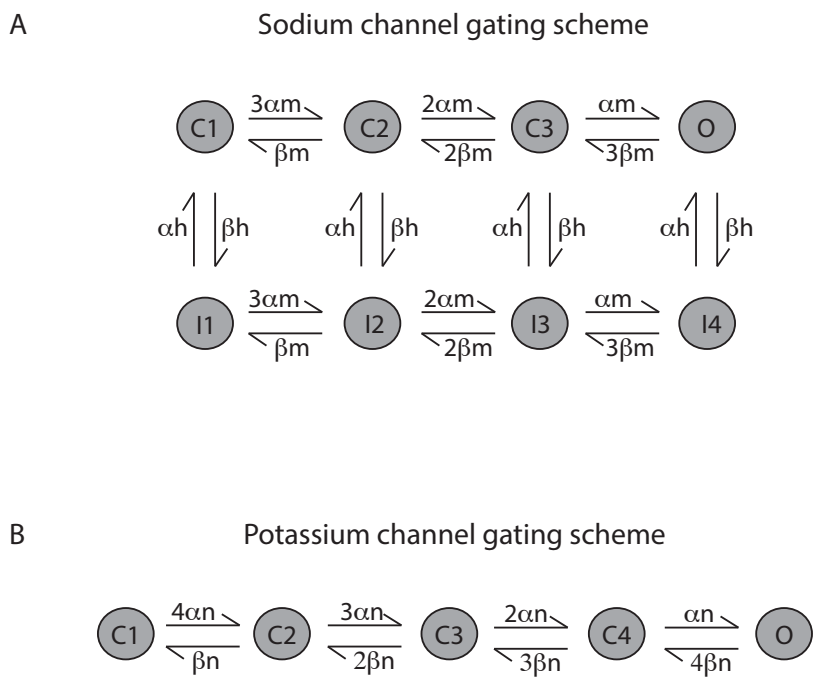


Figure 2.5: Markov gating schemes for sodium and delayed rectifier potassium channels

A. 8-state Markov scheme for sodium channel gating. **B.** 5-state Markov scheme for delayed rectifier potassium channel. O: open state; I: inactivated state; C: closed state. a, b: rate functions; m, n are activation variables for sodium and potassium channels respectively, while h is the inactivation variable for the sodium channel.

Intracellular calcium dynamics are modelled as a single pool of calcium ions coming into the neuron through the opening of voltage-gated L-type calcium channels. Calcium ions are subsequently removed using a decay term that lumps together more complex phenomena like extrusion by pumps and intracellular buffering (Yamada 1989; Anwar, Hong et al. 2012). The activation of SK channel is modelled by assuming that calcium binds to the SK channel with Michaelis-Menton type kinetics with a Hill coefficient of 4 (Xia, Fakler et al. 1998).

2.2.2 Model parameters and rate functions

Model parameters

The model parameters were initially adapted from existing computational models of dopamine neurons (Amini, Clark et al. 1999; Canavier and Landry 2006; Kuznetsova, Huertas et al. 2010) and subsequently modified to fit my model's dynamics.

	Na	K_{dr}	K_A	*CaL*	*SK*	*leak*
$\overline{g}$ (mS/cm^2)	-	-	4	5	5	0.3
E (mV)	55	-72	-75	50	-75	-45

For stochastic sodium and potassium channels,

Single sodium channel conductance, $\gamma_{Na} = 12pS$;

Sodium channel density, $\rho_{Na} = 3/\mu m^2$;

Single potassium channel conductance, $\gamma_{Kdr} = 2pS$;

Potassium channel density, $\rho_{Kdr} = 2/\mu m^2$.

The ion channel densities for the stochastic sodium and potassium channels that have been taken from the literature suggest that these relatively small densities combined with the small diameter of midbrain dopamine neurons would yield an overall small number of ion channels (less than 4000

sodium channels) for the patch of iso-potential membrane being simulated and promise the stochastic effects we expected.

Rate functions

Ion channel open and close primarily in a voltage-dependent manner and the pioneering work by Hodgkin and Huxley made it possible to model these ion channel dynamics using mathematical equations such as ones described here called rate functions. These equations describe how ion channels activate and inactivate with respect to membrane voltage thus allowing current to flow through them. The variables m, a and h, b represent the activation and inactivation variables respectively, and $[Ca]_I$ is the intracellular calcium level.

Sodium channel - I_{Na}

$$\alpha_m = -0.1(V_m+35-5.3)/(\mathbf{exp}(-(V_m+35-5.3)/10)-1)$$

$$\alpha_h = 0.07\ (\mathbf{exp}(-(V_m + 60 - 12)/20))$$

$$\beta_m = 4\ (\mathbf{exp}(-(V_m+60-5.3)/18))$$

$$\beta_h = 1 / (1+\mathbf{exp}(-(V_m+30-12)/10))$$

Delayed rectifier potassium channel - I_{Kdr}

$$\alpha_n = -0.01\ \ (V_m+50-4.3)/(\mathbf{exp}(-(V_m + 50 - 4.3)/10)-1)$$

$$\beta_n = 0.125\ (\mathbf{exp}(-\ (V_m + 60 - 4.3)/80))$$

A-type potassium current - I_A

$$I_A = \overline{g}_A\ a^4\ b\ (V - E_A)$$

$$a_\infty = 1 / (1 + \mathbf{exp}((60- V_m -42)/15));\ \tau_a = 10$$

$$b_\infty = 1 / (1 + \mathbf{exp}(-(V_m+43)/20));\ \ \tau_b = \ 2 * \mathbf{exp}(-\text{pow}((V_m+50),2)/50) + 1.1$$

L-type calcium current - I_{CaL}

$$I_{CaL} = \overline{g}_{CaL}\, a_{CaL}\, (V - E_{CaL})$$

$a_\infty = 1 / (1 + \mathbf{exp}((-V_m + 55)/5))$; $\tau_a = 18 * \mathbf{exp}(-\text{pow}((V_m + 45),2)/625) + 1.5$

Calcium-activated potassium current - I_{SK}

$$I_{SK} = \overline{g}_{SK}\, a_{SK}\, (V - E_{SK})$$

$$a_{SK} = [Ca]_i^{\,4} / [Ca]_i^{\,4} + 0.2^4$$

where $[Ca]_i$ is intracellular calcium concentration governed by the equation

$$d[Ca]_i / dt = (-I_{CaL} / 2Fv) - \beta\, [Ca]_i$$

where F is Faraday constant, v is volume of the soma and β is the time constant of $[Ca]_i$ extrusion.

Background leak - I_L

$$I_L = \overline{g}_L (V - E_L)$$

The above is a description of the model used in both the projects for this thesis. Where there were modifications made to the ion channel currents, this is mentioned in the Methods section of the respective chapters, as also are details of spike train and action potential analyses.

2.2.3 Calibration of *in silico* ion channel currents

We calibrated our model by simulating current approximations to voltage-clamp data obtained from published dopamine neuron literature (Silva, Pechura et al. 1990; Durante, Cardenas et al. 2004; Seutin and Engel 2010) for all of the ion channels included in our model. When recording simulated currents from an individual ion channel type, the maximum conductance of all the remaining channels was set to 0, including leak, so that the current responses represented leak-subtracted values as is normally done in experiments. Voltage clamp protocols were adapted from existing published studies characterising ion channels expressed in midbrain dopamine neurons either in SNc or VTA.

2.3 Results

2.3.1 Spontaneous spike train characteristics and response to simulated pharmacological manipulations

Our stochastic model dopamine neuron fires at a slow spontaneous rate of 3.6 Hz with variability in ISI (Figure 2.6 A (*left*)), that closely resembles some of the average values reported experimentally (3.1 ± 0.9 Hz (Shepard and Bunney 1988), 3.7 ± 0.67 Hz (Brischoux, Chakraborty et al. 2009), 3.43 ± 0.25 Hz (McCutcheon, Conrad et al. 2012), 4.5 ± 1.7 Hz (Grace and Bunney 1984) and within the range 1 – 8 Hz (Grace and Bunney 1983). The CV of ISI is 0.13 (Figure 2.6 A (*right*)), which also falls within ranges reported in experiments for dopamine neurons showing a 'regular' firing pattern for example, 0.01 – 0.02 (Tateno 2010), 0.06 and 0.18 (Wolfart, Neuhoff et al. 2001), 0.13 (Herrik, Christophersen et al. 2010). This also demonstrates that adding stochasticity to sodium and delayed rectifier potassium channels is sufficient to produce a physiologically realistic spike train as compared to the deterministic version of the model that does not give rise to variability in ISI (Figure 2.6 B). Action potentials are broad with a half-maximal width of 2.4ms (2.7 ± 0.5 ms (Grace and Onn 1989); 1.74 ± 0.7 ms to 2.71 ± 0.19 ms (Margolis, Mitchell et al. 2008) and are characterised by a slowly rising depolarisation preceding the action potential followed by a prolonged AHP (Figure 2.6 B). An average action potential obtained from the simulations is compared to those obtained from experiments in Figure 2.6 C.

Slow and regular firing rate and broad action potentials are considered hallmark electrophysiological properties that are used to identify putative dopamine neurons in the midbrain (Sanghera, Trulson et al. 1984; Silva and Bunney 1988; Grace and Onn 1989; Margolis, Lock et al. 2006; Ungless and Grace 2012) and since our model reproduces these features, we can infer that the model captures ion channel dynamics underlying these features of firing. I next wanted to test if my model dopamine neuron responds to simulated pharmacological manipulations in a manner similar

to those seen in experiments in order to further demonstrate that the model is a good representation of an average midbrain dopamine neuron.

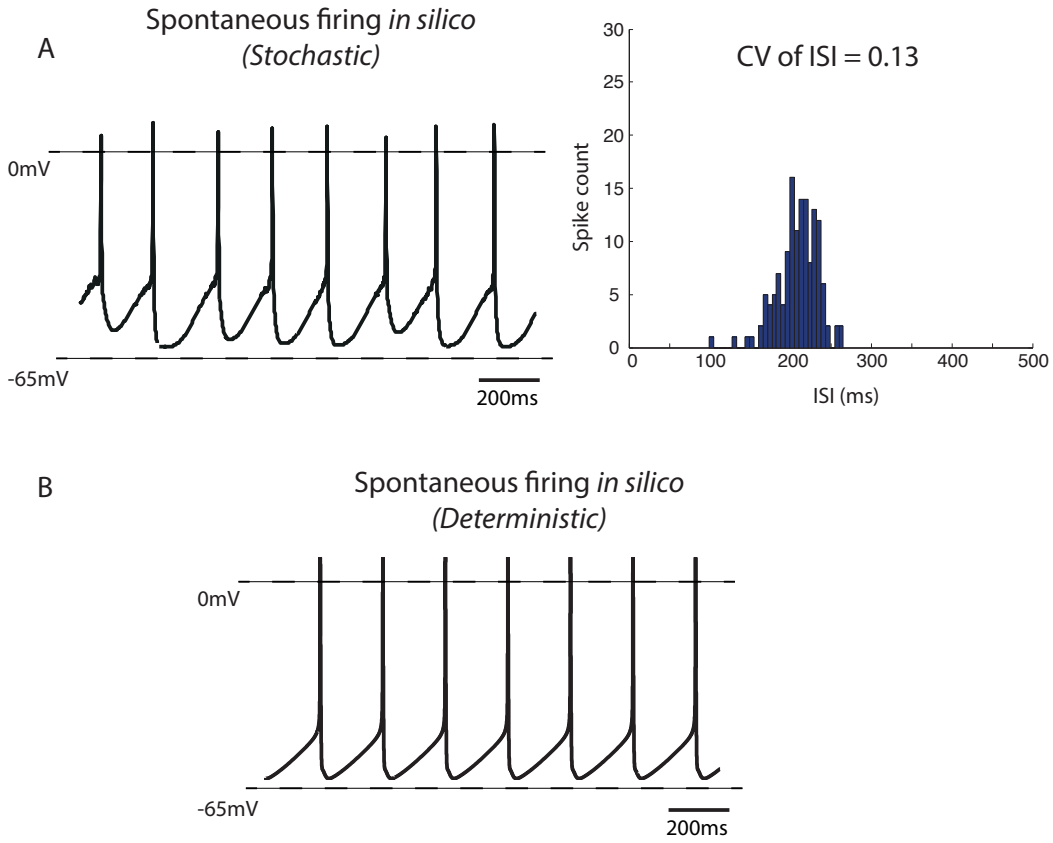

A
Spontaneous firing *in silico*
(Stochastic)
0mV
-65mV
200ms
CV of ISI = 0.13
Spike count
ISI (ms)
B
Spontaneous firing *in silico*
(Deterministic)
0mV
-65mV
200ms
C
Model
Experimental SNc
Experimental VTA
20mV
2ms

Figure 2.6: Spontaneous spike train and action potential characteristics obtained from simulations

A. Spontaneous spike train produced by the stochastic model. The *in silico* dopamine neuron fires at a pacemaker rate of 3.6Hz and CV of ISI equal to 0.13. The spike train is characterised by slow depolarisation leading to the spike, followed by a pronounced AHP. **B**. Spontaneous spike train produced by the deterministic version of the same model demonstrating a lack of variability in ISI. **C.** Average action potential waveforms obtained from the model superimposed with those obtained from the SNc and VTA. (Experimental waveforms adapted from (Ungless and Grace 2012). The average waveforms are alligned at the point of maximum rate of rise.

2.3.2 Ion channel currents regulating the characteristics of spontaneous firing

The A-type potassium channel controls spontaneous firing frequency

A-type potassium channels have been shown to regulate firing frequency by opposing the depolarising current during an ISI in order to delay the subsequent action potential (Connor and Stevens 1971). They are also involved in regulating action potential duration (Zhang and McBain 1995) and latency to first action potential after recovery from membrane hyperpolarisation (Shibata, Nakahira et al. 2000; Koyama and Appel 2006). Midbrain dopamine neurons also express A-type transient potassium currents (Silva, Pechura et al. 1990; Liss, Franz et al. 2001; Koyama and Appel 2006) and have been associated with regulation of pacemaker firing frequency (Liss, Franz et al. 2001; Hahn, Tse et al. 2003). Simulating an inhibition of A-type potassium channels in the model neuron by reducing its maximal conductance by 50% from 4mS/cm^2 to 2mS/cm^2 the firing frequency increased by 1.8-fold from 3.6 Hz (Figure 2.7 A (*left)*) in control to 5.4 Hz (Figure 2.7 B (*left)*). While this is similar to some of the reported values (Kuznetsova, Huertas et al. 2010) it is in contrast to a nearly three-fold increase observed in (Liss, Franz et al. 2001). The increase in firing rate did not affect the firing regularity as seen in Figure 2.7 B (*right)*, compared to control (Figure 2.7 A (*right)*).

4-AP induced inhibition of A-type potassium channels causes a hyperpolarisation in action potential threshold (Grace and Bunney 1983). This could be due to the rapid increase in rate of rise of membrane potential due to lack of any opposing currents. However, we did not observe such a change in spike threshold with a simulated inhibition of this fast potassium channel.

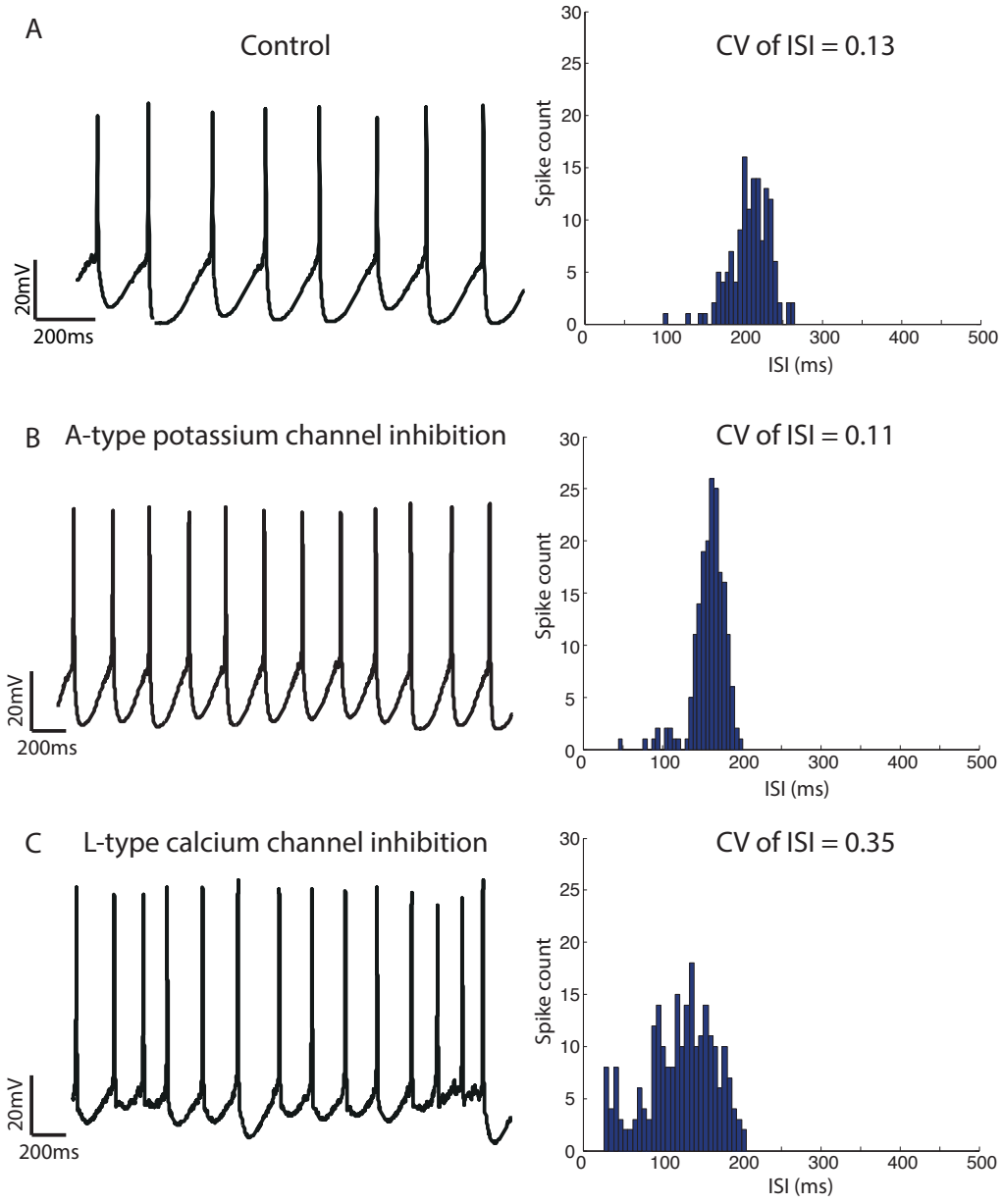

A
Control
CV of ISI = 0.13
Spike count
ISI (ms)
20mV
200ms
B A-type potassium channel inhibition
CV of ISI = 0.11
Spike count
ISI (ms)
20mV
200ms
C L-type calcium channel inhibition
CV of ISI = 0.35
Spike count
ISI (ms)
20mV
200ms
D
Sodium channel inhibition
-45mV
200ms

Figure 2.7: Effects of simulated inhibition of ion channels regulating spontaneous firing in the model dopamine neuron

A. Under control conditions the *in silico* neuron fires spontaneously at a rate of 3.6 Hz (*left*). **B.** When the maximal conductance of A-type potassium channels is reduced by 50% from 4mS/cm^2 to 2mS/cm^2 we observed a 1.8% increase in firing rate. As we can see from the ISI histogram, there was no change in the CV of ISI (*right*), indicating that A-type channels are involved in regulating firing rate and not firing regularity. **C.** When the L-type calcium channel was inhibited by reducing the maximal conductance from 15mS/cm^2 to 5mS/cm^2 there was a marked decrease in firing regularity as can be seen from the spike (*left*) train and the ISI histogram (*right*). The CV of ISI increased from 0.13 to 0.35, which is a similar increase observed during SK channel inhibition. **D.** Simulating a sodium channel block results in cessassion of firing indicating that sodium channels are essential for spike production.

Inhibiting L-type calcium channels decreases firing regularity

Midbrain dopamine neurons especially in the SNc fire single spikes in a regular manner. One of the mechanisms underlying this regular firing is a sub-threshold oscillatory potential, depolarised by L-type calcium channel current and repolarised by SK channel current (Amini, Clark et al. 1999; Drion, Massotte et al. 2011) and blocking L-type calcium channels results in the abolishment of spontaneous firing (Nedergaard, Flatman et al. 1993; Mercuri, Bonci et al. 1994). However, some studies have also shown that such a pacemaker-like firing can continue even in the absence of L-type calcium channel current with co-operation from other ion channel types (Guzman, Sanchez-Padilla et al. 2009; Drion, Massotte et al. 2011) suggesting that L-type channels are not essential for spontaneous firing.

In my model neuron, inhibition of the L-type calcium channel results in a decrease in firing regularity (Figure 2.7 C (*left)*), similar to the decrease in firing regularity observed with inhibition of SK channels. This is because L-type calcium channels are the only source of intracellular calcium used to activate SK channels in our model neuron (Figure 3.4 C). Reducing the maximal conductance of the L-type calcium channel from 15mS/cm^2 to 5mS/cm^2 results in an increase in CV of ISI to 0.35 (Figure 2.7 C (*right)*) from 0.13 in control (Figure 2.7 A (*right)*).

Sodium channel inhibition abolishes spontaneous firing

Sodium channels are essential for spike production in midbrain dopamine neurons (Bunney 2000; Puopolo, Raviola et al. 2007). In agreement with this, our *in slico* neuron stops firing and the membrane potential rests at -45mV when the sodium channel conductance is reduced to zero (Figure 2.7 D) simulating a sodium channel block in TTX (tetrodoxin, a selective sodium channel blocker). While some dopamine neurons especially in the SNc continue to oscillate at a sub-

threshold level after sodium channel inhibition in TTX, not all dopamine neurons exhibit this oscillatory behaviour, especially in the VTA.

2.4 Discussion

My simulation results suggest that the stochastic dopamine neuron model produces electrophysiological features commonly associated with midbrain dopamine neurons and responds well to simulated pharmacological manipulations thereby reinforcing that the model captures underlying ion channel dynamics in accordance with those reported in experiments. The spontaneous firing properties, such as the firing rate and more importantly the firing regularity, associated with the model dopamine neuron, agree well with experimental values suggesting that adding stochasticity to sodium and delayed rectifier potassium channels alone is sufficient to capture the physiological variability present in these neurons.

While majority of the results from the pharmacological manipulations that I simulated agreed well with experimental results and reinforced that the ion channels driving the model were calibrated well, inhibition of the L-type calcium channel conductance produced decreased firing regularity in the model that has not been reported often in experiments, except see (Nedergaard, Flatman et al. 1993). While L-type calcium channels provide the bulk of intracellular calcium in dopamine neurons (Durante, Cardenas et al. 2004), and are associated with SK channel activation (Nedergaard, Flatman et al. 1993), many other types of calcium channels also serve as a source of intracellular calcium (Wolfart and Roeper 2002; Durante, Cardenas et al. 2004) that is used in turn by calcium-dependent SK channels for their activation. Therefore when one type of calcium channel is inhibited there may be other calcium channels that compensate for the loss in intracellular calcium and therefore SK channels would still be activated to provide the hyperpolarisation after a spike to regulate firing precision. For example, T-type calcium channels have also been shown to be functionally coupled to SK channels (Wolfart and Roeper 2002). Because in my model, I only included the L-type calcium channel as the primary source of

intracellular calcium that activates SK channels, it is intuitive to see a decrease in firing regularity with its inhibition.

Having calibrated and tested my model, I next wanted to test and analyse whether and more importantly how SK channel inhibition results in a decrease in firing regularity in midbrain dopamine neurons.

Chapter 3 SK channels control firing precision in midbrain dopamine neurons by regulating the availability of sodium and potassium channels

3.1 Introduction

3.1.1 Calcium-activated potassium channels and their role in dopamine neuron firing

One of the important downstream effects of action potential-mediated calcium influx is activation of calcium-sensitive ion channels, in particular potassium channels (Sah 1992). Two main subtypes based on their molecular and electrophysiological properties have been identified (Sah 1996). The big-conductance (BK) channels have a single channel conductance of 100–200 pS and are both voltage- and calcium-gated and contribute to the repolarisation of the action potential and the initial, fast component of the AHP (fAHP) (Storm 1987; Sah 1996; Faber and Sah 2003). In contrast, small conductance (SK) channels have a unitary conductance of 10-20 pS and are purely activated by an increase in $[Ca^{2+}]_i$ (Sah 1996) and underlie the medium AHP (mAHP). SK channels are selectively blocked by the bee venom apamin (Hugues, Romey et al. 1982). SK channels have been described in many central neurons including midbrain dopamine neurons (Shepard and Bunney 1991; Seutin, Johnson et al. 1993; Ping and Shepard 1996; Tateno 2010), hippocampal pyramidal neurons (Stocker, Krause et al. 1999), cerebellar Pukinje neurons (Womack and Khodakhah 2003), suthalamic nucleus (Hallworth, Wilson et al. 2003), and globus pallidus neurons (Deister, Chan et al. 2009) to name a few.

Midbrain dopamine neurons have a pronounced AHP that is mediated by the SK current and fire in a regular spontaneous manner (Shepard and Bunney 1991; Seutin, Johnson et al. 1993; Ping and Shepard 1996; Tateno 2010). The observation that dopamine neurons in brain slices *in vitro* (in the absence of any synaptic inputs) fire single spikes in a pacemaker like manner (Figure 3.1 A (*left)*) (Silva, Pechura et al. 1990; Hainsworth, Roper et al. 1991) indicates that maintaining firing

regularity is an intrinsic property of these neurons. However in the presence of negative modulators of SK channels like apamin *in vitro,* and *in vivo*, a significant decrease in firing regularity is observed (Figure 3.1 B (*left)*, C), as measured by an increase in CV of ISI (Figure 3.1 A, B (*right)*). This is sometimes accompanied by an increase in burst firing both *in vivo* (Figure 3.1 C (*right)*) and *in vitro,* although often only in the presence of excitatory inputs (Shepard and Bunney 1988; Shepard and Bunney 1991; Gu, Blatz et al. 1992; Nedergaard and Greenfield 1992; Seutin, Johnson et al. 1993; Nedergaard 1999; Waroux, Massotte et al. 2005; Herrik, Christophersen et al. 2010). This is primarily due to a significant decrease in the SK channel mediated AHP (Figure 3.1 D). The fact that VTA dopamine neurons fire more spikes in bursts when compared to SNc dopamine neurons has also been attributed to a lower expression of the SK channel protein in VTA dopamine neurons (Wolfart, Neuhoff et al. 2001) suggesting that SK channels are important for firing regularity.

Although there is experimental evidence that a pharmacological block of SK channels results in a decrease in firing precision in midbrain dopamine neurons (Shepard and Bunney 1988; Ping and Shepard 1996; Waroux, Massotte et al. 2005; Deignan, Lujan et al. 2012), none of these studies predict *how* SK channels might mediate this effect. Understanding the ionic basis of firing regularity is important as decrease in firing regularity, as a result of SK channel hypofunction, has been linked to decreased motor co-ordination in an ataxia mouse model (Walter, Alvina et al. 2006). More importantly, in dopamine neurons in the SNc and the VTA, decreased firing regularity along with the often associated shift in firing pattern from single spiking to burst firing have been observed in rodent models of PD and schizophrenia (Bishop, Chakraborty et al. 2010; Schiemann, Schlaudraff et al. 2012; Krabbe, Duda et al. 2015). In particular, SK channel dysfunction has been observed in a genetic model of PD where by a significant decrease in firing regularity and increase

in burst firing accompanied by a reduction in SK channel mediated AHP, indicating that SK channel function is vital for the healthy firing activity of dopamine neurons (Bishop *et al.* 2010).

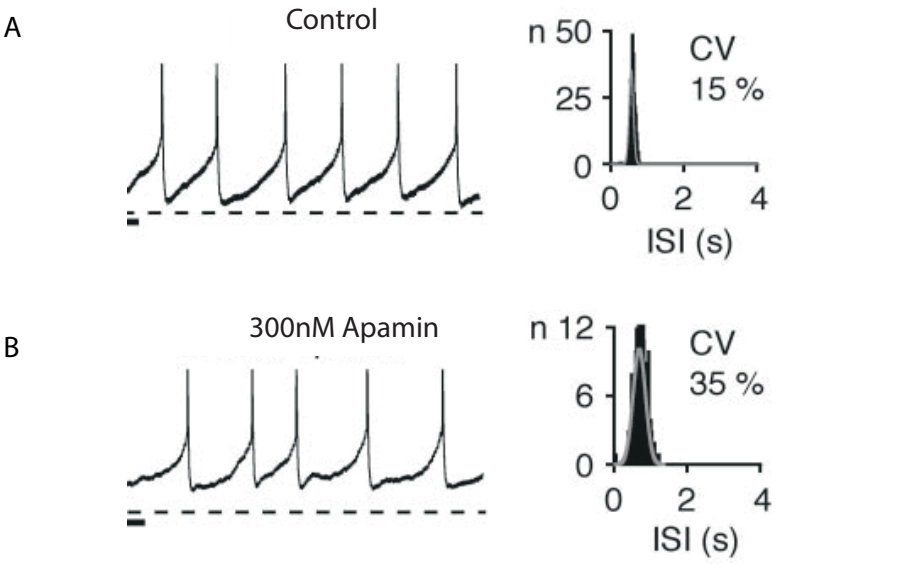

A
Control
n 50
25
0
CV
15 %
0
2
4
ISI (s)
B
300nM Apamin
n 12
6
0
CV
35 %
0
2
4
ISI (s)
C
Control
300nM Apamin
D
Apamin

Figure 3.1: SK channels control firing precision in physiological midbrain dopamine neurons

A. Baseline firing pattern in an example dopamine neuron from the SNc that fires regular action potentials (*left*) with low CV of ISI (*right*). **B.** However the firing regularity is decreased in the presence of apamin (*left*) thus increasing the CV of ISI (*right*). **C.** Sometimes a change in firing pattern from single spike firing to burst firing is also observed when SK channels are inhibited, especially *in vivo*. **D.** These effects of SK channel block are primarily due to the reduction of the AHP that is mediated by the potassium current flowing through SK channels. Figures A, B have been adapted from (Wolfart, Neuhoff et al. 2001) and Figures C, D have been adapted from (Seutin, Johnson et al. 1993).

Many computational and dynamic clamp studies have also indicated that SK channels regulate pacemaker-like firing in deterministic models of dopamine neurons, with special emphasis on their role in repolarising the SOP that is thought to underlie pacemaking and/or to uncover why SK channel block facilitates a transition to burst firing (Li, Bertram et al. 1996; Amini, Clark et al. 1999; Canavier and Landry 2006; Guzman, Sanchez-Padilla et al. 2009; Kuznetsova, Huertas et al. 2010; Tateno 2010; Oster and Gutkin 2011). While one computational study did demonstrate the effect of a decrease in firing regularity with a simulated block of SK channels, this model introduced variability in ISI using a noisy external current injection representative of synaptic inputs (Drion, Massotte et al. 2011). Their model did not account for the intrinsic ion channel noise that we hypothesise is important for firing regularity in dopamine neurons and moreover, studying the underlying mechanisms mediating this effect of SK channel block was not their primary topic of investigation. However another modelling study, using a stochastic leaky conductance, demonstrated that decreased availability of sub-threshold sodium and potassium channels during SK channel inhibition results in a decrease in firing regularity in globus pallidus neurons (Deister, Chan et al. 2009). This seems plausible and could be extended to dopamine neurons as well because the AHP mediated by the SK current provides the hyperpolarised voltage range needed for other voltage-gated ion channels, especially sodium channels to recover from inactivation. Then during the next depolarisation wave, these channels are available for activation and give rise to the next spike. Therefore when the AHP is absent during SK channel inhibition, we hypothesised that due to the stochasticity of ion channels, a variable number of sodium channels would be available for activation thus giving rise to an irregular spike train.

3.1.2 Hypothesis and Aim of the project

The post-spike AHP provided by the current through SK channels standardises the availability of other voltage-gated ion channels such as sodium and potassium channels in order to time each

action potential. With SK channel inhibition, reduced AHP results in a variable amount of sodium channels remaining in the inactivated state, due to ion channel stochasticity, thereby resulting in an irregular spike train.

It is easier to have precise control over individual ion channels and simulate pharmacological effects *in silico* as against experimental settings and therefore our aim was to develop a biophysical *stochastic* model of a dopamine neuron to study the underlying mechanisms of SK channel block. Existing computational models have not been able to demonstrate and/or predict how SK channels might contribute to firing regularity because these models are *deterministic* in nature; i.e. they do not capture the *stochastic* gating of ion channels thereby not being able to simulate the different states an ion channel is capable of existing in. Deterministic models do not produce a physiologically realistic spike train without the addition of an external noisy synaptic input. *Stochastic* models not only produce spike trains with variability in ISI, but also simulate the probabilistic nature of ion channel gating to capture the different states that each ion channel can exist in.

3.2 Methods

To test our hypothesis I have used the hybrid computational model (as described in Chapter 2) of a dopamine neuron with stochasticity in the gating characteristics of sodium and potassium channels in order to evaluate how the SK channel mediated AHP controls the availability of individual ion channels in order to regulate firing regularity.

3.2.1 Data analysis

Customised software was written in MATLAB **(**MATLAB and Statistics Toolbox Release 2012b, The MathWorks, Inc., Natick, Massachusetts, United States**)** for all spike train and action potential related analyses. Spike train histograms and CV of ISI were computed in the presence of SK channel current, ($\overline{g}$ = 5mS/cm^2) and with SK channel inhibition ($\overline{g}$ = 0.5mS/cm^2) in order to study the effects of a simulated block of SK channels. CV of ISI has historically been used as an effective measure of firing regularity (Abbott 2005) and is calculated as the standard deviation (SD) of ISI divided by the mean of ISI. Action potential threshold was measured post-hoc as the voltage at which the third temporal derivative of membrane voltage reaches maximum (Sekerli, Del Negro et al. 2004) (Figure 3.3). This method of threshold calculation is more robust and precise compared to choosing a safe, yet arbitrary, value of membrane voltage that appears to be the threshold upon close visual inspection of spikes and/or phase-plane plots. All statistical analyses were performed on a spike train consisting of 100 consecutive spikes unless mentioned otherwise. Statistics was performed in GraphPad PRISM version 6, GraphPad Software, San Diego California USA, www.graphpad.com. Group means are presented as mean ± SEM and two group comparisons were performed using paired student's t-test with probability level of $p < 0.05$ qualifying as statistically significant.

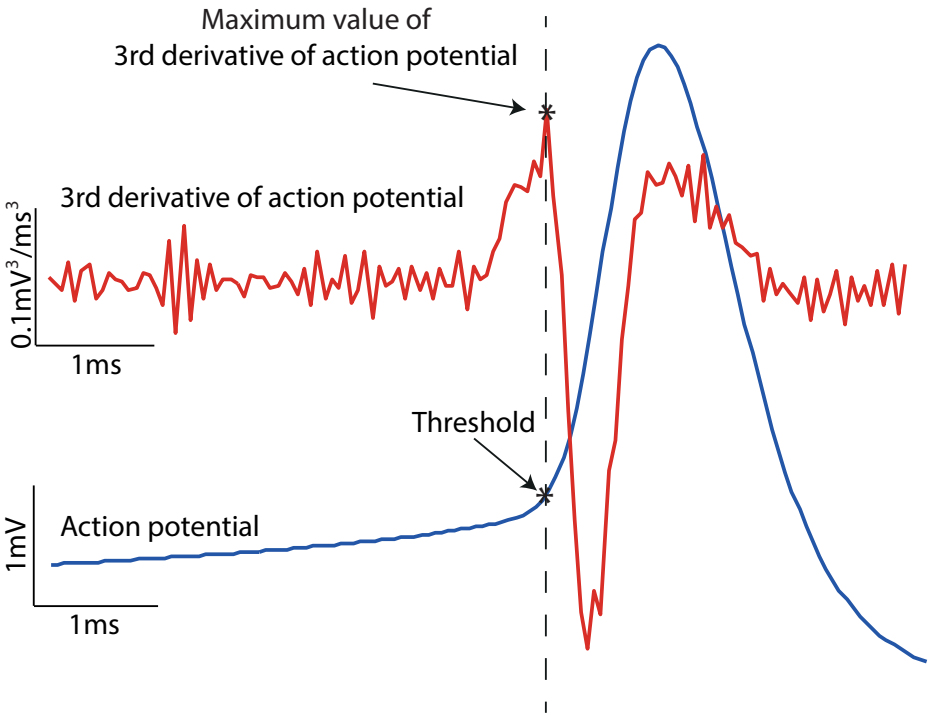


Figure 3.2: Method for calculation of action potential threshold

Action potential threshold is calculated as the voltage corresponding to the maximum value of the third derivative of the membrane potential. This method is more precise and robust compared to an arbitrarily chosen value of dV/dt, voltage corresponding to which is considered as the spike threshold.

3.3 Results

We saw in Chapter 2 that my dopamine neuron model successfully reproduces electrophysiological features common to midbrain dopamine neurons. I next wanted to use this model to test our hypothesis and demonstrate how SK channel inhibition results in a decrease in firing regularity in midbrain dopamine neurons.

3.3.1 A simulated inhibition of SK channels decreases firing regularity and increases firing rate

While the model produces a spontaneous regular spike train (Figure 3.3 A (*left)*), a simulated inhibition of the SK channel (reducing SK conductance from 5mS/cm^2 to 0.5mS/cm^2) results in a significant decrease in firing regularity (Figure 3.3 B *(left)*). Decrease in firing regularity is apparent in the spike train as well as quantified by an increase in the CV of ISI to 0.32 (Figure 3.3 B (*right)*) from 0.13 (Figure 3.3 A (*right)*). This decrease in regularity is accompanied by a significant decrease in the amplitude of the AHP following the spikes (peak AHP: without SK channel inhibition = -60.31 ± 0.03 mV; with SK channel inhibition = -46.36 ± 0.06 mV, $p < 0.05$) (Figure 3.3 C) as compared to control. This result indicates that the AHP provided by the SK current is crucial for maintaining the firing precision in these neurons.

I also observed an increase in the firing rate after a simulated block of SK channels. The firing rate increases by ~36% from 3.6 Hz to 5.6 Hz (Figure 3.3 A, B (*left)*). This is in line with increase in firing rate seen with a pharmacological block of SK channels using apamin in several experiments (Shepard and Bunney 1991; Herrik, Christophersen et al. 2010; Deignan, Lujan et al. 2012). However it is not always the case (Shepard and Bunney 1988; Ji, Hougaard et al. 2009). The discrepancy in firing rate changes observed experimentally could be attributed to a differential expression of SK2 and SK3 subtypes (Deignan, Lujan et al. 2012).

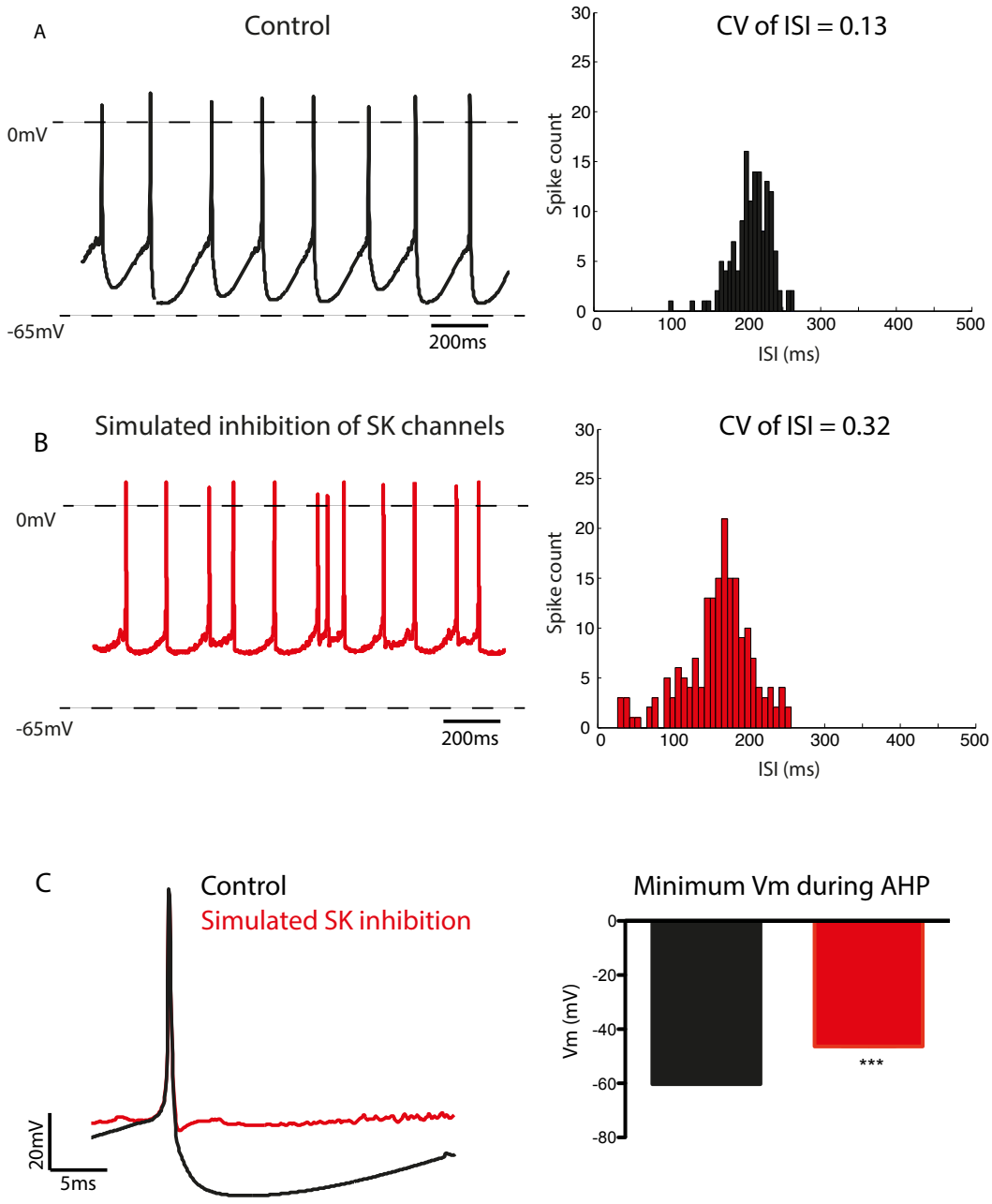


Figure 3.3: Simulated inhibition of SK channels decreases firing regularity and increases firing rate

A. The model dopamine neuron fires spontaneously at a slow and rhythmic rate of 3.6 Hz (*left*) with CV of ISI = 0.13 (*right*). **B.** Simulated SK channel inhibition results in a decrease in the firing regularity (*left*) and the CV of ISI increases to 0.32 (*right*). **C.** This is accompanied by a decrease in the AHP of the action potential (*left*), quantified by a significant decrease in peak AHP (*right*). Error bars represent mean ± S.E.M, not visible due to small range.

It is intuitive that SK channel inhibition would result in an increase in firing rate, as it is the most prominent current during the ISI that prevents depolarisation to next action potential.

3.3.2 SK channels determine action potential threshold and minimise its variability

A plot of membrane voltage against its rate of change (phase-plane plot) is another way of looking at membrane voltage dynamics that can shed light on channel availability and action potential threshold, which may not be easily deciphered from a spike train. I therefore wanted to compare the average phase-plane plot obtained from spontaneous firing with that produced after SK channel inhibition (Figure 3.4 A). Indeed the rate of rise in membrane voltage was also significantly reduced (Figure 3.4 B) with a simulated block of SK channel (maximum rate of rise: without SK channel inhibition = 0.49 ± 0.003 mV/ms; with SK channel inhibition = 0.43 ± 0.004 mV/ms, paired student's t-test, $p < 0.05$), which is a strong indication of reduced availability of sodium channels. This also suggested that if indeed there were reduced sodium channels available during spiking, action potential threshold must also be depolarised. We therefore next analysed action potential threshold.

I observed a depolarisation in the average threshold for action potential generation when SK channel is blocked in our model (Figure 3.5 A, B). The mean action potential threshold depolarises from -45.06 ± 0.08 mV to -43.83 ± 0.08 mV ($p < 0.05$, paired student's t-test). A visual inspection of the thresholds as plotted on individual spikes (Figure 3.5 B) showed spike-to-spike variability and so I wanted to quantify this. The CV of spike threshold increases from 0.06 to 1.8. The effect of apamin on action potential threshold has not been reported in experiments in midbrain dopamine neurons and so this effect is also an important prediction of our model.

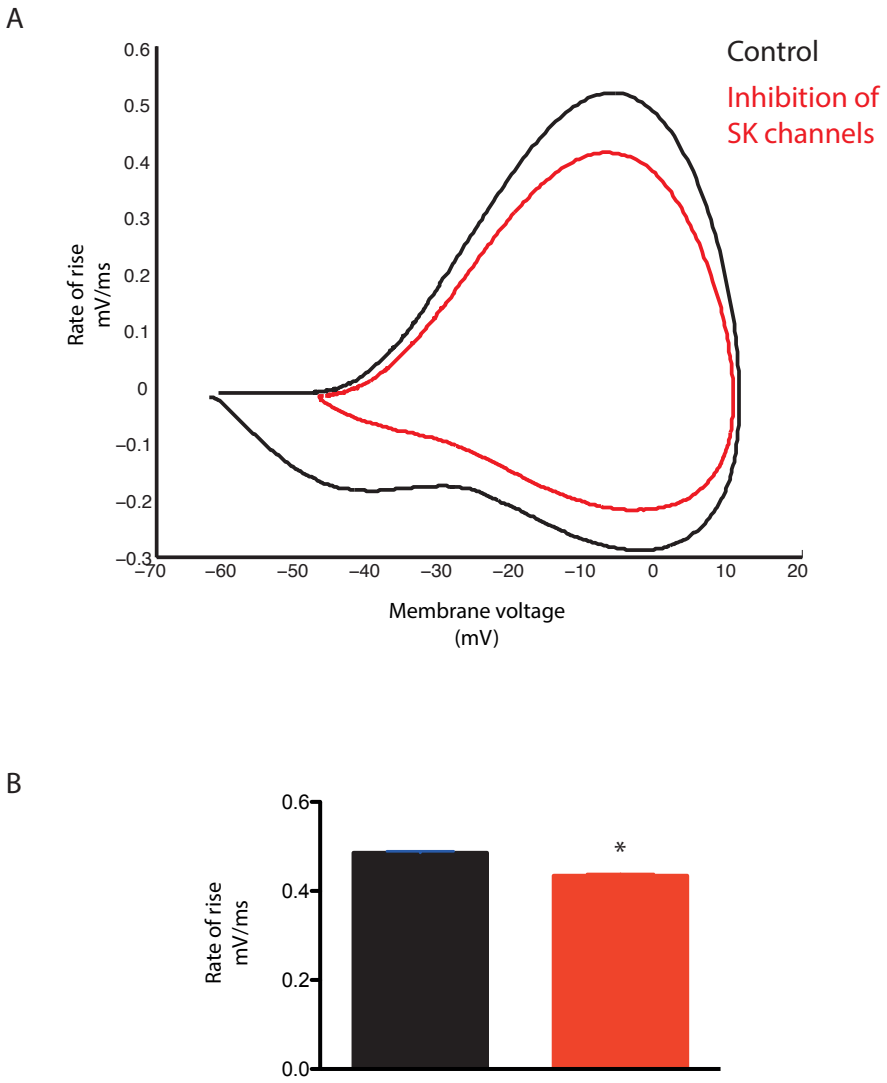


Figure 3.4: SK channel inhibition causes a decrease in rate of change in membrane voltage

A. Phase-plane plot shows a clear reduction in rate of change in membrane voltage during a simulated SK channel inhibition (*red*) compared to control (*black*). **B**. This is quantified by a significant decrease in the maximum value of rate of rise of membrane voltage, which is indicative of sodium channel unavailability. Error bars indicate mean ± S.E.M, not visible due to small range.

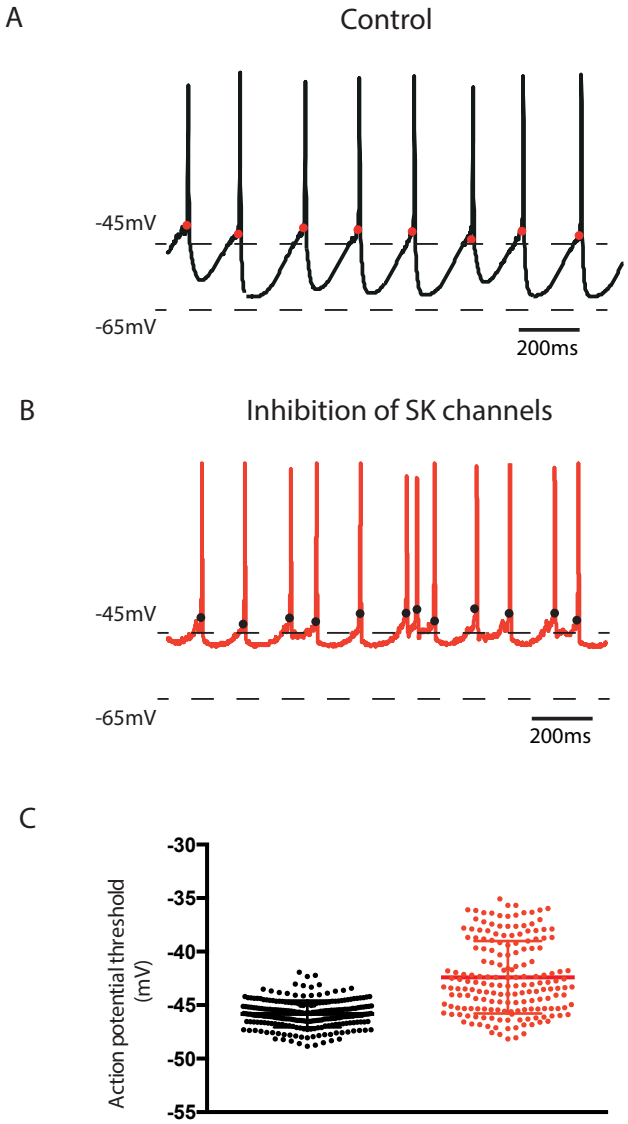


Figure 3.5: Action potential threshold depolarises and becomes more variable with simulated SK channel inhibition

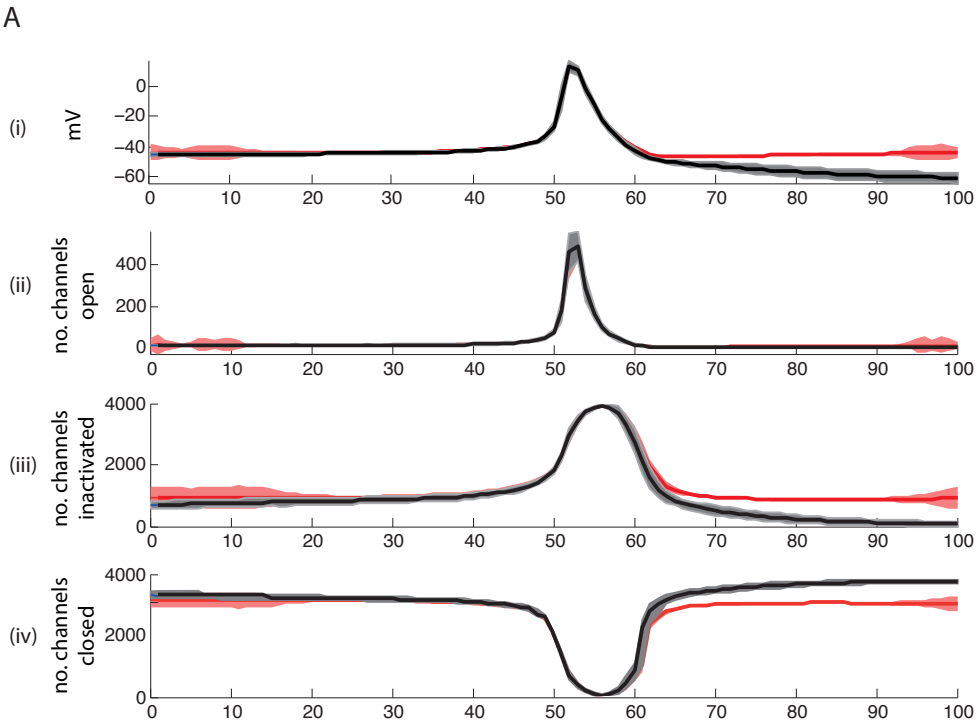
A, B. When SK channels are inhibited in the model, action potential threshold depolarises and becomes more variable (B) compared to control (A). The red and black dots indicate spike threshold. **C.** Quantification of depolarisation in spike threshold as an effect of SK channel block in the model. Error bars represent mean ± S.E.M. The dots are individual threshold values obtained from the spikes.

3.3.3 SK channel inhibition causes insufficient recovery from inactivation of sodium channels

Now that we had an indication of reduced sodium channel availability, we were able to investigate exactly how and why there was such a reduction in sodium channel availability because of the underlying Markov gating scheme used in my model for sodium channels. We therefore looked at the number of sodium channels in each of the open, closed, and inactivated states during the action potential (Figure 3.6 A (*i*)). I found that as the membrane remains hyperpolarised before the spike, a large number of sodium channels remain closed; as the membrane begins to depolarise, a number of sodium channels begin to open to fire the spike (Figure 3.6 A (*ii*), *black, red*). Once the spike begins to repolarise, the number of open channels returns to minimum, thereby increasing the number of channels moving into the inactivated state (*iii*). However, when SK channels are inhibited, the number of channels in the closed state is reduced (*iv*) and more variable in the AHP region as shown by the shaded region due to a large number of them failing to recover from inactivation (*iii*). Moreover, there is increased variability in the number of channels open during the post-spike AHP, during SK channel inhibition, indicating that sometimes there maybe enough sodium channels to open in order to fire a spike while sometimes there may not (Figure 3.6 A (*ii*), *red*). This is primarily because those sodium channels that did not go back to the closed state, failed to recover from inactivation, due to the decreased AHP portion of the spike (Figure 3.6 A (*iii, iv*)). This means that there are fewer channels available to open during the subsequent spikes.

We also found that the total number of open channels during the spike is reduced, and while the amount of reduction is only small, it is still statistically significant (Figure 3.6 B (*left*)). Moreover, the variability in the number of ion channels in the open state is of greater importance because this shows that sometimes there are enough channels open to fire a spike while sometimes this is not the case. This is what is instrumental in giving rise to the irregularity associated with the spike train during SK channel inhibition.

The inactivation variable h in sodium channel dynamics indicates amount of recovery from inactivation – a value of 1 indicating complete recovery. We therefore also looked at the amount of recovery from inactivation for both cases with and without SK channel inhibition at the point of peak AHP. We can see from Figure 3.6 B (*right*) that during SK channel inhibition, recovery from inactivation at peak AHP is significantly reduced compared to control.


A
(i)
mV
0
−20
−40
−60
0 10 20 30 40 50 60 70 80 90 100
(ii)
no. channels open
400
200
0
(iii)
no. channels inactivated
4000
2000
0
(iv)
no. channels closed
4000
2000
0

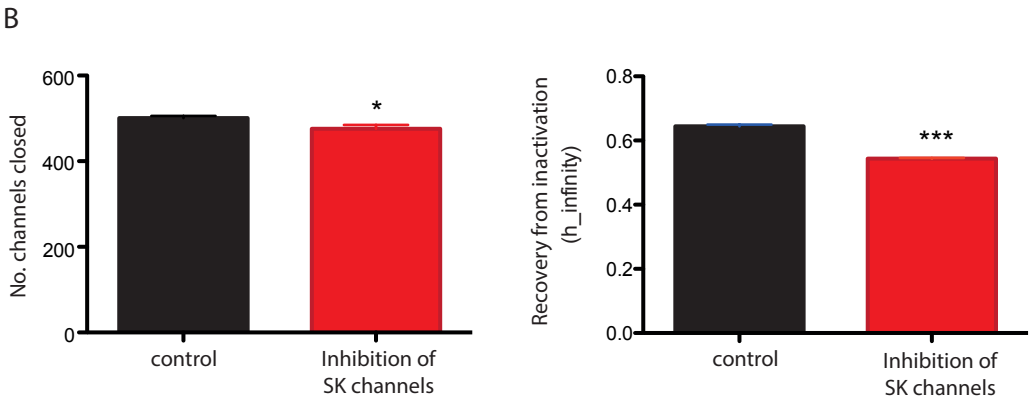

B
No. channels closed
600
400
200
0
*
control
Inhibition of SK channels
Recovery from inactivation (h_infinity)
0.8
0.6
0.4
0.2
0.0
***
control
Inhibition of SK channels

Figure 3.6: Failure of recovery from inactivation of sodium channels underlies decrease in firing regularity with SK channel inhibition

A. Shows the availability of sodium channels (*ii* - *iv*) during the course of the action potential (*i*). The number of sodium channels open increases steadily with depolarisation (*ii*) following the start of the action potential. This is accompanied by a steady increase in the number of inactivated channels (*iii*). While the number of open channels goes back to zero as soon as the action potential has passed, there is a significant difference between the number of channels that remain in the inactivated state (*iii*). As the channels recover from inactivation, they become closed (*iv*); however once again, a large number of channels fail to go to the closed state because they remained inactivated. Shaded region in A represents standard deviation around the mean. **B.** Although we cannot see a reduction in the number of open channels during the peak of the action potential, there is small yet statistically significant reduction in the number of open channels during the spike (*i*). The reduction in recovery from inactivation is explained by the reduction in the *h* parameter of sodium channels inactivation dynamics (*ii*). Error bars represent mean ± S.E.M, sometimes not visible due to extremely small range.

3.3.4 SK channel inhibition causes reduction in A-type sub-threshold potassium current

A-type potassium channels activate at sub-threshold membrane voltages after they have recovered from inactivation during the AHP. Insufficient AHP due to SK channel inhibition must result in insufficient activation of A-type potassium channels, thereby promoting further increase in firing rate observed with SK channel block. In our model, SK channel inhibition results in a significant decrease in A-type potassium channel current (average peak current: without SK channel inhibition = 0.035 ± 0.0004 nA; with SK channel inhibition = 0.031 ± 0.0004 nA; $p < 0.05$, paired student's t-test) that reflects a lack of A-type potassium channel activation (Figure 3.7). This is an important prediction of the model.

Decrease in firing regularity is accompanied by increased firing rate in many experiments with apamin-induced block of SK channels in midbrain dopamine neurons however this has not been related to decreased A-type potassium channel activity. However, (Deister, Chan et al. 2009) do give evidence of reduced availability of A-type potassium channels during SK channel inhibition in their model of globus pallidus neurons that was also related to the increase in firing rate they observed with a simulated SK channel inhibition.

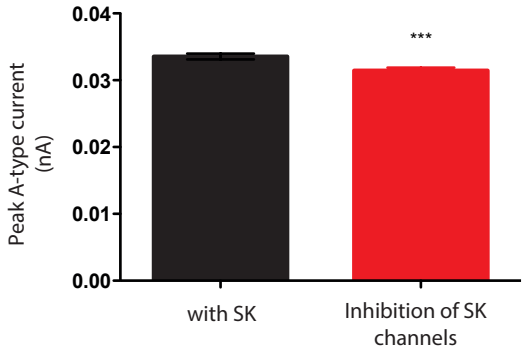


Figure 3.7: Simulated inhibition of SK channels results in a significant decrease in the peak sub-threshold activated A-type potassium current

The peak A-type potassium channel current is significantly reduced when SK channel are blocked in the model. Error bars indicate mean ± S.E.M.

3.4 Discussion

The firing pattern of a neuron is both a result of its intrinsic membrane properties as well as the sum of its synaptic inputs from other neurons (Stemmler and Koch 1999; Koch and Segev 2000). Most midbrain dopamine neurons fire spontaneously in the presence and absence of extrinsic synaptic inputs (Llinas, Greenfield et al. 1984; Grace and Onn 1989; Harris, Webb et al. 1989; Blythe, Wokosin et al. 2009) and dynamically modulate their firing activity by changing their firing rate and pattern in response to stimuli such as rewards (Schultz 1998) and aversive events (Brischoux, Chakraborty et al. 2009). While many experimental studies have demonstrated that SK channels appear to selectively control firing regularity in midbrain dopamine neurons, no hypotheses have been put forth as to *why* or *how* this effect is mediated by SK channels.

Sodium ions are essential for spike generation in midbrain dopamine neurons (Grace and Bunney 1983). As the membrane is depolarised, increasing numbers of sodium channels are activated until enough are available to fire an action potential in an all-or-none manner; once the action potential peaks, sodium channels begin to inactivate (Hille 1992; Abbott 2001). Once inactivated, the neuronal membrane needs to be hyperpolarised to facilitate recovery of these channels from inactivation in order to be available for activation when the next round of depolarisation occurs (Abbott 2001). Potassium currents flowing through calcium-activated potassium channels provide the bulk of the post-spike hyperpolarising drive that helps in recovery from inactivation.

We therefore hypothesised that the AHP mediated by SK channel current provides enough hyperpolarisation to help sodium channels recover from inactivation after the preceding spike such that there are always enough available to activate/open to fire subsequent spikes at regular intervals. Our stochastic model not only produces a spike train with variability in ISI as seen in biological dopamine neurons but also demonstrates the changes in regularity of firing when we simulate an SK

channel inhibition. The reduction in AHP gives rise to irregularity in firing, and also increases the number of action potentials fired, a feature that is commonly observed in experiments, but not always. At the molecular level, it has been demonstrated that two different subtypes of SK channels also present in dopamine neurons – SK2 and SK3 - differentially control the firing rate (SK3) and precision (SK2 and SK3) (Deignan, Lujan et al. 2012). The inconsistent effect of SK channel block on firing rate observed in experiments could depend on the relative and/or co-expression of these two SK channel subtypes in the neurons recorded from.

In our model dopamine neuron, an increase in firing rate is expected because of a reduction in the time to reach action potential threshold as a result of a reduction in the AHP. In addition, the *relative* availability of sub-threshold ion channels is also critical in determining the effect on firing rate after SK channel inhibition as demonstrated in their computational study (Deister, Chan et al. 2009) in globus pallidus neurons where the proportion of open *sub-threshold* sodium and potassium channels determines the firing rate after a simulated SK channel inhibition. Similarly, our simulations also demonstrate a reduction in sub-threshold activated A-type potassium channel, which explains the increase in firing rate, which is an important prediction of our model. While SK channel inhibition resulted in a reduction in A-type potassium current thereby perhaps resulting in an increase in the firing rate of the model neuron, modulation of the A-type potassium conductance can have other important consequences *in vivo,* such as increased excitability in turn making the neuron more susceptible to burst firing. This could support the fact that pharmacological inhibition of SK channels sometimes facilitates burst firing (Shepard and Bunney 1988; Shepard and Bunney 1991).

Another interesting result from our modelling study is that of SK channel's role in regulating and maintaining action potential threshold. SK channels not only maintain variability in firing, but also

seem to minimise variability in spike threshold. This however seems intuitive because if SK channels control availability of spike producing ion channels such as the sodium channels, it is expected to have an effect on spike threshold as sodium channel inactivation alone has been shown to cause variability in spike threshold (Platkiewicz and Brette 2011). Moreover, the depolarisation in threshold due to slowing of membrane dynamics after SK channel block also agrees well with the fact that membrane voltage and spike threshold have an inverse correlation (Henze and Buzsaki 2001). This is referred to as threshold adaptation and has profound effects on the neurons input-output properties such as enhanced coincidence detection (Azouz and Gray 2000), improved feature selection (Wilent and Contreras 2005), and temporal coding (Kuba, Ishii et al. 2006). Therefore our results suggest that SK channels regulate and reduce the variability of spike threshold in midbrain dopamine neurons.

Our results have demonstrated how a single ion channel exerts its influence on a number of other ion channels and regulates the firing properties of the neuron. Our results also illustrate the importance of ion channel noise in dopamine neuron electrophysiology and that channel noise is sufficient to explain *how* SK channels regulate the neurons' firing precision.

Chapter 4 Quantitative analysis of burst waveforms from VTA dopamine neurons

4.1 Introduction

In vivo, dopamine neurons in the SNc and VTA fire bursts of action potentials both spontaneously as well as in response to unexpected rewards (Schultz 1998). Burst firing is associated with large phasic increases in dopamine levels in target regions (Chergui, Suaud-Chagny et al. 1994) that play a major role in orchestrating a variety of behaviours. This is in part due to a non-linear increase in dopamine as a result of saturation of dopamine transporters because of a difference in time scales between release and uptake (Gonon 1988; Chergui, Suaud-Chagny et al. 1994; Prasad and Amara 2001). One of the most widely investigated functions of dopamine neuron burst firing is related to reinforcement learning by encoding reward prediction errors (Glimcher 2011). Abnormal burst firing has been reported in mouse models of schizophrenia (Fabricius, Helboe et al. 2010), and PD (Bishop, Chakraborty et al. 2010; Schiemann, Schlaudraff et al. 2012). Therefore burst firing in dopamine neurons is vital for its role in regulating mental health and that understanding mechanisms controlling burst firing is an important step towards developing treatment modalities for disorders.

4.1.1 Characteristics of burst firing in midbrain dopamine neurons *in vivo*

Bursts are characterised as two or more closely spaced spikes, defined as starting with an ISI of 80 ms or less and terminating with an ISI of greater than 160ms (Grace and Bunney 1984), typically with decreasing amplitude and increasing ISI with intra-burst frequencies reaching up to 50Hz *in vivo* (Tepper, Martin et al. 1995; Paladini, Iribe et al. 1999; Hyland, Reynolds et al. 2002). An ISI histogram for a neuron displaying high levels of burst firing typically consists of two peaks

(whereas for a neuron that fires single spikes is uni-modal); the first peak represents the shorter intra-burst ISIs and the second peak corresponds to longer duration inter-burst ISIs.

While burst firing is generally associated with higher rates of firing in many neuronal types, in dopamine neurons there does not seem to be a correlation between baseline firing rates and bursting (Grace and Bunney 1984). In fact, slowly firing neurons have been shown to fire large number of bursts and vice versa, sometimes, fast firing neurons do not show any bursts (Grace and Bunney 1984). Dopamine neurons fire anywhere between a handful of bursts to more than 70% of their spikes in bursts (Grace and Bunney 1984; Robinson, Smith et al. 2004; Zweifel, Parker et al. 2009). The number of spikes within a burst varies with two-spike bursts (doublets) being more common. On average, there seem to be between 3 and 4 spikes within a burst (Grace and Bunney 1984; Hyland, Reynolds et al. 2002), with a maximum of 22 spikes in a burst in freely moving rats (Hyland, Reynolds et al. 2002). Some of the qualitative observations of *in vivo* intracellular burst waveforms were that bursts ride on a 'depolarising wave', progressively shorten in height and become broader as the burst progressed (Grace and Bunney 1984). Using pharmacological manipulations it was hypothesised that burst firing arises from the calcium-induced inactivation of a potassium conductance due to increased calcium entry into the neuron during a burst and that a burst is terminated by a calcium-dependent potassium current, such as the SK, that is possibly activated by the sustained depolarised wave a burst is superimposed on (Grace and Bunney 1984).

While dopamine neurons fire bursts spontaneously *in vivo*, they do not do so *in vitro*. Somatic current depolarisation does not reliably generate burst firing due to depolarisation block (Grace and Bunney 1983; Richards, Shiroyama et al. 1997; Blythe, Wokosin et al. 2009). Burst firing can however be reliably induced by electrical stimulation of glutamatergic afferents, bath application of NMDA and AMPA receptor agonists, and sometimes SK channel inhibition, though often only in

the presence of NMDA (Ping and Shepard 1996; Johnson and Wu 2004; Kim, Choi et al. 2004). There is also evidence for a preferential role of NMDARs in burst firing (Chergui, Charlety et al. 1993; Christoffersen and Meltzer 1995; Tong, Overton et al. 1996).

Some of the mechanisms that have been postulated for burst firing in dopamine neurons include the coupled oscillator model (Wilson and Callaway 2000), where the dendrites and somatic compartments maintain an intrinsic oscillation driven by the co-ordination of L-type calcium channels and SK channels. When there is no synaptic activation, the neuron fires at the frequency of the larger compartment, the soma, however, synaptic stimulation of the dendrites gives rise to high frequency firing due to amplification of the dendritic firing frequency (Kuznetsov, Kopell et al. 2006). Preferential role for NMDARs has been attributed to its voltage-sensitive magnesium block that allows for hyperpolarising currents to dampen the effects of synaptic depolarisation whereas AMPAR activation does not elicit bursts always due to depolarisation block (Kuznetsov, 2006). A number of potassium channels have been hypothesised to terminate bursts including SK channels (Li, Bertram et al. 1996), M-type channels (Drion, Bonjean et al. 2010), and ERG (Canavier, Oprisan et al. 2007). While most of these studies have been conducted *in vitro*, *in vivo* intracellular data is lacking. Analysis of *in vivo* intracellular membrane voltage dynamics could shed light on mechanisms that drive endogenous bursts and can help elucidate ion channels underlying this mode of firing.

4.1.2 Hypothesis and aim of the project

As mentioned previously, although there have been many studies both experimental and computational that have tried to elucidate mechanisms underlying burst firing, *in vivo* intracellular recordings are lacking. While extracellular recordings are the most commonly used method in neuronal electrophysiology especially *in vivo* and can be sufficient to study firing patterns and

response to stimuli, intracellular waveforms can be valuable for analysing neuronal membrane dynamics that are a reflection of the currents flowing through ion channels in the neuron as we saw in Figure 1.2. We wanted to analyse the *in vivo* whole-cell recordings that were obtained from seven immunohistochemically identified dopamine neurons in the VTA (experiments performed by Frederic Brischoux) in anesthetised rats, in order to provide a comprehensive quantitative description of membrane dynamics during endogenous burst firing and try to relate changes in membrane voltage trajectory to underlying ion channel dynamics.

Aim

I used the following approach to analyse the *in vivo* membrane voltage waveforms during burst firing:

i) Since ion channel currents define membrane voltage trajectory, any differences in action potential waveforms could be related to dynamic changes in the respective ion channel mechanisms that would be driving the respective portion of the action potential. Therefore, as a first step, I compared average membrane voltage waveforms of non-burst single spikes with spikes from within bursts, using simple statistical measures, to look for differences, if any, in action potential features such as height, width, rate of change in membrane voltage, threshold, and AHP.

ii) PCA is a powerful mathematical technique used for feature extraction from high dimensional data. I therefore used PCA, as a complementary technique, of the membrane voltage data to extract features, if any, of spikes within a burst that were different from non-burst single spikes, that could not be deciphered from simple analysis of average waveforms as in (i).

iii) I then used my computational model of dopamine neuron to test whether I could relate results from PCA analysis to ion channels. In order to this, I took advantage of the fact that because the PCs are a linear combination of the underlying variables, reconstructing the membrane voltage waveforms after modifying the PCs will be reflected as changes in the underlying currents. Therefore by reconstructing the spike trains after modifying the important PCs and using those reconstructed waveforms as voltage commands to my model, I would be able to extract ion channel currents that are modified as a result. This is a novel idea and has never been used before in such an analysis in neurophysiology. This technique is detailed in the Methods section.

iv) I next used the model neuron again to run the original spike trains with the endogenous bursts in a spike train clamp protocol and have a direct look at the evolution of ion channel currents underlying single spikes and spikes within a burst.

4.2 Methods

4.2.1 Waveform analysis and spike statistics

In this study, our primary aim was to perform a quantitative analysis of *in vivo* whole-cell bursts recorded from immunohistochemically identified VTA dopamine neurons in anesthetised rats, in order to elucidate differences in membrane and current dynamics, if any, between non-burst single spikes and spikes from within a burst. To this effect and as a first step, customised software was written for the automated detection and analysis of all burst and non-burst waveforms and other parameters associated with spikes in MATLAB (MATLAB and Statistics Toolbox Release 2012b, The MathWorks, Inc., Natick, Massachusetts, United States). Spike trains from all seven neurons were imported into MATLAB using the open-source sigTOOL package (Lidierth 2009). A spike was detected each time the membrane voltage crossed a threshold value of -20mV in the positive direction. Bursts in a spike train were detected using the ISI criterion, in which a burst starts with an ISI < 80ms and ends with ISI > 160ms (Grace and Bunney 1984); i.e. the first two spikes in a burst are temporally coupled to each other with an interval of <80ms between them. As the burst proceeds, spikes within the burst progressively decrease in amplitude and become further apart, finally ending with a large ISI > 180ms (Grace and Bunney 1984). Firing patterns were visualised using ISI histograms that were compiled using all spikes detected in a thirty-second baseline recording for each neuron. Firing regularity was measured as the CV of ISI and was computed as standard deviation of ISI divided by the mean of ISI.

All statistical analyses were performed in GraphPad PRISM version 5, GraphPad Software, San Diego California USA, www.graphpad.com. For comparisons between burst and non-burst waveforms, spikes were separated as belonging to one of three groups – first spike of a burst, last spike of a burst and, non-burst single spike. Group means are presented as mean ± SEM unless stated otherwise. Comparison of group means between two groups were performed using the paired

student's t-test while the means of multiple groups were compared using repeated measures one-way ANOVA followed by the Newman-Keuls test for multiple comparisons.

To analyse and compare membrane voltage dynamics, average membrane voltage and phase plane waveforms (first temporal difference of membrane voltage plotted against membrane voltage), were computed by aligning single spikes at the point of maximum rate of rise. Quantitative measurements were obtained from all spikes within each of the three groups. Action potential height was measured as the absolute maximum value of membrane voltage. Action potential width was measured at half of peak height. Maximum rate of rise and fall of membrane voltage were obtained from maximum and minimum values of its first temporal derivative respectively. To understand changes in AHP, the AHP was divided into three segments. Minimum membrane voltage values at 5ms (corresponding to fast-AHP mediated by the BK current), 25ms and 80ms (corresponding to medium/slow AHP mediated by the SK current) from peak of action potential were obtained. Time to peak (TTP) for AHP was measured as the time elapsed between action potential peak and the minimum trough of the action potential. Action potential threshold was measured as the voltage at which the third temporal derivative of membrane voltage reaches maximum (Sekerli, Del Negro et al. 2004).

As a complementary and novel approach, I also used PCA to extract differences between waveforms present in the above three groups. In general, mathematical analysis of neural waveforms has been mostly applied to identifying and separating spikes belonging to different neuronal populations from multi-unit recordings, referred to as spike sorting. The most common and computationally inexpensive methods that were initially used for this purpose were based on spike amplitude, or spike shape using window discriminators (Rey, 2015), and template matching techniques (Gerstein, 1964; Lewicki, 1998). However these techniques did not prove effective

because spike amplitude and width were not found to be the best predictors of spike shape, thus requiring manual intervention to sort out spikes accurately. More recently, PCA (Lewicki, 1998; Adamos, 2008) and wavelet transforms (Shoham, 2003) have been more successfully used for feature extraction and subsequently spike sorting.

4.2.2 Principal Components Analysis (PCA)

PCA is a mathematical concept that enables meaningful representation and visualisation of high dimensional data in a lower dimensional space (Dunteman 1989). It is a series of steps that first normalises the data and then using algebraic concepts, produces a new representation of the original data in the principal components (PC) space. Each PC represents the data in the direction of maximum variance of the underlying variables. Usually the first few PCs explain greater than 80% - 90% of the variability in a data set. The data is then reconstructed using these first few important PCs rather than all the variables that originally described the data. In other words, a multi-dimensional data (that is difficult to visualise) can now be reduced to a few dimensions that can be visualised in a 2-D or 3-D space. Furthermore, since each of the PCs is a linear combination of all the underlying variables that describe the original data, a loadings plot can be used to visualise how much each of these underlying variables contributes to respective PCs.

While PCA has often been used to cluster spikes from multi-unit recordings (Lewicki 1998), it has not been used to analyse membrane voltage dynamics. Our approach of using PCA as a method to extract features of action potential waveform in terms of differences in epochs of membrane voltage between the different groups of spikes, i.e. non-burst and burst spikes, is a novel data-driven technique for such analysis. Further, because the changes in membrane voltage epochs during a spike reflect changes in ion channel currents, we use PCA as an indirect method to relate changes in spike waveforms to ion channel dynamics, as described in more detail in the following sub-section.

4.2.3 Spike train clamp using PC-reconstructed and raw waveforms

Each PC in our analysis is computed as a linear combination of the underlying membrane voltage values. We therefore hypothesised that the PCs could be inferred as one or more ion channel currents that drive the changes in membrane voltage. In order to test this hypothesis, all the spikes used in PCA were reconstructed after increasing each of the four PCs by a factor of 50%. These reconstructed waveforms were then used as voltage commands in a computational model of a midbrain dopamine neuron (model described in Chapter 2). Peak currents underlying these reconstructed waveforms were compared with the original currents before reconstruction using the standard t-test. The currents that were modified as a result of the PC reconstruction were believed to represent the PC that was increased by 50%. Once again, this method of relating changes in PC loadings to changes in ion channel currents is a novel and interesting technique that can be used in the future to perform waveform analysis to understand ion channel dynamics driving changes in action potential waveforms in any neuronal type.

Furthermore, as a complementary approach to waveform analysis and PCA, we also simulated voltage clamp using the original spike trains in order to study underlying currents that operate during a burst. In other words, we used the raw spike trains from the in vivo recordings as voltage command to the model neuron and analysed how the underlying ion channel currents evolved, especially during burst firing. The clamp was simulated in the same mathematical model mentioned above. As we did for membrane voltage, current spikes were detected for all the ion channels present in the model. Current spikes were separated as first spike of burst, last spike of burst and non-burst single spike. Peak currents were compared across the groups using repeated measures one-way ANOVA followed by post-hoc Newman-Keuls test to correct for multiple comparisons in PRISM.

4.3 Results

I analysed action potential waveforms recorded from seven immuno-histochemically identified VTA dopamine neurons from anesthetised rats, in the whole-cell configuration, in order to compare differences in membrane dynamics between single spikes and spikes during bursts. I used two methods for my analysis – PCA to look at membrane voltage dynamics and burst clamp using my computational dopamine neuron model to study ion channel currents underlying burst firing. PCA based feature extraction helped in identifying epochs of membrane voltage trajectory before, during, and after the action potential that were different between burst spikes and single spikes. Spike train clamp (or burst clamp) using the whole-cell recordings were used as voltage command to my model dopamine neuron to analyse the currents flowing through non-burst single spikes and during bursts in order to uncover the role of ion channels during burst firing in these neurons. However, before performing PCA and clamping experiments, I performed basic statistical analyses on some of the parameters that could be extracted from the intracellular membrane voltage traces.

4.3.1 Spike train and action potential characteristics

A variety of spike train characteristics with varying degrees of bursting and irregularity in firing were observed among the seven neurons that were recorded from. Qualitatively, majority of burst contained two to four spikes and resembled the example shown in Figure 4.1 A. However, sometimes a burst appeared to ride on a depolarised "wave", especially in long-duration bursts as well as in neurons that fired majority of their spikes in bursts (Figure 4.1 B). The neurons fired at an average rate of 4.91 ± 1.89 Hz. They displayed a fairly irregular firing pattern with average CV of ISI of 0.56 ± 0.07. All seven neurons recorded from displayed at least some amount of bursting (Figure 4.2 A), with average percentage of spikes appearing as bursts being 39.11% (Range: 8.2% - 73.73%). Average number of spikes within a burst was 3.97, with majority of the bursts being fired

as doublets (two-spike bursts) *(*Figure 4.2 B). All of these measures were found to be very similar to those reported for extracellular as well as intracellular studies *in vivo* (Grace and Bunney 1984; Chergui, Charlety et al. 1993; Floresco, West et al. 2003; McCutcheon, Conrad et al. 2012), highlighting the fact that the intracellular configuration does not adversely affect the physiology of the neuron.

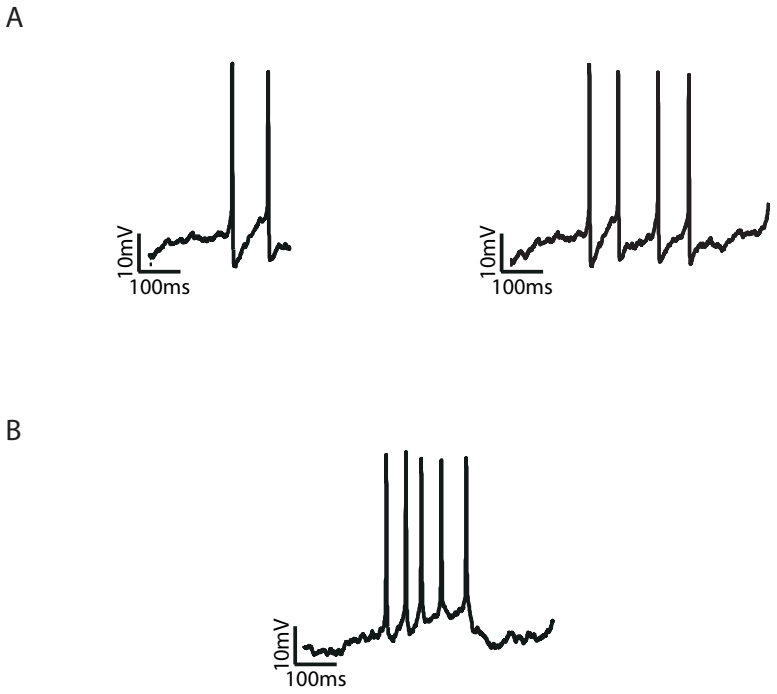


Figure 4.1: Spike train characterisitcs of in vivo whole-cell recordings from dopamine neurons in the VTA

A. Majority of neurons fired bursts consisting of two-four spikes. **B.** Some neurons that fired majority of their spikes in bursts fired bursts that appeared to ride on a "depolarising wave". All bursts appeared to have spikes with increasing ISI and decreasing spike height (A, B).

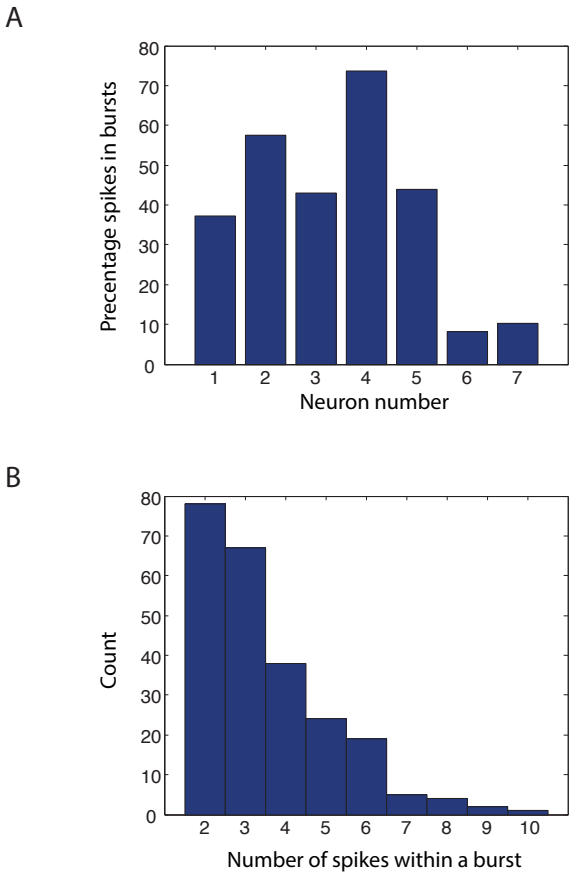


Figure 4.2: Burst statistics

A: All neurons displayed bursting activity with more than 2 neurons firing greater than 30% of their spikes in bursts. **B:** Doublets or two-spike bursts were the most common type of bursts and there were no bursts with more than 10 spikes in them.

We next separated spikes into three groups to analyse differences in membrane voltage dynamics between spikes within a burst and non-burst single spikes – first spikes of bursts, last spikes of bursts and non-burst single spikes and looked at specific action potential features that qualitatively appear to be modified during a burst, namely, spike height, width and threshold and certain additional parameters such as AHP, and rate of change in membrane voltage. Membrane voltage differences between first spikes of bursts and non-burst single spikes could reflect ion channels facilitating burst generation, while differences between last spikes of bursts and non-burst single spikes could reflect ion channels underlying burst termination.

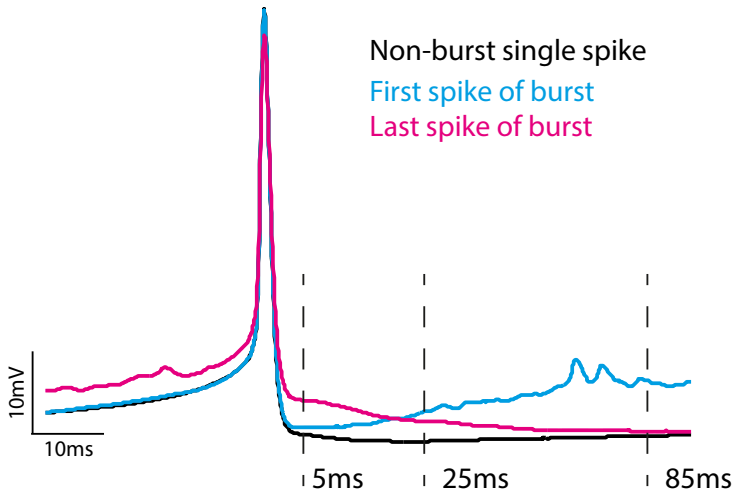
4.3.2 Reduced post-spike AHP is the first detectable change in membrane dynamics during a burst

When we averaged action potential waveforms for non-burst single spikes, first spikes of bursts and last spikes of bursts and superimposed them, we could distinctly observe that there was a marked difference between the averages of these three groups especially in the approach to action potential threshold and in particular the AHP region (Figure 4.3 A). We therefore measured the amplitude of the AHP at three specific time stamps from the peak of action potential – 5ms (fast-AHP), 25ms (medium-AHP) and 85ms (slow-AHP) (Figure 4.3 A). These time stamps also have a physiological interpretation; calcium and voltage activated potassium BK channels are known to be present in many central neurons including midbrain dopamine neurons and are responsible for the repolarisation of the action potential and also contribute to the fast component of the AHP (Faber and Sah 2003) that generally lasts between 3ms to 7ms from action potential upstroke.

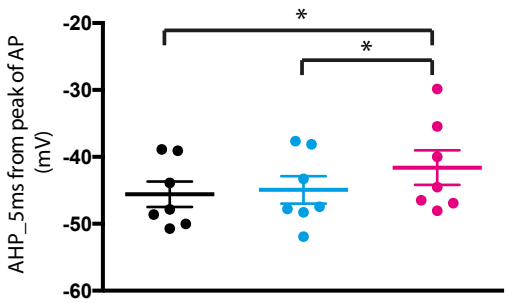
Therefore analysing the AHP at the 5ms position, we could relate any changes in the AHP in this region to BK channel activity. AHP at 25ms from action potential peak represents the AHP mediated by SK channels that are expressed in midbrain dopamine neurons that peak at few tens of

milliseconds from action potential peak (Faber and Sah 2007). We also looked the AHP at 85ms to determine if a prolonged AHP terminates a burst and so we wanted to assess the AHP long after the spike has passed and around the duration in which SK channels would have inactivated (50ms – 100ms).

A


Non-burst single spike
First spike of burst
Last spike of burst
10mV
10ms
5ms
25ms
85ms

B


AHP_5ms from peak of AP (mV)
-20
-30
-40
-50
-60
*
*

C

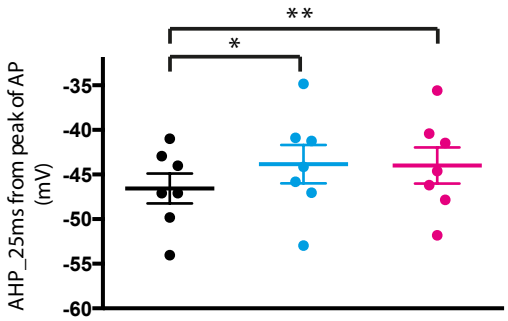

AHP_25ms from peak of AP (mV)
-35
-40
-45
-50
-55
-60
**
*

Figure 4.3: Reduction in endogenous is the first detectable change in membrane dynamics during burst firing

A: A superimposition of the average non-burst single spike (*black*), average first spike of bursts (*cyan*), and the average last spike of bursts (*magenta*) reveals that a reduction in the post-spike AHP is the first detectable change in membrane dynamics during a burst. The average first spike of bursts looks identical to the average non-burst single spike all the way from the beginning up to the end of the repolarisation phase, including the fast AHP. However, after this, the average first spike of bursts does not show the typical AHP but begins to depolarise again to fire the next closely spaced spike. **B**: At 5ms from peak of action potential, which represents the fast AHP mediated by the BK current, there is no difference in the amplitude of AHP between average non-burst single spike and average first spike of bursts, however there is a significant difference between the average first spike and average last spike indicating that the fast AHP perhaps is inactivated during a burst. **C:** At 25ms from action potential peak, the amplitude of AHP is significantly depolarised for the average first and last spikes of bursts compared to average non-burst single spikes, indicating a reduction in the medium AHP mediated by SK channel current. Error bars represent mean ± S.E.M.

I found a significant difference in the peak AHP measured at 5ms from peak of action potential (Figure 4.3 A) between the three average waveforms (one-way repeated measures ANOVA, $p < 0.05$). Post-hoc multiple comparisons using Neuman-Keuls test revealed that the peak AHP was significantly depolarised for the average last spike of bursts compared to both average non-burst single spike and average first spike of bursts (peak AHP at 5ms from peak of action potential; average non-burst single spike = -45.58 ± 1.89 mV; average first spike of bursts = -44.92 ± 2.05 mV; average last spike of bursts = -41.61 ± 2.58 mV) (Figure 4.3 B). This could indicate inactivation of a repolarising current during the course of burst firing. Dopamine neuron action potentials are primarily repolarised by the currents mediated by delayed rectifier potassium channels (Silva, Pechura et al. 1990), but it is possible that BK channels known to be present in dopamine neurons (Su, Song et al. 2010) also contribute. In particular, 5ms from action potential peak represents the fast component of the AHP (fAHP) that is mediated by BK channels in many neuronal types. Reduction in BK currents during burst firing has also been demonstrated in hippocampal pyramidal neurons (Shao, Halvorsrud et al. 1999). Reduction in fAHP could either be a consequence of inhibition by modulators acting during burst firing or simply because of failure of recovery from inactivation due to the fast succession of spikes.

The most striking difference we found was the significant reduction in AHP in the average first spike of a burst (Figure 4.3 A) mediated by the SK current. The AHP measured at 25ms from peak of action potential was significantly different between the average waveforms (one-way repeated measures ANOVA, $p < 0.05$). Post-hoc multiple comparisons using Neuman-Keuls test revealed that the peak AHP for the average first spike of bursts was depolarised by 7% compared to the average non-burst single spike (peak AHP at 25ms from peak of action potential; average first spike of bursts = -42.92 ± 2.25 mV; average non-burst single spike = -46.54 ± 1.64 mV; $p < 0.05$) (Figure 4.3 C). This reduction in SK channel mediated AHP at 25ms from action potential peak appears to

be the first detectable change in membrane dynamics leading up to endogenous bursting in dopamine neurons.

4.3.3 SK channels may not contribute to burst termination in VTA dopamine neurons

It has sometimes been suggested that akin to other neurons such as Purkinje neurons (Swensen and Bean 2003), bursts in dopamine neurons are terminated due to activation of SK channels (Li, Bertram et al. 1996) and are followed by a prolonged AHP. If this were the case, we would find that the AHP for the average last spike of bursts, should be more hyperpolarised compared to the average non-burst single spike. Contrary to this though, we found no significant difference in the AHP at 85ms (since the AHP lasts between 50ms – 100ms) after action potential peak, between the average last spike of bursts and average non-burst single spike (peak AHP at 85ms from action potential peak; average last spike of bursts = -44.64mV ± 1.6mV; average non-burst single spike = -45.67mV ± 1.51mV; $p > 0.05$, paired student's t-test) (Figure 4.3 A; Figure 4.4 A), indicating that perhaps SK channels are not involved in terminating endogenous bursts in dopamine neurons. We also do not find AHP of average last spikes more hyperpolarised than the AHP of non-burst single spikes at any point after the action potential peak. While there seems to be a prolonged period of silence after a burst, as has been suggested (Grace and Bunney 1984) (mean ISI; after non-burst single spike = 188.92 ± 74.34 ms; after a burst = 376.34 ± 53.79 ms; $p > 0.05$, paired student's t-test), this is not statistically significant (Figure 4.4 A).

Moreover, when we use the spike trains as voltage commands in our model neuron, there is a progressive decrease in the peak SK channel current during bursts (Figure 4.4 B). This however could be an anomaly of the model design because SK channels are dependent on incoming calcium ions through sub-threshold activated L-type calcium channels, which is the only source of calcium in our model. Since there seems to be a reduction in AHP during the beginning of a burst, L-type

calcium channels are perhaps unable to activate resulting in a decrease in L-type calcium current leading to subsequent decrease in $[Ca]_i^{2+}$ that in turn results in a corresponding decrease in SK channel current. However, in physiological dopamine neurons, although L-type channels carry the bulk of calcium current (Durante, Cardenas et al. 2004), it is possible that other calcium channels compensate for this reduced L-type calcium channel current.

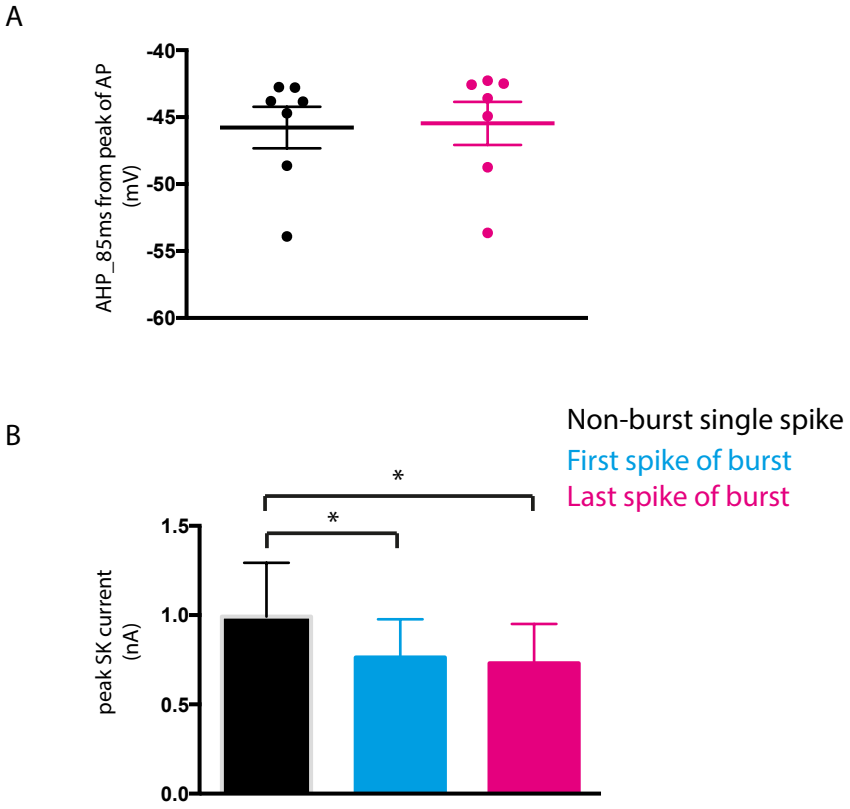


Figure 4.4: VTA dopamine neuron bursts are not terminated by prolonged AHP due to greater SK channel activation

A. At 85ms from action potential peak, there is no significant difference in peak AHP amplitude between the average last spike of bursts and average non-burst single spike suggesting that there is no prolonged SK channel activation that would perhaps terminate the burst. **B.** There is a significant decrease in peak SK channel current during the beginning of a burst as revealed by spike train clamp using my computational model. Error bars represent mean ± S.E.M.

4.3.4 Progressive decrease in recovery from inactivation of sodium channels results in slow membrane dynamics and depolarisation in action potential threshold during burst firing

Sometimes, spikes within a burst appear to ride on a depolarising wave, with each successive spike having a higher threshold for firing (Grace 1988) (Figure 4.5 A, B). We wanted to validate this notion and therefore calculated action potential threshold for non-burst single spikes, first spikes in bursts and last spikes in bursts. Indeed, we found that the action potential threshold is significantly different between the three groups (one-way repeated measures ANOVA, $p < 0.05$). Post-hoc multiple comparisons using Neuman-Keuls test revealed that the action potential threshold was significantly depolarised for average the last spike of bursts compared to both non-burst single spikes and first spikes of bursts (mean action potential threshold; average last spike of bursts = -36.42mV ± 1.74mV; average non-burst single spikes = -38.84mV ± 1.55mV; average first spike of bursts -38.23mV ± 1.74mV; $p < 0.05$) (Figure 4.5 C). We hypothesised that this depolarisation in action potential threshold was due to a progressive decrease in rate of change of membrane potential as result of failure of recovery from inactivation of sodium channels.

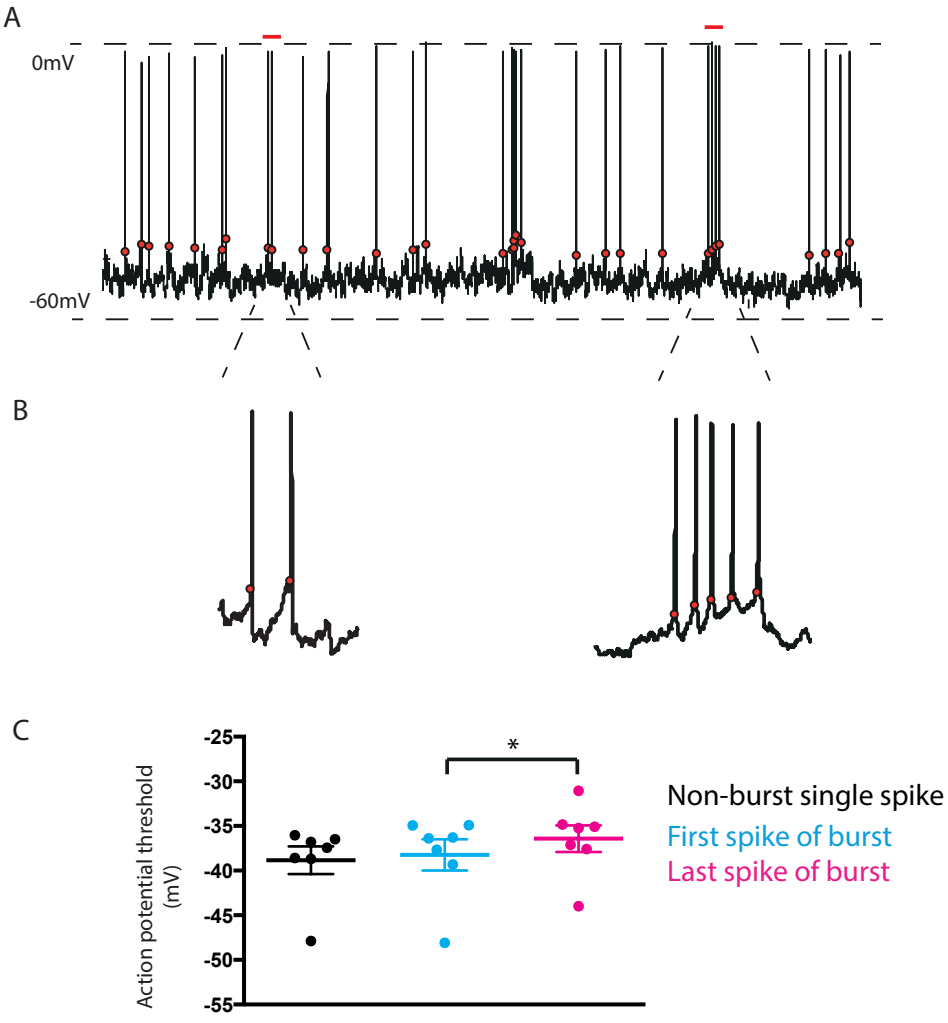


Figure 4.5: Action potential threshold progressively depolarises during burst firing in VTA dopamine neurons

A. Example of a spike train with bursts where we can see a progressive increase in spike threshold (indicated by red circles) during bursts. **B.** The burst with the horizontal bar in A is expanded on the time scale to highlight the progressive depolarisation in spike threshold, that has been quantified in **C.** Error bars indicate mean ± S.E.M.

When we plotted the membrane voltage against its rate of rise (phase-plane plots), it was evident that the average last spike of bursts was significantly slower than the average first spike of bursts (Figure 4.6 A). Slowing of membrane voltage is indicative of reduced availability of sodium channels since maximum rate of rise (dV/dt) of membrane voltage is proportional to sodium channel availability (Mann 1997). Maximum dV/dt was reduced from 3.48 ± 0.22 mV/ms in average first spikes to 2.98 ± 0.24 mV/ms in average last spike of bursts (paired student's t-test, $p < 0.05$) (Figure 4.6 B). We next used our model to test if it was failure of recovery from inactivation of sodium channels during bursts that was underlying the reduction in rate of change in membrane voltage and the resulting depolarisation in action potential threshold. We found that there was a progressive decrease in recovery from inactivation during a burst as illustrated by Figure 4.7; this is dealt with in more detail in section 4.3.5. This also correlates well with what we observed with SK channel inhibition in the previous chapter.

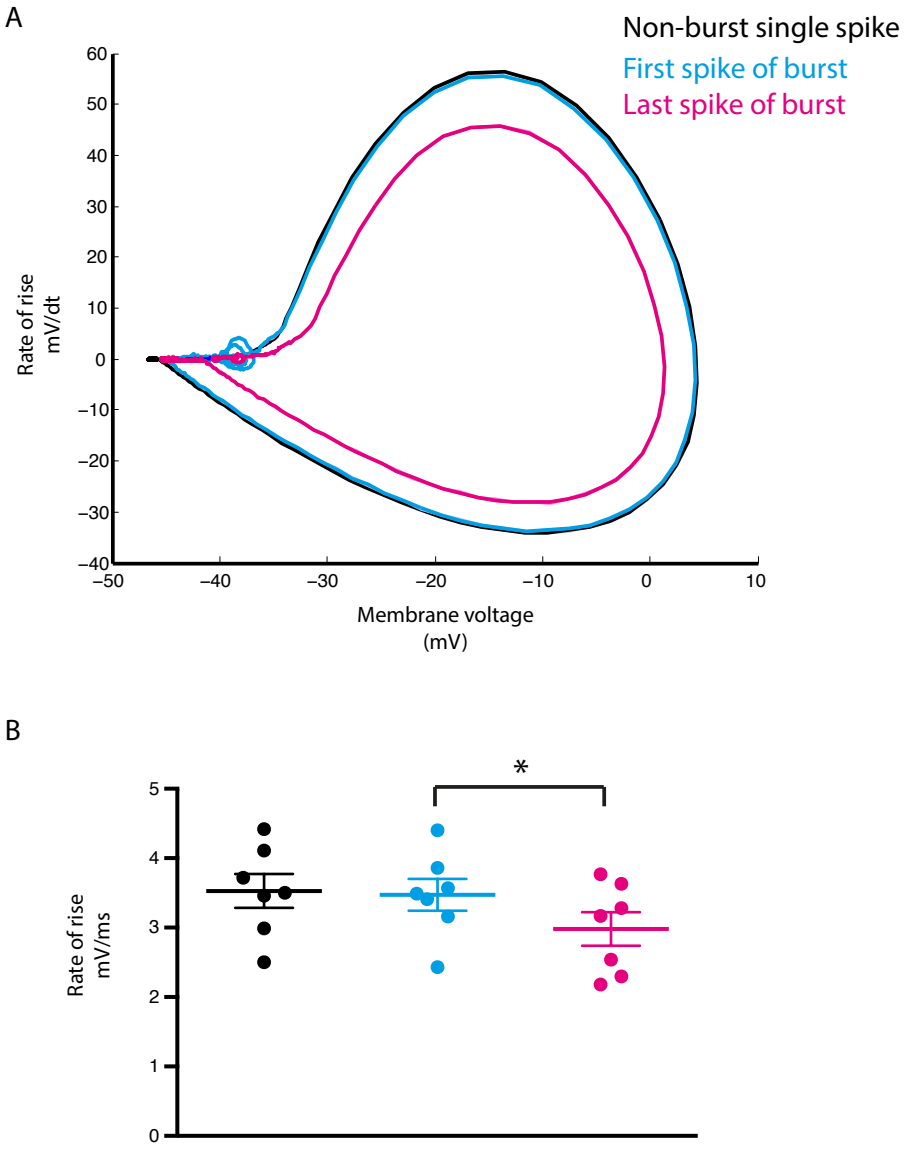


Figure 4.6: Rate of rise in membrane voltage is reduced during burst firing in dopamine neurons

A: Phase-plane plot of membrane voltage against rate of change of membrane voltage shows that there is no difference in the rate of change of membrane voltage between the average first spike of bursts (blue) and average non-burst single spikes (black); however the rate of change in membrane voltage slows during bursts such that the average last spike of bursts (magenta) appears to have much slower kinetics compared to the other two groups. **B:** This is quantified by a significant reduction in maximum rate of change in membrane voltage suggesting reduced availability of sodium channels. Error bars indicate mean ± S.E.M.

4.3.5 Sodium channel inactivation underlies burst termination

The above results suggest that there is a progressive increase in sodium channel inactivation during burst firing, resulting in depolarisation of spike threshold and slowing of membrane dynamics. I therefore used my stochastic model to look at sodium channel inactivation during burst firing. I used the concept of voltage clamp to run the raw *in vivo* spike trains as command voltage to my model dopamine neuron and looked at the progression of sodium channel states during burst firing. As we can see for the example burst in Figure 4.7 A, as the burst progresses, the number of open sodium channels progressively decreases (Figure 4.7 B) and the number of sodium channels inactivated increases (Figure 4.7 C). This gives direct evidence of reduction in sodium channel availability that perhaps facilitates burst termination.

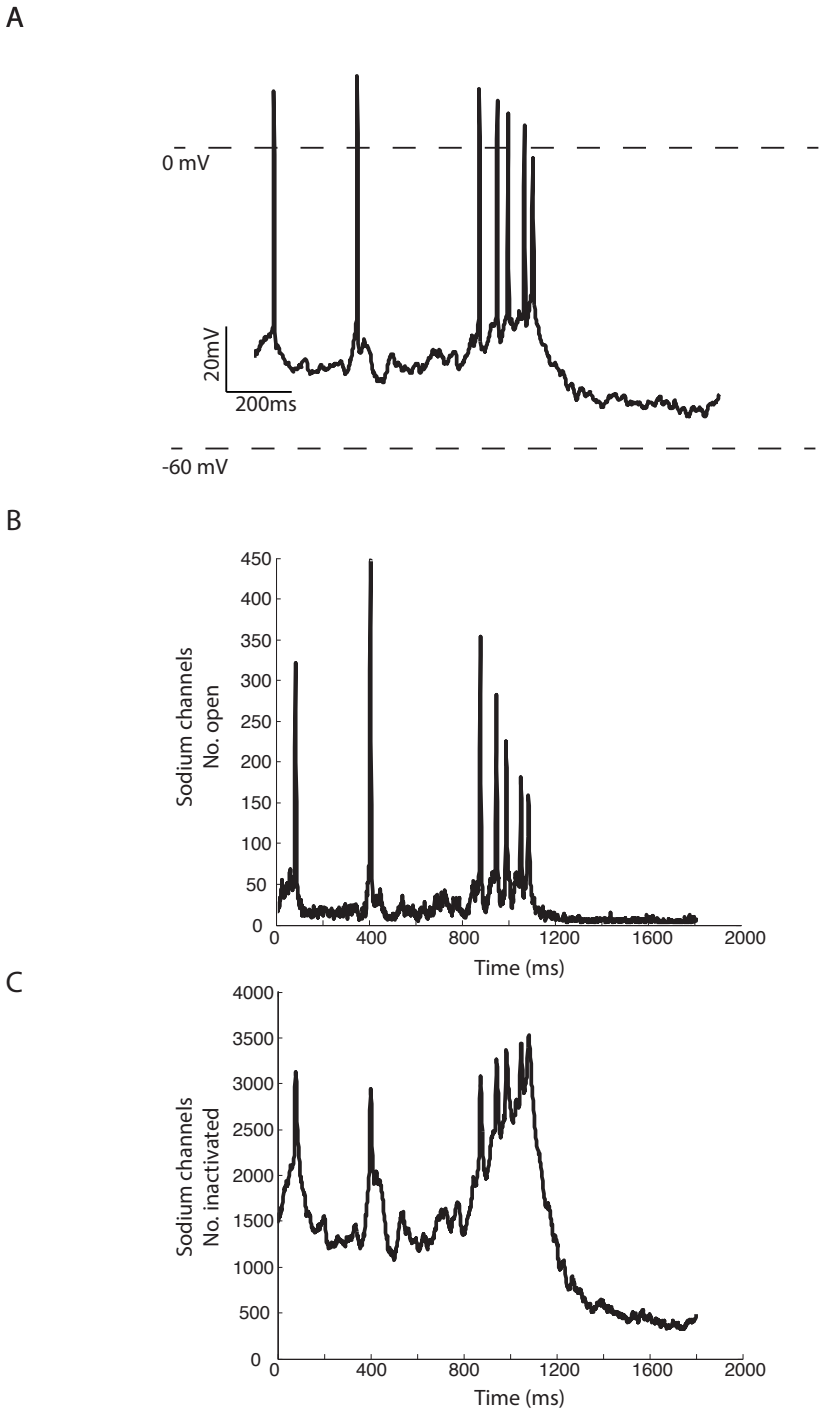


Figure 4.7: Progressive inactivation of sodium channels during a burst

A: An example burst that shows a progressive decrease in spike height and depolarisation in spike threshold. **B:** This decrease in height and depolarisation in spike threshold is perhaps due to the reduction in the number of sodium channels open. **C:** This is due to an increase in the number of sodium channels that remain in the inactivated state.

4.3.6 Other changes in action potential characteristics during burst firing

Action potential width during burst firing

Bursts are typically defined as a series of spikes of decreasing amplitude and increasing width (Grace and Bunney 1984). Action potential width was calculated at half of peak height. While on average, action potential width increased by 14.11% between the average first spike of bursts and the average last spike of bursts (mean action potential width: first spikes of bursts = 1.63 ± 0.09 ms; last spikes of bursts = 1.86 ± 0.19 ms, paired student's t-test, n.s), this did not reach statistical significance across all neurons (Figure 4.8 A, B). However, four out of seven neurons did show a significant increase in action potential width for last spikes of bursts compared to first spikes of bursts (unpaired student's t-test for individual neurons, $p < 0.05$).

Action potential height

Bursts are also described as consisting of spikes of decreasing amplitude. Indeed, average last spike of bursts is significantly shorter than average first spike in bursts (mean action potential height: first spikes of bursts = 5.17 ± 2.47 mV; last spikes of bursts = 3.32 ± 1.98 mV, $p < 0.05$; paired student's t-test) (Figure 4.8 A, C). Such a decrease in spike height can be attributed to reduced sodium channel availability as a result of sustained depolarisation during the burst resulting in sodium channels being unable to recover from inactivation.

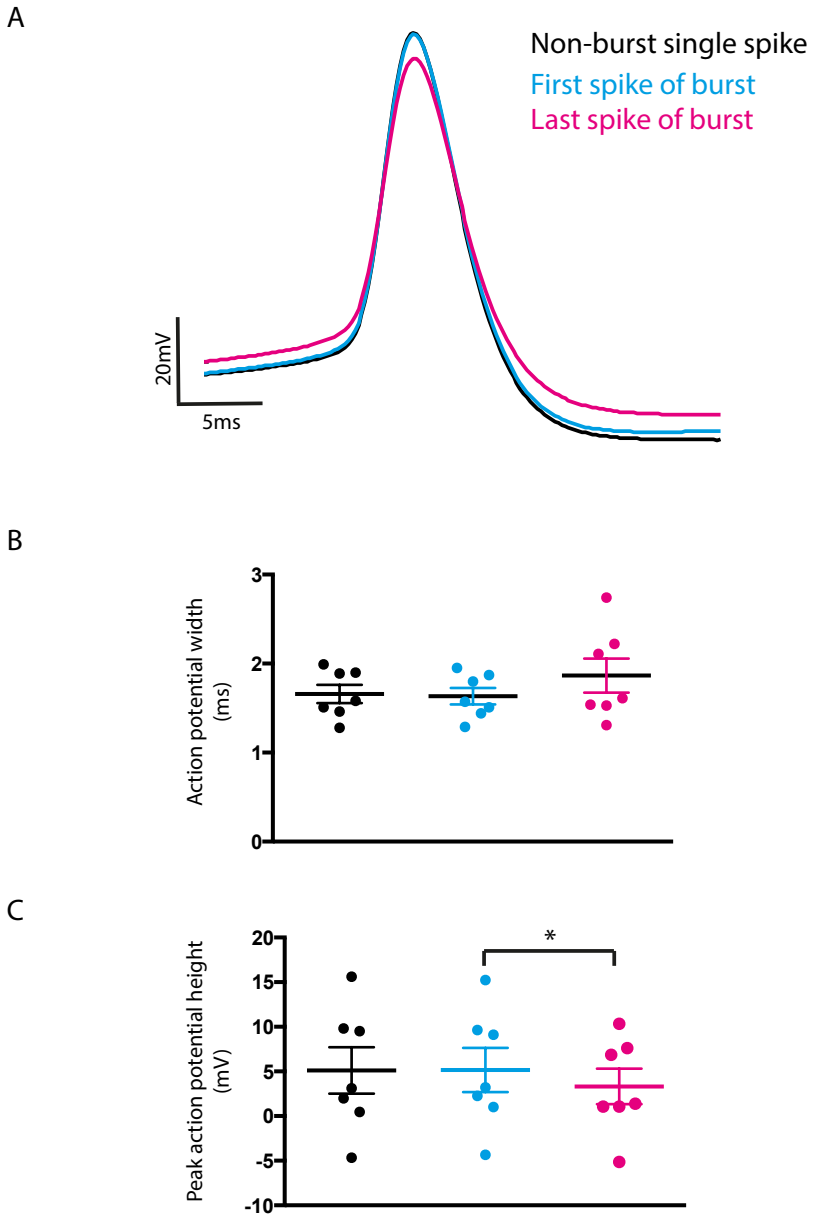


Figure 4.8: Action potential height and width are significantly reduced during burst firing in VTA dopamine neurons

A. Average action potential waveforms of non-burst single spikes (black), first spikes of bursts (blue), and last spikes of bursts (magenta) aligned at the point of maximum rate of rise. **B.** Decrease in action potential height for average last spike of bursts is evident in A and statistically significant while the increase in spike width although significant for five out of seven neurons, is not significant across the population. Error bars represent mean ± S.E.M.

4.3.7 PCA of action potential waveforms, as a novel method for studying neuronal membrane dynamics, identifies key ion channels implicated in burst firing

Neural action potentials are characterised by a large number of membrane voltage values depending on the sampling rate and so a single spike can be considered as a multi-dimensional signal, where each membrane voltage value is one dimension. PCA extracts, from these waveforms, few dimensions that account for maximum variability across all spikes or in other words, those features that can be used to differentiate groups of spikes that maybe present in the spike trains. In our case, the data consists of *in vivo* whole cell recordings of action potentials from dopamine neurons in the VTA of the midbrain. For using PCA to analyse this data set, we consider each spike as a 300 dimensional signal, where each dimension is the membrane voltage value at each time point over 180ms. However it is impossible to visualise this 300-dimension space. For example, if the spike was only characterised by two or three membrane voltage values (V1, V2) (Figure 4.9 A), then we could use a simple scatter plot (V1 vs V2) to see the relationship between all the spikes based on these two variables but this becomes difficult when there are hundreds of variables (Figure 4.9 B). Using the first few PCs, however, we can re-represent the data in two or three dimensions and see the relationships between spikes. Each spike in the data set has a PC score that places it in the PC space (Figure 4.9 C). Once again, spikes were detected as described above and separated into non-burst single spikes, first spikes of a burst and last spikes of the bursts. These spikes were aligned at the point of maximum rate of rise in membrane potential and PCA was performed on all these spikes.

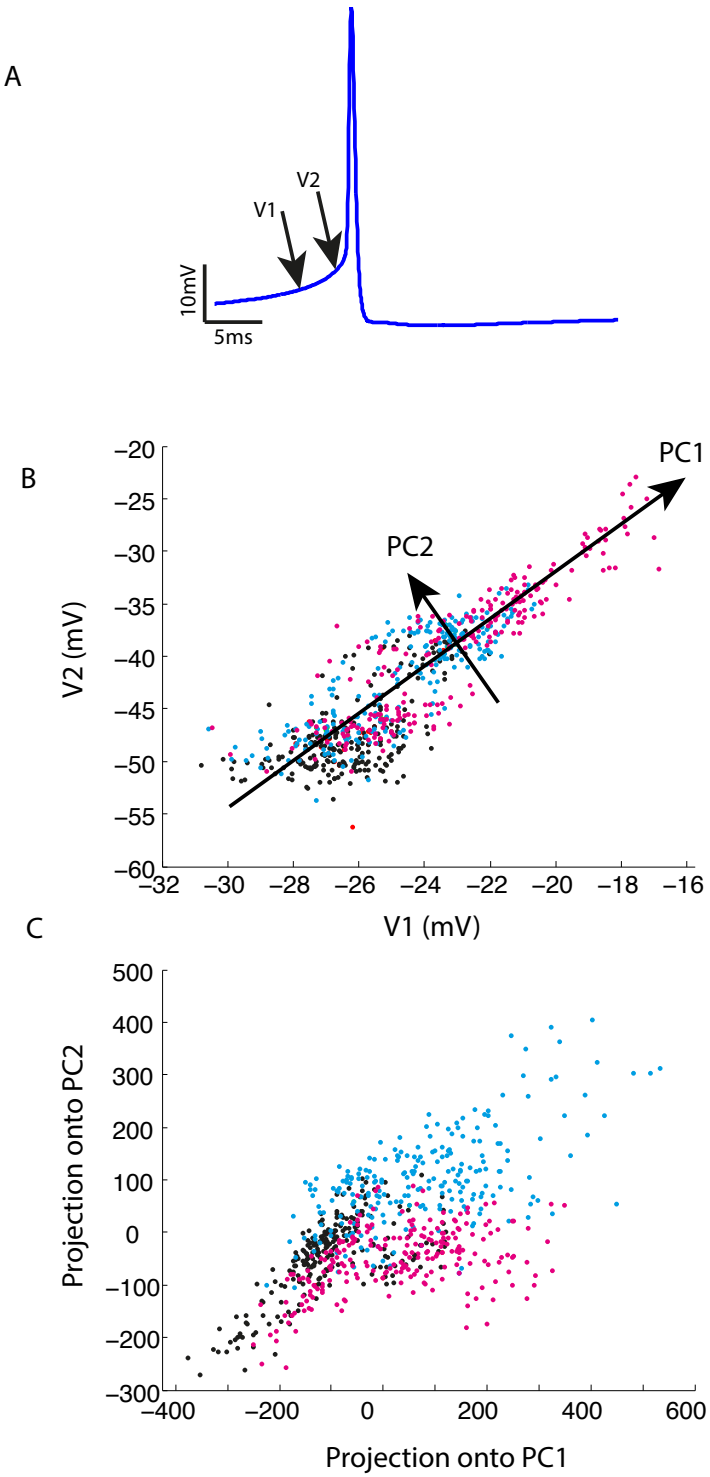

A
V2
V1
10mV
5ms
B
PC1
PC2
V2 (mV)
V1 (mV)
C
Projection onto PC2
Projection onto PC1

Figure 4.9: Schematic explanation for PCA

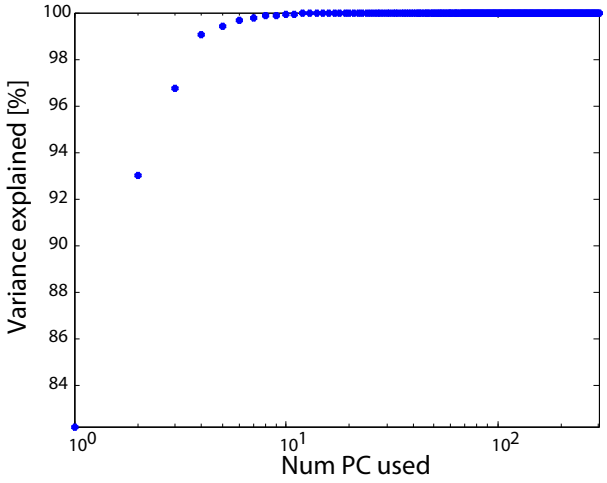
A: An example action potential where V1 and V2 are two values of membrane voltage. **B:** Scatter plot of V1 against V2, where each spot is a spike from the VTA data, colour coded according to whether a spike is a non-burst single spike (black), first spike of burst (cyan) or last spike of a burst (magenta). It is easy to see the relationship between two such membrane voltage values, however it will be difficult to visualise the relationship between 300 membrane voltage values. **C:** All the spikes are now plotted as a linear combination of all the 300 variables using just the first two PCs that account for maximum variance in the data.

We used PCA as a novel complementary approach to look for any other changes in membrane dynamics during burst firing that we may have missed using the simple methods described in the previous analyses. We expected that the first few PCs would explain the variance between spikes within a burst and non-burst single spikes based on differences in epochs of membrane voltage that could be ultimately related to specific ion channel currents. The scree plot shows the percentage variance explained by each of the PCs (Figure 4.10 A). For our analysis we can see that the first four PCs account for nearly 100% of the variability in the spikes. We therefore used these four PCs for all further analyses.

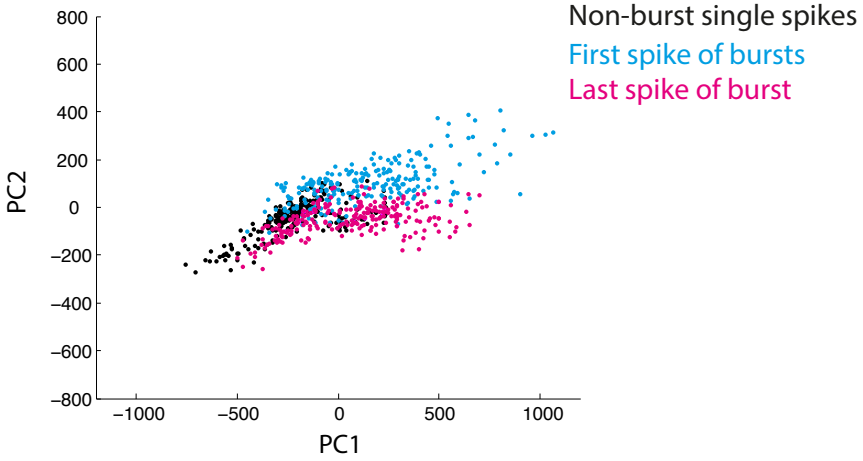
PC scores – do similar spikes group together?

Looking at the scores plot (Figure 4.10 B), which is a plot of the reconstructed data set projected in the PC-space, using the first two PCs in our analysis, we can see that non-burst single spikes (black), first spike of bursts (blue) and last spikes of bursts (magenta) seem to form overlapping yet separable groups. However, since all these groups overlap with each other, we also looked at the mean PC scores for each PC and see how each of these groups are in relation to one another. We visualised this using a spider plot (Figure 4.10 C). This plot helps in visualising multi-dimensional data using multiple axes and so can compare how each group's mean PC score sits on each PC axis. From the above spider plots we can clearly see a separation of means of PC scores on all four PCs between the groups of spikes. For example, PC1 separates non-burst single spikes from spikes within a burst, PC2 captures the variance between first spikes of bursts compared to both non-burst single spikes and last spikes of bursts, and finally PC3 and PC4 separate last spikes of bursts from both non-burst single spikes and first spikes of bursts. We now looked at which of the underlying variables contribute more to the PCs. This would tell us which part of the action potential is responsible for the separation that is observed between the groups based on the PCs.

A


Variance explained [%]
100
98
96
94
92
90
88
86
84
10^0
10^1
10^2
Num PC used

B


Non-burst single spikes
First spike of bursts
Last spike of burst
PC2
800
600
400
200
0
−200
−400
−600
−800
−1000
−500
0
500
1000
PC1

C

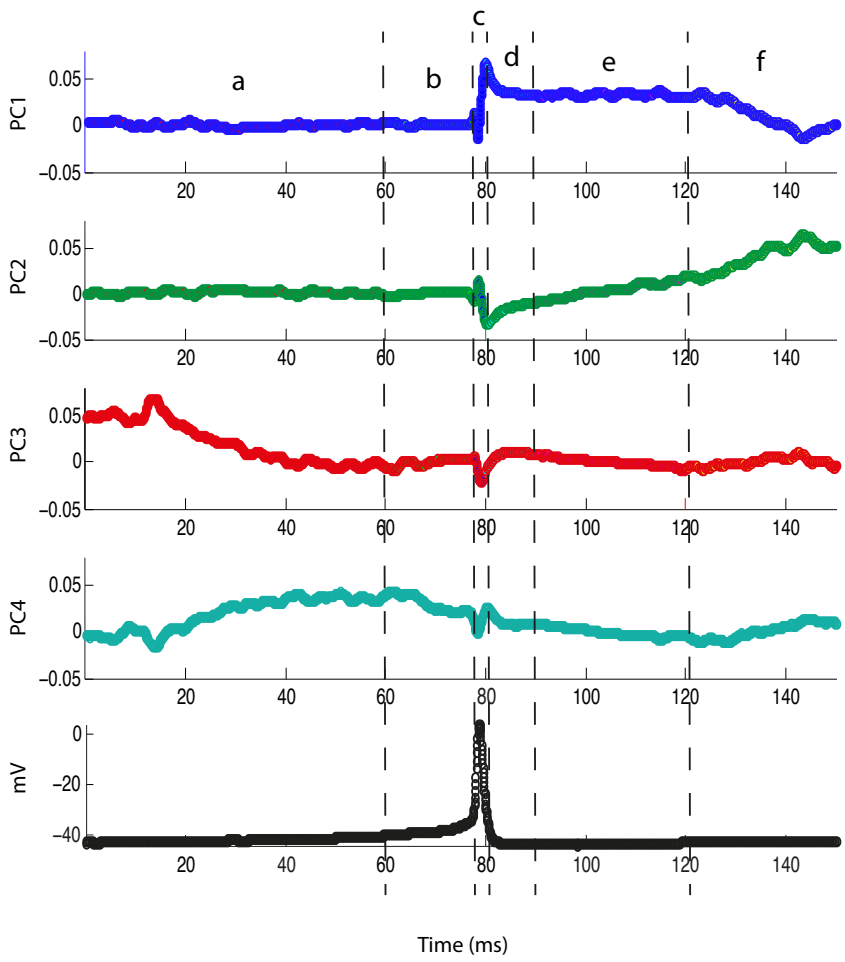

PC 4
PC 3
PC 1
PC 2

Figure 4.10: Principal components analysis of burst and non-burst waveforms

A. Scree plot shows the percentage of variance explained by each of the PCs; in our case, the first four PCs (blue dots) explain nearly 99% of the variance present across the spikes in our analysis. **B.** Scores plot shows how the first two PCs are able to separate the spikes into three overlapping yet distinct groups belonging to non-burst single spikes (black), first spikes of bursts (cyan), and last spikes of bursts (magenta). **C.** Spider plot shows mean values of PC1 – PC4 for the three groups of spikes following the same colour coding as in B.

PC loadings – which variables contribute most to the variability and what is the relationship between the variables?

In our case, there are 300 variables or membrane voltage values and so each PC has 300 values both in the negative and positive directions. A high value of a variable in either direction would indicate greater contribution of that variable to the PC. This is visualised using the loadings plot in Figure 4.11. We can see from the loadings plot, that PC1 has larger values around the peak as well as the AHP region of the action potential. Because PC1 separates non-burst single spikes from first and last spikes of bursts, we can infer that this separation is based on differences in action potential peak and AHP. This also agrees well with our previous analysis that last spikes of bursts are significantly shorter in peak height and differ in AHP properties. Similarly, PC2 separates first spikes of bursts due to the contribution of the slow hyperpolarisation region of the action potential. PC3 seems to represent the increased activity before the last spikes of bursts and PC4 captures the variance in spike threshold, thus separating last spikes of bursts from the other two groups.



a: subthreshold before spike b: pre-threshold/ threshold c: peak d: fAHP e: mAHP f: sAHP

Figure 4.11: Temporal profile of the first four PCs during the different phases of the action potential

The PCs have been divided into specific regions a - f corresponding to particular phases of the action potential. The region during which each of the PCs has larger values can then be related to changes in those ion channel currents that mediate the corresponding phase of the spike. fAHP: fastAHP, mAHP: mediumAHP, sAHP: slowAHP.

Spike train clamp using PC-reconstructed waveforms

I next wanted to see if I could relate each of these PCs to the underlying ion channel currents. I therefore reconstructed the individual spike waveforms using the first four PCs after increasing the PCs by 50%. We then compared the ion channel currents produced by the model under spike train clamp in control and PC-reconstructed modes to see which ion channel currents are modulated in the PC-reconstructed mode. Indeed, I found that when the spikes were reconstructed after increasing PC1 by 50%, sodium and SK currents were increased (Figure 4.12 A). Similarly, PC3 reconstructed waveform clamp resulted in an increase in SK current alone (Figure 4.12 B) while PC4 reconstructed waveform clamp caused an increase in A-type potassium current (Figure 4.12 C). While it may appear that the differences are small and may not denote a functional change in the neuron, this technique is used merely as a method to identify *which* ion channel currents are altered when a particular PC is altered so that I can justify my method of using PCA as an efficient method of waveform analysis for the purpose of my project.

In summary, PCA provided a complementary approach to support our previous analysis well and showed that bursts differ from single spikes primarily in the AHP region, spike height, and spike threshold. The currents underlying these differences in membrane dynamics as reflected by the action potential waveforms were the sodium current that regulates spike height, and the SK current that regulates the AHP. It also appears that the A-type potassium current is involved in maintaining spike threshold.

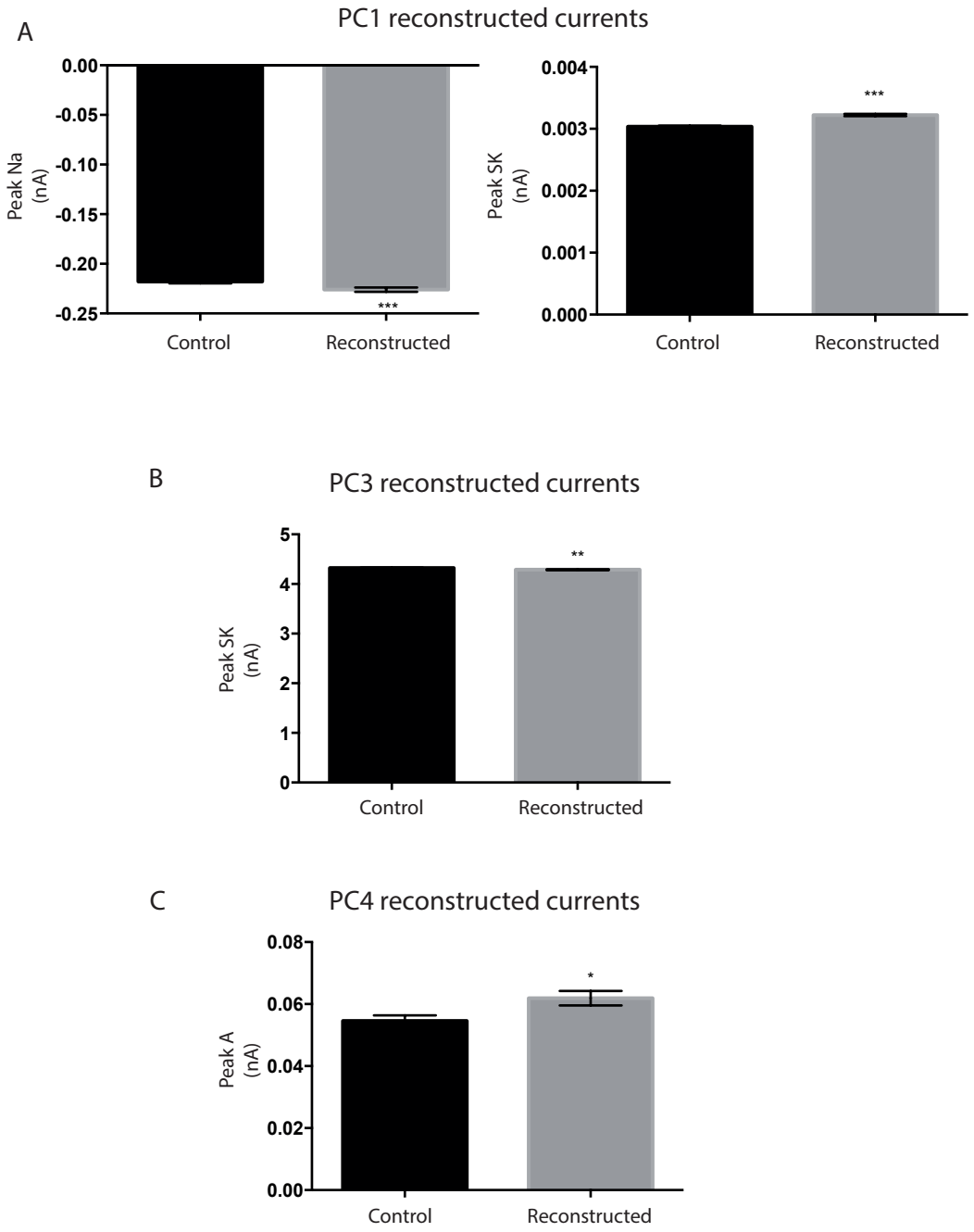


Figure 4.12: Peak currents obtained from spike train clamp after increasing PCs by 50%

A: PC1 results in an increase in peak sodium channel and SK channel currents. This agrees well with Figure 4.10 B because PC1 varies most around action potential peak and AHP. **B:** Similarly, PC3 appears to encode SK channel current alone because this was the only current that was increased significantly after modifying PC3. **C:** PC4 modification results in an increase in peak A type current implying that this current is involved in spike threshold because PC4 explains the variance in the region preceding threshold as in Figure 4.10. Error bars represent mean ± S.E.M.

4.3.8 Burst clamp – voltage clamp simulation using the raw *in vivo* spike train obtained from recording in the VTA

In order to elucidate ion channel currents during endogenous burst firing, we used burst clamp to look at how current flowing through each of the ion channels in our model drive the membrane voltage during the course of bursts. The model dopamine neuron was clamped using the spike trains as the command voltage for each of the seven neurons and the average peak currents from the ion channels included in the model were compared between average non-burst single spikes, average first spike of bursts, and average last spike of bursts across all the neurons. As expected, sodium channel current differed significantly between the groups (one-way repeated measures ANOVA, $p < 0.05$) (Figure 4.13 A). Post-hoc multiple comparisons using Neuman-Keuls test revealed that there was a significant difference in sodium currents between all three groups (peak sodium current; average non-burst single spike = -0.48 ± 0.03 nA, average first spike of bursts = -0.39 ± 0.04 nA, average last spike of bursts = -0.33 ± 0.03 nA, $p < 0.05$). The difference between average first spike and average last spike sodium current agrees well with our observation of decrease in rate of change in membrane rate and depolarisation in action potential threshold, all indicative of reduced availability of sodium channels. However, the reduction in sodium current at the average first spike compared to non-burst single spikes is not understood.

Burst clamp also revealed that there is a difference in the A-type potassium channel current between the groups (one-way repeated measures ANOVA, $p < 0.05$) (Figure 4.13 C). Post-hoc multiple comparisons using Neuman-Keuls test revealed that there is a reduction in A-type current in both average first and last spike of bursts compared to average non-burst single spikes (peak A-type potassium current; average non-burst single spike = 0.42 ± 0.03 nA, average first spike of bursts = 0.35 ± 0.05 nA, average last spike of bursts = 0.28 ± 0.04 nA, $p < 0.05$). This perhaps is due to insufficient activation of A-type channels due to the reduction in post-spike AHP during burst firing

because A-type potassium channels are activated in the sub-threshold range (Silva, Pechura et al. 1990). A-type potassium channels regulate firing frequency and so a reduction in this current during burst firing could also facilitate in transiently elevating the instantaneous firing frequency during bursting.

It also appears that there is a decrease in peak L-type calcium channel current between the three groups, although this did not achieve statistical significance (Figure 4.13 D). L-type calcium channels are activated sub-threshold to provide the depolarisation drive to bring the membrane voltage to action potential threshold after every spike (Amini, Clark et al. 1999). Because we previously found that the AHP of the first spike is greatly reduced during the start of a burst, it is possible that L-type calcium channels are unable to activate enough because the membrane voltage does not reach the hyperpolarised voltage range needed for their activation.

SK channel current was also reduced between the groups (one-way repeated measures ANOVA, $p < 0.05$) (Figure 4.13 E). Post-hoc multiple comparisons using Neuman-Keuls test revealed that the current was significantly reduced at the average first and last spikes of bursts compared to average non-burst single spike (peak SK current; average non-burst single spike = 0.99 ± 0.3 nA, average first spike of bursts = 0.76 ± 0.21 nA, average last spike of bursts = 0.73 ± 0.22 nA, $p < 0.05$). This was expected because of the reduction in the AHP at the first spike of burst that I previously found in membrane voltage analysis. Burst clamp gives us direct evidence of ion channel currents underlying endogenous burst firing in VTA dopamine neurons.

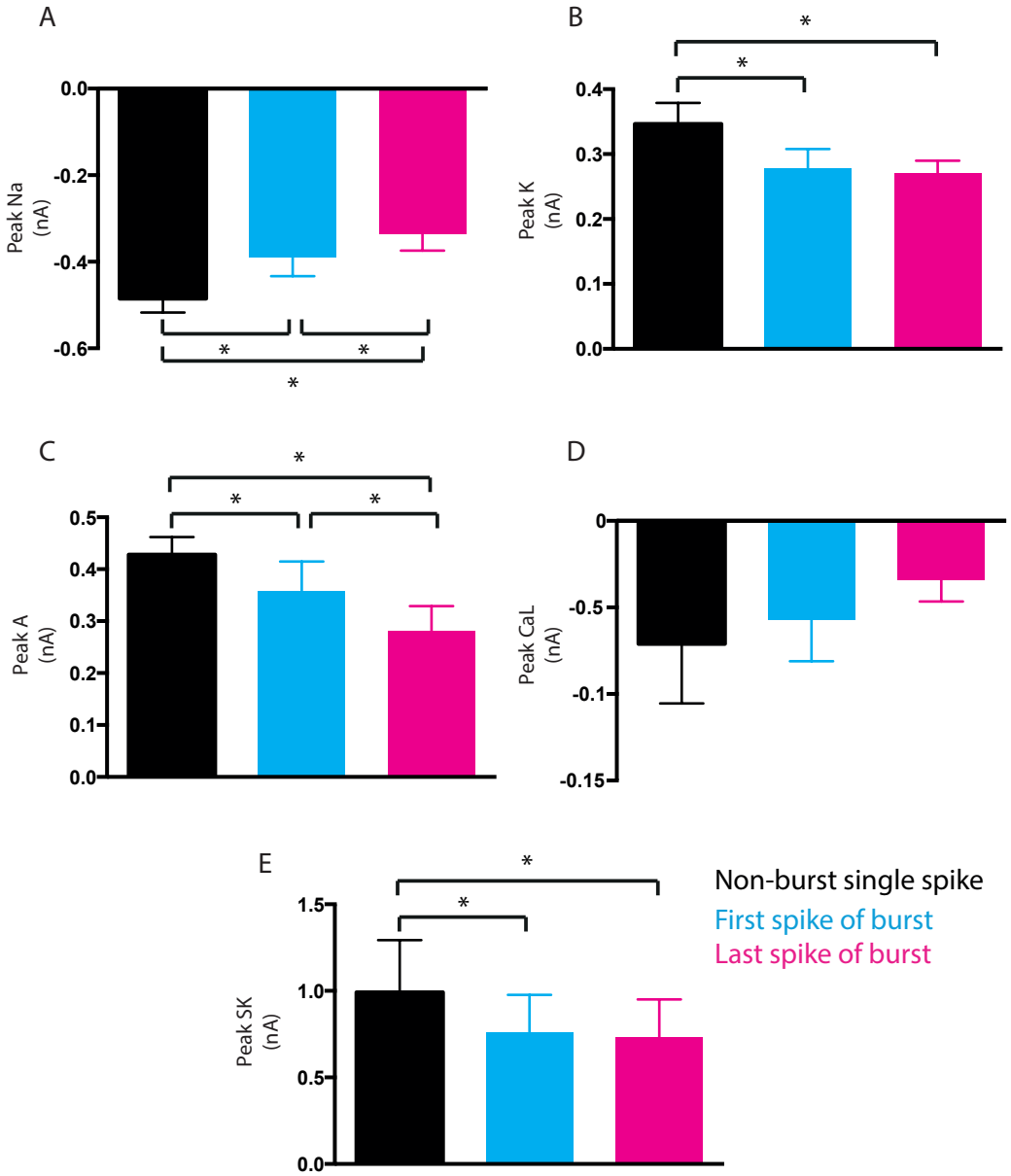


Figure 4.13: Burst clamp

A: Peak sodium current is reduced during burst firing indicating unavailability of sodium channels during a burst. **B:** Delayed rectifier potassium current is also reduced between the non-burst single spike and first spike of bursts. **C:** Peak A-type potassium current is reduced during burst firing perhaps because of reduced activation as a result of reduced AHP during burst firing. **D:** L-type calcium channel current also is reduced even at the start of a burst perhaps again due to insufficient activation as a result of reduced AHP. **E:** SK channel current is also reduced at the start of a burst that results in the reduction in AHP, which appears to be the first detectable change in membrane dynamics during burst firing. Error bars represent mean ± S.E.M.

4.4 Discussion

Some computational studies have tried to simulate endogenous bursting in dopamine neurons and put forth credible hypotheses for the generation of bursts in these neurons (Penney and Britton 2002; Komendantov, Komendantova et al. 2004; Canavier and Landry 2006). However, because of a lack of experimental whole-cell recordings from the intact brain, we did not have a comprehensive view of the membrane dynamics during burst firing. I analysed whole-cell records of endogenous burst firing obtained from dopamine neurons in the VTA of anesthetised rats in order to quantify membrane voltage features and thereby identify underlying ion channel currents during bursting with the aim of hypothesising mechanisms underlying burst firing. I used simple statistical comparisons of membrane waveforms during and outside of burst firing, as well as more sophisticated methods such as PCA, to better understand the evolution of membrane voltage that might lead to and terminate bursts. I also used our model to identify key ion channels implicated during burst firing using spike train clamp.

My results primarily suggest that SK channel inhibition is the key event that triggers a burst *in vivo,* and that sodium channel inactivation plays a crucial role in shaping the spikes during a burst, and hypothesise that it may also facilitate burst termination. Membrane waveform analysis and PCA identified differences in the AHP, spike height, and threshold as the main features that distinguish single spikes from spikes within a burst. Therefore PCA also indicates that modulation of the SK current underlies endogenous bursting, and reduction in sodium current (that could be due to sustained sodium channel inactivation) underlies changes in spike height and depolarisation in spike threshold. Interestingly, PCA suggests that the A-type potassium channel plays a crucial role in maintaining spike threshold in these neurons. Finally, burst clamp using my stochastic dopamine neuron model gives direct evidence of progressive sodium channel inactivation during the burst that

underlies slowing of membrane voltage dynamics, reduction in spike height and depolarisation in action potential threshold during a burst.

NMDAR-dependent modulation of SK channels

In vitro, midbrain dopamine neurons do not demonstrate burst firing in the absence of synaptic inputs and experimental evidence suggests that NMDAR activation results in an increase in burst firing in midbrain dopamine neurons (Johnson, Seutin et al. 1992; Chergui, Charlety et al. 1993; Zweifel, Parker et al. 2009). Bursting is further augmented by the selective blockade of SK channels in the presence of NMDAR stimulation (Seutin, Johnson et al. 1993); blockade of SK channels alone has also been shown to give rise to burst firing in these neurons (Shepard and Bunney 1988; Shepard and Stump 1999). *In vivo*, endogenous bursts also appear to depend primarily on NMDAR activation and SK channel inhibition results in an increase in burst firing (Chergui, Charlety et al. 1993; Waroux, Massotte et al. 2005).

Because, from my results, reduction in SK channel current mediated AHP appears to trigger bursts *in vivo*, I sought to research the published literature for evidence of what might cause this effect. While only one study provides direct evidence of a down regulation in SK channel current as a direct result of NMDAR activation (Paul, Keith et al. 2003), it does corroborate well with our prediction and other studies that have demonstrated increase in burst firing in apamin. However, SK channels have primarily been shown to dampen NMDAR-dependent EPSPs due to a negative feedback loop formed by tight coupling with calcium influx through NMDAR in some other neuronal types (Ngo-Anh, Bloodgood et al. 2005; Nanou, Alpert et al. 2013). The association of SK channels with calmodulin (CaM), whose phosphorylated state determines the calcium affinity of the SK-CaM protein complex, in turn confers the calcium sensitivity of SK channels (Maylie, Bond et al. 2004). There does exist evidence of neurotransmitter-dependent inhibition of SK channels due to

decreased calcium sensitivity by the CK2-mediated phosphorylation of SK channel bound CaM during activation of adrenergic receptors by norepinephrine (Maingret, Coste et al. 2008). Muscarinic inhibition of SK channels has also been shown to enhance excitatory effects NMDAR stimulation facilitating long-term potentiation (LTP) (Buchanan, Petrovic et al. 2010).

In VTA dopamine neurons, however, activation of muscarinic receptors results in post-synaptic hyperpolarisation due to activation of SK channels as a result of increased intracellular calcium release from internal stores (Fiorillo and Williams 2000). Therefore, further experimental work needs to be carried out to determine whether there exists an intracellular mechanism that might inhibit SK channels via the CK2-pathway on NMDAR stimulation in VTA dopamine neurons.

Sodium channel inactivation during burst firing could facilitate termination of bursts

TTX-sensitive, action potential generating sodium currents have fast activation and inactivation dynamics and play an important regulatory role in determining action potential shape, threshold, and height. In my analysis of endogenous burst waveforms from VTA dopamine neurons, I observed a progressive decrease in sodium channel current due to failure of recovery from inactivation as a result of decrease in the AHP during burst firing. This in turn manifested as a progressive decrease in spike height, slowing of membrane rate of change, and depolarisation in spike threshold. As the burst progressed, recovery from inactivation progressively decreases until there are insufficient sodium channels available to fire any more spikes. This perhaps results in burst termination.

Relationship to existing models of bursting

My thesis uses mathematical techniques and a stochastic dopamine neuron model to analyse membrane voltage trajectories and corresponding ion channel currents during endogenous burst

firing in VTA dopamine neurons in order to hypothesise mechanisms underlying generation and termination of bursts. The first few computational models of dopamine neurons have focussed on the role of NMDAR activation and the sodium pump for the generation and termination of bursts respectively (Li, Bertram et al. 1996; Canavier 1999).

Mechanisms by which SK channel block facilitates burst firing were explored in some other modelling studies that predicted sub-threshold plateaux potentials driven by L-type calcium channels and repolarised by ERG current as underlying burst firing (Amini, Clark et al. 1999; Canavier, Oprisan et al. 2007; Oster and Gutkin 2011). However with our results we hypothesise that a transient inhibition of SK channels, perhaps via NMDAR activation, triggers bursts. Moreover, all these studies concentrated on *in vitro* models of bursting; *in vivo* models are primarily based on electro-tonic coupling between dopamine neurons (Komendantov and Canavier 2002), electrical coupling between dendrites and soma (Wilson and Callaway 2000), and summation of effects of a concomitant increase in excitatory drive and reduction of inhibitory synaptic conductances along with SK channel inhibition (Canavier and Landry 2006). Most existing models predict roles for potassium conductances such as SK (Li, Bertram et al. 1996), ERG (Canavier, Oprisan et al. 2007), and M-type (Drion, Bonjean et al. 2010) to repolarise bursts in dopamine neurons. However our prediction is that sodium channels progressively fail to recover from inactivation during the course of a burst until there are insufficient sodium channels available to initiate any further action potentials and therefore the burst terminates.

Chapter 5 Conclusions and Discussion

Ion channels shape the excitability of neurons and a multitude of ion channels work in concert to influence the membrane voltage to give rise to the neuronal action potential. Because of their role in reward-related learning and the presence of abnormal firing patterns in disorders such as schizophrenia and PD, a lot of work has gone into elucidating the role of ion channels controlling the different aspects of firing in midbrain dopamine neurons. We developed a novel stochastic model representative of midbrain dopamine neurons in order to uncover mechanism(s) by which SK channels maintain firing regularity and further used the model to analyse ion channel currents during burst firing in voltage clamp mode using whole-cell membrane voltage spike trains. We also employed mathematical techniques like PCA as a complimentary approach to identify epochs during spiking, especially during burst firing that differentiated burst waveforms from non-burst waveforms and relate these differences to ion channel currents that might be driving those effects.

5.1 Summary of findings

Our first hypothesis stated that "*the post-spike AHP provided by the current through SK channels standardises the availability of other voltage-gated ion channels such as sodium and potassium channels in order to time each action potential. With SK channel inhibition, reduced AHP results in a variable amount of sodium channels remaining in the inactivated state, due to ion channel stochasticity, thereby resulting in an irregular spike train."* To test this hypothesis, I developed a biophysical model of a midbrain dopamine neuron with ion channel stochasticity (Figure 5.1). My primary results suggest that SK channels control the availability of sodium channels by providing a hyperpolarising current after each spike in order to facilitate recovery of these channels from inactivation such that enough are always available to open during the next depolarising wave to fire a spike. When SK channels are blocked, spike timing becomes irregular because, due to the stochastic nature of ion channels, sometimes there are enough sodium channels available to open

and so the neuron fires a spike whereas at other times, the neuron remains silent for a longer period of time to enable enough sodium channels to recover from inactivation an then fires a spike after a longer ISI. We also find that decrease in firing regularity is accompanied by a depolarisation and increase in variability in spike threshold due to the overall reduced availability of sodium channels.

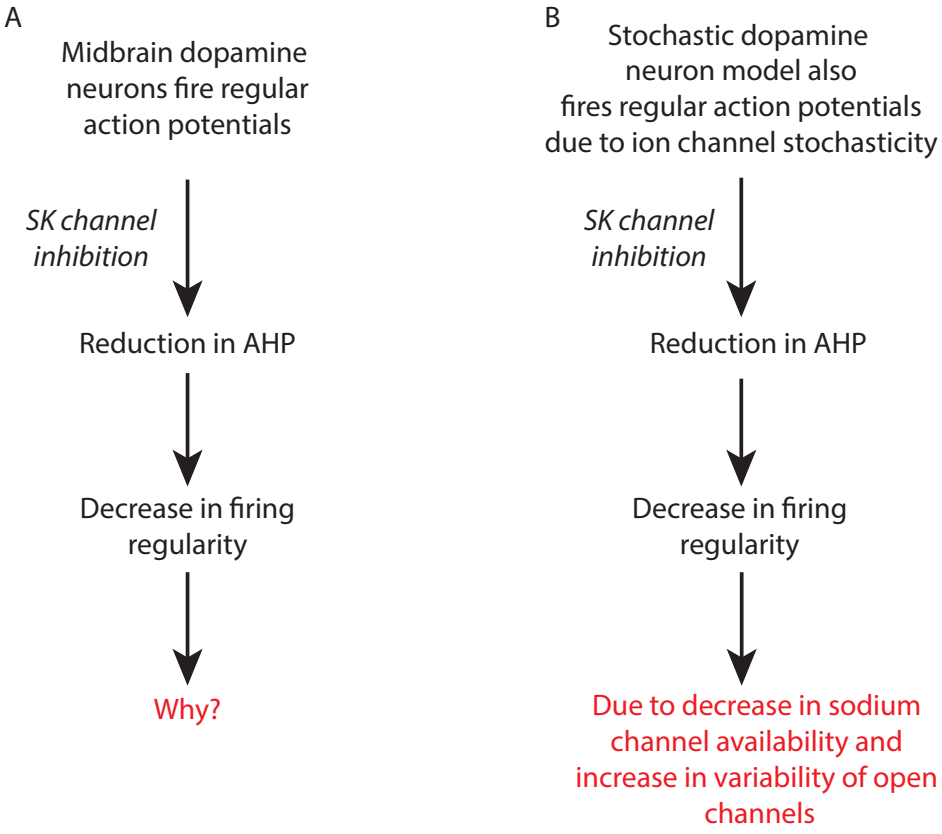


Figure 5.1: Schematic representation of firing regularity in midbrain dopamine neurons

A. In physiological midbrain dopamine neurons, while experiments demonstrated that inhibition of SK channels results in a decrease in firing regularity, it was not clear why. **B.** Using a stochastic dopamine neuron model that reproduced regular spiking in the presence of SK channels, revealed that a simulated inhibition of SK channels results in a decrease in the availability of sodium channels along with an increase in the variability of open channels thus giving rise to an decrease in firing regularity.

For the data driven analysis of membrane voltage waveforms to understand burst-firing mechanisms, we used mathematical techniques and computational modelling to elucidate ion channel mechanisms underlying endogenous bursting in VTA dopamine neurons (Figure 5.2). Preliminary analysis of voltage traces led to the following hypotheses:

i) SK channel current is significantly reduced during burst firing

ii) There is a progressive depolarisation in action potential threshold during a burst

iii) The depolarisation in action potential threshold is due to accumulation of sodium channel inactivation

Such a data-driven analysis of whole-cell *in vivo* bursts revealed that a reduction in the AHP mediated by SK channels is the first detectable change in the membrane voltage trajectory during the first spike of a burst suggesting that perhaps neurotransmitter and/or NMDAR-activation dependent SK-channel inhibition is key for endogenous burst generation *in vivo*. The other significant result demonstrates that decreased recovery of sodium channels from inactivation during the course of a burst plays a crucial role in shaping the spikes especially causing reduction in spike height, slowing membrane dynamics, and depolarisation in spike threshold. We further predict that due to a progressive increase in number of sodium channels that remain inactive, the burst finally terminates due to unavailability of sodium channels to fire any further spikes.

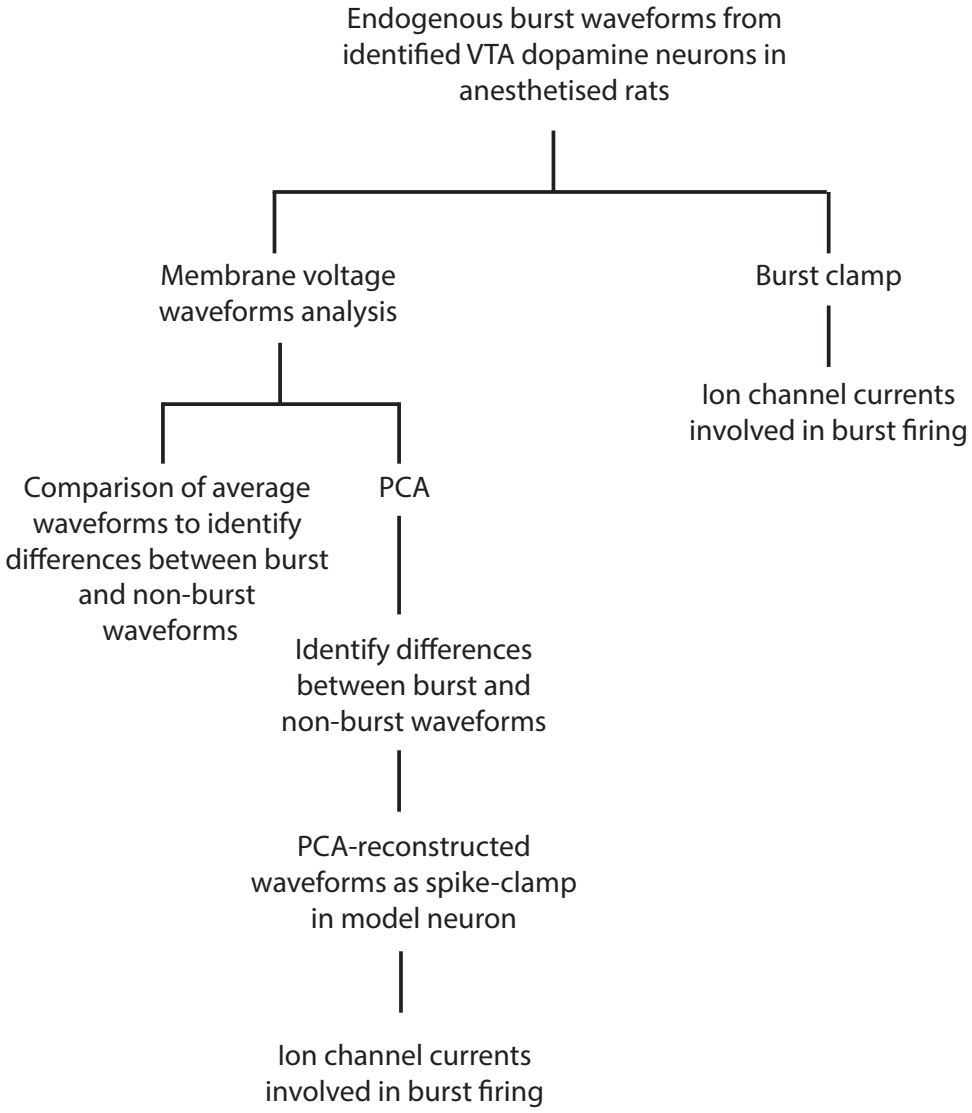


Figure 5.2: Schematic for the novel and complementary methods used in the analysis of endogenous burst firing data obtained from dopamine neurons in the VTA

In order to elucidate ion channel mechanisms underlying endogenous burst firing in VTA dopamine neurons, complementary methods of membrane voltage waveform analysis using average waveform comparisons and PCA was used along with burst clamp technique using our model dopamine neuron.

5.2 Significance of computational modelling

A number of mathematical models have been recently developed, each seeking to answer specific questions regarding dopamine neuron physiology and have made important predictions about the role of ion channels in a myriad of electrophysiological features of these neurons (Amini, Clark et al. 1999; Wilson and Callaway 2000; Komendantov and Canavier 2002; Komendantov, Komendantova et al. 2004; Canavier and Landry 2006; Canavier, Oprisan et al. 2007; Kuznetsova, Huertas et al. 2010; Drion, Massotte et al. 2011; Ha and Kuznetsov 2013). One of the strengths of computational modelling is that it gives control over individual ion channels, in that a number of combinations of conductance values, half-activation voltage, and densities can easily be adjusted to simulate different conditions. Moreover, the neuron can be reduced to a simple system of variables thereby reducing its complexity, yet retaining much of its electrophysiological features such that one can concentrate on a particular set of ion channels most relevant to the question at hand. For example the model developed for my thesis is a single compartment representation of the dopaminergic soma with only those ion channels required to simulate electrophysiological features and responses to pharmacological manipulations relevant to our study. Another benefit of a model neuron is that it can be used in dynamic clamp experiments to establish a real-time interaction between an *in silico* and a biological neuron (Sharp, O'Neil et al. 1993). This enables easy addition or removal of virtual ion channel currents and/or synaptic inputs to the biological neuron to test their effects.

Only a few computational studies have successfully developed neuron models with ion channel stochasticity, representative of a specific neuronal type (Mercer, Chan et al. 2007; Xu and Clancy 2008; Deister, Chan et al. 2009; Masoli, Solinas et al. 2015) and my study is the first such model for midbrain dopamine neurons. Adding ion channel stochasticity allowed me to reproduce spike trains with firing regularity akin to those seen in *in vitro* and dissociated preparations of midbrain

dopamine neurons and then test our hypothesis that it is the availability of ion channels that critically controls firing regularity in these neurons (Figure 5.1). Because of the availability of whole-cell membrane voltage data from *in vivo* recordings, using the stochastic model we were also able to identify and explain mechanisms underlying some of the features associated with endogenous burst firing such as depolarisation in spike threshold, slowing in membrane rate of change due to unavailability of sodium channels.

Finally, having developed a biophysical model of midbrain dopamine neurons, with ion channel stochasticity, it can be maintained and developed further to test hypotheses and make predictions about dopamine neuron physiology in the future.

5.3 Novel methodology for data-driven analysis of membrane voltage waveforms and underlying ion channel currents

I used PCA as a complimentary approach for the data-driven analysis of *in vivo* membrane voltage waveforms (Figure 5.2). While PCA itself is not a novel technique for data analysis, and has sometimes been used in spike sorting after multi-unit recordings (Lewicki 1998), it has not been used to identify ion channel mechanisms underlying differences in membrane voltage waveforms between groups of spikes. I used my model dopamine neuron to elucidate ion channel currents that might be driving the differences in membrane voltage dynamics, that were identified using PCA, as a novel method to identify the roles of different ion channels in burst firing in midbrain dopamine neurons.

I also extended the concept of voltage clamp (Hodgkin and Huxley 1952) to run the raw whole-cell VTA spike trains obtained from dopamine neurons *in vivo,* through my model dopamine neuron to analyse how ion channel currents change with time during burst firing (Figure 5.2). This has

allowed me to make predictions about some of the ion channels that may be involved in driving and terminating bursts in these neurons. This is a novel technique that can be used to quickly test hypotheses arising from experiments and/or make preliminary predictions that can be tested experimentally, about ion channel currents that might be regulating specific electrophysiological features of a neuron.

5.4 Predictions from our study that could be tested experimentally

Our model predicts that sodium channels become unavailable to open because the membrane does not reach hyperpolarised potentials required for recovery from inactivation when SK channels are inhibited. Due to the stochastic nature of ion channels, this results in an increase in the variability of available sodium channels for activation; in other words, sometimes enough sodium channels recover from inactivation and therefore open to fire a spike, whereas sometimes it takes longer for enough sodium channels to recover from inactivation and therefore it takes longer to fire the next spike, thus giving rise to an irregular spike train. Under experimental conditions, ion channel availability can be calculated indirectly using peak current measurements, however these are only approximations. Whereas, a computational model with simulated stochastic ion channels can be used as a replacement in a dynamic clamp protocol after pharmacologically or genetically silencing the equivalent neuronal channels. This way one can monitor exactly the number of ion channels in each of the states during the different manipulations performed in the experiments.

The other predictions from our modelling study such as depolarisation in spike threshold with SK channel inhibition can be tested by recording spiking activity and comparing spike thresholds in the presence and absence of SK channel inhibitors like apamin. Our model predicts that the increase in firing rate observed after SK channel inhibition could be facilitated due to the associated reduction in A-type potassium current in our model. In an experimental setting, when SK channel inhibition with apamin results in an increase in firing rate, using dynamic clamp, we could inject virtual A-type potassium current from our model to test if this facilitates a reversal of firing rate to baseline before application of apamin.

An important hypothesis from our analysis of whole cell bursts is that a transient SK channel inhibition as a result of NMDAR activation triggers burst firing *in vivo* (Figure 5.3). As discussed in

Chapter 4, such a hypothesis is plausible because similar neurotransmitter dependent inhibition of SK channels has been observed in other neurons and linked to LTP (Maingret, Coste et al. 2008). Only one study gives evidence of SK channel inhibition as a direct result of NMDAR stimulation in VTA dopamine neurons (Paul, Keith et al. 2003) however they do not demonstrate nor hypothesise what the intracellular mechanisms might be. While this result has not gained much attention, it is worth testing and if indeed SK currents are reduced with NMDAR stimulation, then the pathway via which NMDAR activation results in SK channel inhibition needs to be investigated further. The first candidate could be the CK2-PP2A pathway because SK channels are known to form protein complexes with these kinases and phosphatases (Allen, Fakler et al. 2007) in association with CaM. Calcium sensitivity of SK channels is indirectly reduced due to the phosphorylation of SK-bound CaM by CK2. However there is no evidence to suggest that NMDAR activation directly causes such a downstream effect in midbrain dopamine neurons.

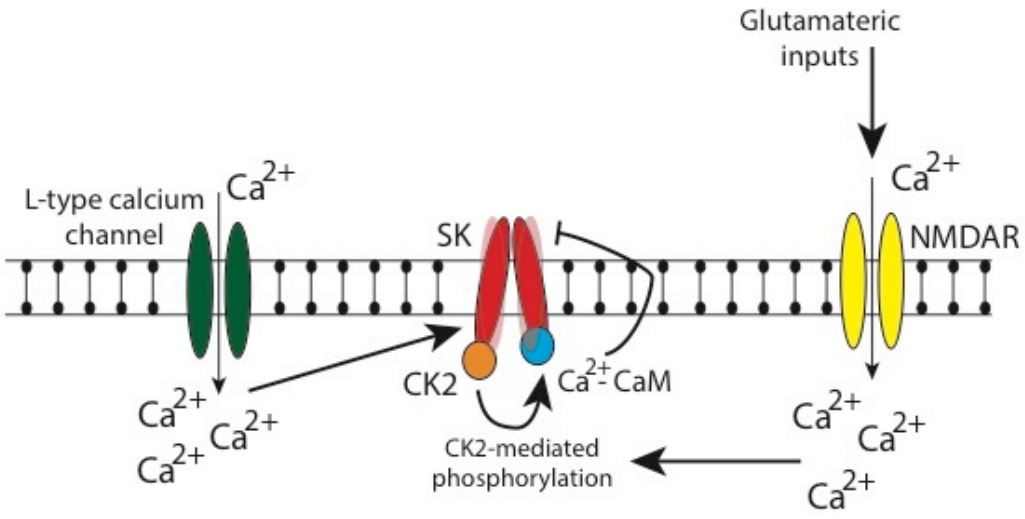


Figure 5.3: Schematic to demonstrate our prediction that NMDAR-dependent SK channel inhibition triggers endogenous burst firing in VTA dopamine neurons

SK channels are activated by incoming calcium ions through L-type calcium channels via binding of CaM. Because a reduction in AHP is the first change in membrane voltage waveform during burst firing in VTA dopamine neurons, we predict that during synaptic stimulation, activation of NMDARs inhibits SK channels via CK2-mediated phosphorylation of SK-bound CaM thereby decreasing the calcium sensitivity of SK channels and inhibiting them, thus resulting in a burst.

Once again, dynamic clamp could be used to study sodium channel inactivation related predictions during burst firing using our stochastic model. We showed that spike threshold progressively depolarises due to inactivation of sodium channels during the course of burst firing and predict that it is perhaps complete failure of recovery from inactivation that results in the termination of bursts (Figure 5.4). It has been demonstrated in other models of dopamine neurons that depolarisation block occur due to sodium channel inactivation where the neuron ceases to fire after discharging a series of closely spaced spikes similar to bursts (Kuznetsova, Huertas et al. 2010; Qian, Yu et al. 2014; Yu and Canavier 2015). Therefore our prediction seems plausible and can be tested by introducing virtual sodium channels just before burst termination to see if that prevents termination by producing further spiking**.**

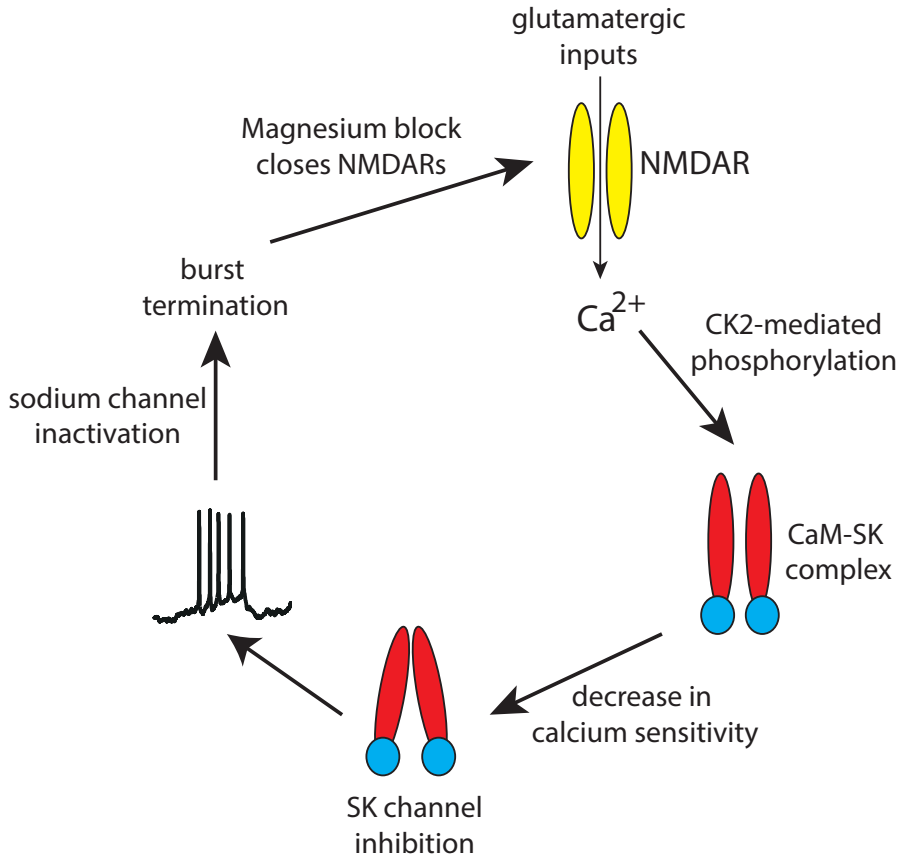


Figure 5.4: Schematic for endogenous burst generation and termination in VTA dopamine neurons

My analysis predicts that bursts are generated due to the transient inhibition of SK channels due to NMDAR activation via the CK2-mediated phosphorylation of SK-bound CaM. I also predict that bursts are terminated due to a failure of recovery from inactivation of sodium channels during burst firing, such that enough sodium channels are not available to fire further spikes.

References

Abbott, P. D. a. L. F. (2001). Model Neurons I: Neuroelectronics. Theoretical Neuroscience: Computational and Mathematical Modeling of Neural Systems, The MIT Press

Abbott, P. D. a. L. F. (2005). Theoretical Neuroscience: Computational and Mathematical Modeling of Neural Systems, The MIT Press.

Allen, D., B. Fakler, et al. (2007). "Organization and regulation of small conductance Ca2+-activated K+ channel multiprotein complexes." The Journal of neuroscience : the official journal of the Society for Neuroscience **27**(9): 2369-2376.

Amini, B., J. W. Clark, Jr., et al. (1999). "Calcium dynamics underlying pacemaker-like and burst firing oscillations in midbrain dopaminergic neurons: a computational study." Journal of neurophysiology **82**(5): 2249-2261.

Anwar, H., S. Hong, et al. (2012). "Controlling Ca2+-activated K+ channels with models of Ca2+ buffering in Purkinje cells." Cerebellum **11**(3): 681-693.

Azouz, R. and C. M. Gray (2000). "Dynamic spike threshold reveals a mechanism for synaptic coincidence detection in cortical neurons in vivo." Proceedings of the National Academy of Sciences of the United States of America **97**(14): 8110-8115.

Beeler, J. A., N. Daw, et al. (2010). "Tonic dopamine modulates exploitation of reward learning." Frontiers in behavioral neuroscience **4**: 170.

Bishop, M. W., S. Chakraborty, et al. (2010). "Hyperexcitable substantia nigra dopamine neurons in PINK1- and HtrA2/Omi-deficient mice." Journal of neurophysiology **104**(6): 3009-3020.

Blythe, S. N., D. Wokosin, et al. (2009). "Cellular mechanisms underlying burst firing in substantia nigra dopamine neurons." The Journal of neuroscience : the official journal of the Society for Neuroscience **29**(49): 15531-15541.

Bonci, A., G. Bernardi, et al. (2003). "The dopamine-containing neuron: maestro or simple musician in the orchestra of addiction?" Trends in pharmacological sciences **24**(4): 172-177.

Brischoux, F., S. Chakraborty, et al. (2009). "Phasic excitation of dopamine neurons in ventral VTA by noxious stimuli." Proceedings of the National Academy of Sciences of the United States of America **106**(12): 4894-4899.

Brodie, M. S., M. A. McElvain, et al. (1999). "Pharmacological reduction of small conductance calcium-activated potassium current (SK) potentiates the excitatory

effect of ethanol on ventral tegmental area dopamine neurons." The Journal of pharmacology and experimental therapeutics **290**(1): 325-333.

Buchanan, K. A., M. M. Petrovic, et al. (2010). "Facilitation of long-term potentiation by muscarinic M(1) receptors is mediated by inhibition of SK channels." Neuron **68**(5): 948-963.

Bunney, A. A. G. a. B. S. (2000). Electrophysiological Properties of Midbrain Dopamine Neurons Psychopharmacology - 4th Generation of Progress, Raven Press, New York, New York, 1995

Calabresi, P., B. Picconi, et al. (2007). "Dopamine-mediated regulation of corticostriatal synaptic plasticity." Trends in neurosciences **30**(5): 211-219.

Canavier, C. C. (1999). "Sodium dynamics underlying burst firing and putative mechanisms for the regulation of the firing pattern in midbrain dopamine neurons: a computational approach." Journal of computational neuroscience **6**(1): 49-69.

Canavier, C. C. and R. S. Landry (2006). "An increase in AMPA and a decrease in SK conductance increase burst firing by different mechanisms in a model of a dopamine neuron in vivo." Journal of neurophysiology **96**(5): 2549-2563.

Canavier, C. C., S. A. Oprisan, et al. (2007). "Computational model predicts a role for ERG current in repolarizing plateau potentials in dopamine neurons: implications for modulation of neuronal activity." Journal of neurophysiology **98**(5): 3006-3022.

Cardozo, D. L. and B. P. Bean (1995). "Voltage-dependent calcium channels in rat midbrain dopamine neurons: modulation by dopamine and GABAB receptors." Journal of neurophysiology **74**(3): 1137-1148.

Chan, C. S., J. N. Guzman, et al. (2007). "'Rejuvenation' protects neurons in mouse models of Parkinson's disease." Nature **447**(7148): 1081-1086.

Chan, C. S., R. Shigemoto, et al. (2004). "HCN2 and HCN1 channels govern the regularity of autonomous pacemaking and synaptic resetting in globus pallidus neurons." The Journal of neuroscience : the official journal of the Society for Neuroscience **24**(44): 9921-9932.

Chergui, K., H. Akaoka, et al. (1994). "Subthalamic nucleus modulates burst firing of nigral dopamine neurones via NMDA receptors." Neuroreport **5**(10): 1185-1188.

Chergui, K., P. J. Charlety, et al. (1993). "Tonic activation of NMDA receptors causes spontaneous burst discharge of rat midbrain dopamine neurons in vivo." The European journal of neuroscience **5**(2): 137-144.

Chergui, K., M. F. Suaud-Chagny, et al. (1994). "Nonlinear relationship between impulse flow, dopamine release and dopamine elimination in the rat brain in vivo." Neuroscience **62**(3): 641-645.

Chiodo, L. A. and G. Kapatos (1992). "Membrane properties of identified mesencephalic dopamine neurons in primary dissociated cell culture." Synapse **11**(4): 294-309.

Christoffersen, C. L. and L. T. Meltzer (1995). "Evidence for N-methyl-D-aspartate and AMPA subtypes of the glutamate receptor on substantia nigra dopamine neurons: possible preferential role for N-methyl-D-aspartate receptors." Neuroscience **67**(2): 373-381.

Connor, J. A. and C. F. Stevens (1971). "Voltage clamp studies of a transient outward membrane current in gastropod neural somata." The Journal of physiology **213**(1): 21-30.

Cousins, M. S. and J. D. Salamone (1996). "Involvement of ventrolateral striatal dopamine in movement initiation and execution: a microdialysis and behavioral investigation." Neuroscience **70**(4): 849-859.

Cui, G., T. Okamoto, et al. (2004). "Spontaneous opening of T-type Ca2+ channels contributes to the irregular firing of dopamine neurons in neonatal rats." The Journal of neuroscience : the official journal of the Society for Neuroscience **24**(49): 11079-11087.

Dahan, L., B. Astier, et al. (2007). "Prominent burst firing of dopaminergic neurons in the ventral tegmental area during paradoxical sleep." Neuropsychopharmacology : official publication of the American College of Neuropsychopharmacology **32**(6): 1232-1241.

Dahlstrom, A. and K. Fuxe (1964). "Localization of monoamines in the lower brain stem." Experientia **20**(7): 398-399.

Dauer, W. and S. Przedborski (2003). "Parkinson's disease: mechanisms and models." Neuron **39**(6): 889-909.

de Polavieja, G. G., A. Harsch, et al. (2005). "Stimulus history reliably shapes action potential waveforms of cortical neurons." The Journal of neuroscience : the official journal of the Society for Neuroscience **25**(23): 5657-5665.

Deignan, J., R. Lujan, et al. (2012). "SK2 and SK3 expression differentially affect firing frequency and precision in dopamine neurons." Neuroscience **217**: 67-76.

Deister, C. A., C. S. Chan, et al. (2009). "Calcium-activated SK channels influence voltage-gated ion channels to determine the precision of firing in globus pallidus neurons." The Journal of neuroscience : the official journal of the Society for Neuroscience **29**(26): 8452-8461.

Deister, C. A., M. A. Teagarden, et al. (2009). "An intrinsic neuronal oscillator underlies dopaminergic neuron bursting." The Journal of neuroscience : the official journal of the Society for Neuroscience **29**(50): 15888-15897.

Di Chiara, G. and V. Bassareo (2007). "Reward system and addiction: what dopamine does and doesn't do." Current opinion in pharmacology **7**(1): 69-76.

Dorval, A. D., Jr. and J. A. White (2005). "Channel noise is essential for perithreshold oscillations in entorhinal stellate neurons." The Journal of neuroscience : the official journal of the Society for Neuroscience **25**(43): 10025-10028.

Dragicevic, E., J. Schiemann, et al. (2015). "Dopamine midbrain neurons in health and Parkinson's disease: emerging roles of voltage-gated calcium channels and ATP-sensitive potassium channels." Neuroscience **284**: 798-814.

Drion, G., M. Bonjean, et al. (2010). "M-type channels selectively control bursting in rat dopaminergic neurons." The European journal of neuroscience **31**(5): 827-835.

Drion, G., L. Massotte, et al. (2011). "How modeling can reconcile apparently discrepant experimental results: the case of pacemaking in dopaminergic neurons." PLoS computational biology **7**(5): e1002050.

Dunteman, G. H. (1989). Principal components analysis, Sage.

Durante, P., C. G. Cardenas, et al. (2004). "Low-threshold L-type calcium channels in rat dopamine neurons." Journal of neurophysiology **91**(3): 1450-1454.

Erhardt, S., H. Nissbrandt, et al. (1999). "Activation of nigral dopamine neurons by the selective GABA(B)-receptor antagonist SCH 50911." Journal of neural transmission **106**(5-6): 383-394.

Faber, E. S. and P. Sah (2003). "Ca2+-activated K+ (BK) channel inactivation contributes to spike broadening during repetitive firing in the rat lateral amygdala." The Journal of physiology **552**(Pt 2): 483-497.

Faber, E. S. and P. Sah (2003). "Calcium-activated potassium channels: multiple contributions to neuronal function." The Neuroscientist : a review journal bringing neurobiology, neurology and psychiatry **9**(3): 181-194.

Faber, E. S. and P. Sah (2007). "Functions of SK channels in central neurons." Clinical and experimental pharmacology & physiology **34**(10): 1077-1083.

Fabricius, K., L. Helboe, et al. (2010). "Increased dopaminergic activity in socially isolated rats: an electrophysiological study." Neuroscience letters **482**(2): 117-122.

Faisal, A. A. (2013). Noise in neurons and other constraints. Computational Systems Neurobiology. N. L. Novere, Springer**:** 227-257.

Faisal, A. A. and S. B. Laughlin (2007). "Stochastic simulations on the reliability of action potential propagation in thin axons." PLoS computational biology **3**(5): e79.

Faisal, A. A., L. P. Selen, et al. (2008). "Noise in the nervous system." Nature reviews. Neuroscience **9**(4): 292-303.

Faisal, A. A., J. A. White, et al. (2005). "Ion-channel noise places limits on the miniaturization of the brain's wiring." Current biology : CB **15**(12): 1143-1149.

Fallon, J. H., D. A. Koziell, et al. (1978). "Catecholamine innervation of the basal forebrain. II. Amygdala, suprarhinal cortex and entorhinal cortex." The Journal of comparative neurology **180**(3): 509-532.

Fallon, J. H. and R. Y. Moore (1978). "Catecholamine innervation of the basal forebrain. III. Olfactory bulb, anterior olfactory nuclei, olfactory tubercle and piriform cortex." The Journal of comparative neurology **180**(3): 533-544.

Fallon, J. H. and R. Y. Moore (1978). "Catecholamine innervation of the basal forebrain. IV. Topography of the dopamine projection to the basal forebrain and neostriatum." The Journal of comparative neurology **180**(3): 545-580.

Finlay, J. M. (2001). "Mesoprefrontal dopamine neurons and schizophrenia: role of developmental abnormalities." Schizophrenia bulletin **27**(3): 431-442.

Fiorillo, C. D. and J. T. Williams (2000). "Cholinergic inhibition of ventral midbrain dopamine neurons." The Journal of neuroscience : the official journal of the Society for Neuroscience **20**(20): 7855-7860.

Floresco, S. B., C. L. Todd, et al. (2001). "Glutamatergic afferents from the hippocampus to the nucleus accumbens regulate activity of ventral tegmental area dopamine neurons." The Journal of neuroscience : the official journal of the Society for Neuroscience **21**(13): 4915-4922.

Floresco, S. B., A. R. West, et al. (2003). "Afferent modulation of dopamine neuron firing differentially regulates tonic and phasic dopamine transmission." Nature neuroscience **6**(9): 968-973.

Fujimura, K. and Y. Matsuda (1989). "Autogenous oscillatory potentials in neurons of the guinea pig substantia nigra pars compacta in vitro." Neuroscience letters **104**(1-2): 53-57.

Gerfen, C. R., M. Herkenham, et al. (1987). "The neostriatal mosaic: II. Patch- and matrix-directed mesostriatal dopaminergic and non-dopaminergic systems." The

Journal of neuroscience : the official journal of the Society for Neuroscience **7**(12): 3915-3934.

Glimcher, P. W. (2011). "Understanding dopamine and reinforcement learning: the dopamine reward prediction error hypothesis." Proceedings of the National Academy of Sciences of the United States of America **108 Suppl 3**: 15647-15654.

Goldwyn, J. H. and E. Shea-Brown (2011). "The what and where of adding channel noise to the Hodgkin-Huxley equations." PLoS computational biology **7**(11): e1002247.

Gonon, F. G. (1988). "Nonlinear relationship between impulse flow and dopamine released by rat midbrain dopaminergic neurons as studied by in vivo electrochemistry." Neuroscience **24**(1): 19-28.

Grace, A. A. (1988). "In Vivo and in Vitro Intracellular Recordings from Rat Midbrain Dopamine Neurons." Annals of the New York Academy of Sciences **537**: 51–76.

Grace, A. A. (1990). "Evidence for the functional compartmentalization of spike generating regions of rat midbrain dopamine neurons recorded in vitro." Brain research **524**(1): 31-41.

Grace, A. A. (1991). "Phasic versus tonic dopamine release and the modulation of dopamine system responsivity: a hypothesis for the etiology of schizophrenia." Neuroscience **41**(1): 1-24.

Grace, A. A. and B. S. Bunney (1983). "Intracellular and extracellular electrophysiology of nigral dopaminergic neurons--2. Action potential generating mechanisms and morphological correlates." Neuroscience **10**(2): 317-331.

Grace, A. A. and B. S. Bunney (1983). "Intracellular and extracellular electrophysiology of nigral dopaminergic neurons--3. Evidence for electrotonic coupling." Neuroscience **10**(2): 333-348.

Grace, A. A. and B. S. Bunney (1984). "The control of firing pattern in nigral dopamine neurons: burst firing." The Journal of neuroscience : the official journal of the Society for Neuroscience **4**(11): 2877-2890.

Grace, A. A. and B. S. Bunney (1984). "The control of firing pattern in nigral dopamine neurons: single spike firing." The Journal of neuroscience : the official journal of the Society for Neuroscience **4**(11): 2866-2876.

Grace, A. A., S. B. Floresco, et al. (2007). "Regulation of firing of dopaminergic neurons and control of goal-directed behaviors." Trends in neurosciences **30**(5): 220-227.

Grace, A. A. and S. P. Onn (1989). "Morphology and electrophysiological properties of immunocytochemically identified rat dopamine neurons recorded

in vitro." The Journal of neuroscience : the official journal of the Society for Neuroscience **9**(10): 3463-3481.

Grenhoff, J., G. Aston-Jones, et al. (1986). "Nicotinic effects on the firing pattern of midbrain dopamine neurons." Acta physiologica Scandinavica **128**(3): 351-358.

Grenhoff, J., L. Ugedo, et al. (1988). "Firing patterns of midbrain dopamine neurons: differences between A9 and A10 cells." Acta physiologica Scandinavica **134**(1): 127-132.

Gu, X., A. L. Blatz, et al. (1992). "Subtypes of substantia nigra dopaminergic neurons revealed by apamin: autoradiographic and electrophysiological studies." Brain research bulletin **28**(3): 435-440.

Guzman, J. N., J. Sanchez-Padilla, et al. (2009). "Robust pacemaking in substantia nigra dopaminergic neurons." The Journal of neuroscience : the official journal of the Society for Neuroscience **29**(35): 11011-11019.

Guzman, J. N., J. Sanchez-Padilla, et al. (2010). "Oxidant stress evoked by pacemaking in dopaminergic neurons is attenuated by DJ-1." Nature **468**(7324): 696-700.

Ha, J. and A. Kuznetsov (2013). "Interaction of NMDA receptor and pacemaking mechanisms in the midbrain dopaminergic neuron." PloS one **8**(7): e69984.

Hahn, J., T. E. Tse, et al. (2003). "Long-term K+ channel-mediated dampening of dopamine neuron excitability by the antipsychotic drug haloperidol." The Journal of neuroscience : the official journal of the Society for Neuroscience **23**(34): 10859-10866.

Hainsworth, A. H., J. Roper, et al. (1991). "Identification and electrophysiology of isolated pars compacta neurons from guinea-pig substantia nigra." Neuroscience **43**(1): 81-93.

Hallworth, N. E., C. J. Wilson, et al. (2003). "Apamin-sensitive small conductance calcium-activated potassium channels, through their selective coupling to voltage-gated calcium channels, are critical determinants of the precision, pace, and pattern of action potential generation in rat subthalamic nucleus neurons in vitro." The Journal of neuroscience : the official journal of the Society for Neuroscience **23**(20): 7525-7542.

Hansen, H. H., C. Ebbesen, et al. (2006). "The KCNQ channel opener retigabine inhibits the activity of mesencephalic dopaminergic systems of the rat." The Journal of pharmacology and experimental therapeutics **318**(3): 1006-1019.

Harris, N. C., C. Webb, et al. (1989). "A possible pacemaker mechanism in pars compacta neurons of the guinea-pig substantia nigra revealed by various ion channel blocking agents." Neuroscience **31**(2): 355-362.

Henze, D. A. and G. Buzsaki (2001). "Action potential threshold of hippocampal pyramidal cells in vivo is increased by recent spiking activity." Neuroscience **105**(1): 121-130.

Herrik, K. F., P. Christophersen, et al. (2010). "Pharmacological modulation of the gating properties of small conductance Ca2+-activated K+ channels alters the firing pattern of dopamine neurons in vivo." Journal of neurophysiology **104**(3): 1726-1735.

Hille, B. (1992). Ionic channels of excitable membrane. Sunderland, MA, Sinauer Associates.

Hille, B. (1992). Ionic channels of excitable membranes. 3rd. Sunderlan, MA, Sinauer Assoc.

Hodgkin, A. L. and A. F. Huxley (1952). "Currents carried by sodium and potassium ions through the membrane of the giant axon of Loligo." The Journal of physiology **116**(4): 449-472.

Hodgkin, A. L. and A. F. Huxley (1952). "A quantitative description of membrane current and its application to conduction and excitation in nerve." The Journal of physiology **117**(4): 500-544.

Howes, O. D. and S. Kapur (2009). "The dopamine hypothesis of schizophrenia: version III--the final common pathway." Schizophrenia bulletin **35**(3): 549-562.

Hugues, M., G. Romey, et al. (1982). "Apamin as a selective blocker of the calcium-dependent potassium channel in neuroblastoma cells: voltage-clamp and biochemical characterization of the toxin receptor." Proceedings of the National Academy of Sciences of the United States of America **79**(4): 1308-1312.

Humphries, M. D., M. Khamassi, et al. (2012). "Dopaminergic Control of the Exploration-Exploitation Trade-Off via the Basal Ganglia." Frontiers in neuroscience **6**: 9.

Hyland, B. I., J. N. Reynolds, et al. (2002). "Firing modes of midbrain dopamine cells in the freely moving rat." Neuroscience **114**(2): 475-492.

Hyman, S. E., R. C. Malenka, et al. (2006). "Neural mechanisms of addiction: the role of reward-related learning and memory." Annual review of neuroscience **29**: 565-598.

Ikemoto, S. (2007). "Dopamine reward circuitry: two projection systems from the ventral midbrain to the nucleus accumbens-olfactory tubercle complex." Brain research reviews **56**(1): 27-78.

Ji, H., C. Hougaard, et al. (2009). "Tuning the excitability of midbrain dopamine neurons by modulating the Ca2+ sensitivity of SK channels." The European journal of neuroscience **29**(9): 1883-1895.

Ji, H. and P. D. Shepard (2006). "SK Ca2+-activated K+ channel ligands alter the firing pattern of dopamine-containing neurons in vivo." Neuroscience **140**(2): 623-633.

Ji, H., K. R. Tucker, et al. (2012). "Functional characterization of ether-a-go-go-related gene potassium channels in midbrain dopamine neurons - implications for a role in depolarization block." The European journal of neuroscience **36**(7): 2906-2916.

Johnson, S. W. and V. Seutin (1997). "Bicuculline methiodide potentiates NMDA-dependent burst firing in rat dopamine neurons by blocking apamin-sensitive Ca2+-activated K+ currents." Neuroscience letters **231**(1): 13-16.

Johnson, S. W., V. Seutin, et al. (1992). "Burst firing in dopamine neurons induced by N-methyl-D-aspartate: role of electrogenic sodium pump." Science **258**(5082): 665-667.

Johnson, S. W. and Y. N. Wu (2004). "Multiple mechanisms underlie burst firing in rat midbrain dopamine neurons in vitro." Brain research **1019**(1-2): 293-296.

Kang, Y. and S. T. Kitai (1993). "Calcium spike underlying rhythmic firing in dopaminergic neurons of the rat substantia nigra." Neuroscience research **18**(3): 195-207.

Khaliq, Z. M. and B. P. Bean (2008). "Dynamic, nonlinear feedback regulation of slow pacemaking by A-type potassium current in ventral tegmental area neurons." The Journal of neuroscience : the official journal of the Society for Neuroscience **28**(43): 10905-10917.

Khaliq, Z. M. and B. P. Bean (2010). "Pacemaking in dopaminergic ventral tegmental area neurons: depolarizing drive from background and voltage-dependent sodium conductances." The Journal of neuroscience : the official journal of the Society for Neuroscience **30**(21): 7401-7413.

Kim, S. H., Y. M. Choi, et al. (2004). "Two different Ca2+-dependent inhibitory mechanisms of spontaneous firing by glutamate in dopamine neurons." Journal of neurochemistry **91**(4): 983-995.

Koch, C. and I. Segev (2000). "The role of single neurons in information processing." Nature neuroscience **3 Suppl**: 1171-1177.

Komendantov, A. O. and C. C. Canavier (2002). "Electrical coupling between model midbrain dopamine neurons: effects on firing pattern and synchrony." Journal of neurophysiology **87**(3): 1526-1541.

Komendantov, A. O., O. G. Komendantova, et al. (2004). "A modeling study suggests complementary roles for GABAA and NMDA receptors and the SK

channel in regulating the firing pattern in midbrain dopamine neurons." Journal of neurophysiology **91**(1): 346-357.

Koyama, S. and S. B. Appel (2006). "A-type K+ current of dopamine and GABA neurons in the ventral tegmental area." Journal of neurophysiology **96**(2): 544-554.

Krabbe, S., J. Duda, et al. (2015). "Increased dopamine D2 receptor activity in the striatum alters the firing pattern of dopamine neurons in the ventral tegmental area." Proceedings of the National Academy of Sciences of the United States of America **112**(12): E1498-1506.

Krekora, L. (1992). THE PHYSICAL BASIS OF ION CHANNEL KINETICS: THE IMPORTANCE OF DYNAMICS. Proceedings of the Institute for Mathematics and its Applications (IMA), University of Minnesota.

Kuba, H., T. M. Ishii, et al. (2006). "Axonal site of spike initiation enhances auditory coincidence detection." Nature **444**(7122): 1069-1072.

Kuznetsov, A. S., N. J. Kopell, et al. (2006). "Transient high-frequency firing in a coupled-oscillator model of the mesencephalic dopaminergic neuron." Journal of neurophysiology **95**(2): 932-947.

Kuznetsova, A. Y., M. A. Huertas, et al. (2010). "Regulation of firing frequency in a computational model of a midbrain dopaminergic neuron." Journal of computational neuroscience **28**(3): 389-403.

Lavoie, B. and A. Parent (1991). "Dopaminergic neurons expressing calbindin in normal and parkinsonian monkeys." Neuroreport **2**(10): 601-604.

Lewicki, M. S. (1998). "A review of methods for spike sorting: the detection and classification of neural action potentials." Network **9**(4): R53-78.

Li, Y. X., R. Bertram, et al. (1996). "Modeling N-methyl-D-aspartate-induced bursting in dopamine neurons." Neuroscience **71**(2): 397-410.

Lidierth, M. (2009). "sigTOOL: A MATLAB-based environment for sharing laboratory-developed software to analyze biological signals." Journal of neuroscience methods **178**(1): 188-196.

Liss, B., O. Franz, et al. (2001). "Tuning pacemaker frequency of individual dopaminergic neurons by Kv4.3L and KChip3.1 transcription." The EMBO journal **20**(20): 5715-5724.

Liss, B. and J. Roeper (2008). "Individual dopamine midbrain neurons: functional diversity and flexibility in health and disease." Brain research reviews **58**(2): 314-321.

Llinas, R., S. A. Greenfield, et al. (1984). "Electrophysiology of pars compacta cells in the in vitro substantia nigra--a possible mechanism for dendritic release." Brain research **294**(1): 127-132.

Lobb, C. J., T. W. Troyer, et al. (2011). "Disinhibition bursting of dopaminergic neurons." Frontiers in systems neuroscience **5**: 25.

Lobb, C. J., C. J. Wilson, et al. (2010). "A dynamic role for GABA receptors on the firing pattern of midbrain dopaminergic neurons." Journal of neurophysiology **104**(1): 403-413.

Lodge, D. J. and A. A. Grace (2006). "The laterodorsal tegmentum is essential for burst firing of ventral tegmental area dopamine neurons." Proceedings of the National Academy of Sciences of the United States of America **103**(13): 5167-5172.

Luthi, A. and D. A. McCormick (1998). "H-current: properties of a neuronal and network pacemaker." Neuron **21**(1): 9-12.

Maingret, F., B. Coste, et al. (2008). "Neurotransmitter modulation of small-conductance Ca2+-activated K+ channels by regulation of Ca2+ gating." Neuron **59**(3): 439-449.

Mann, M. D. (1997). Properties of Excitable Membranes: The Spike. The Nervous System in Action.

Margolis, E. B., H. Lock, et al. (2006). "The ventral tegmental area revisited: is there an electrophysiological marker for dopaminergic neurons?" The Journal of physiology **577**(Pt 3): 907-924.

Margolis, E. B., J. M. Mitchell, et al. (2008). "Midbrain dopamine neurons: projection target determines action potential duration and dopamine D(2) receptor inhibition." The Journal of neuroscience : the official journal of the Society for Neuroscience **28**(36): 8908-8913.

Marrion, N. V. and S. J. Tavalin (1998). "Selective activation of Ca2+-activated K+ channels by co-localized Ca2+ channels in hippocampal neurons." Nature **395**(6705): 900-905.

Masoli, S., S. Solinas, et al. (2015). "Action potential processing in a detailed Purkinje cell model reveals a critical role for axonal compartmentalization." Frontiers in cellular neuroscience **9**: 47.

Matsuda, W., T. Furuta, et al. (2009). "Single nigrostriatal dopaminergic neurons form widely spread and highly dense axonal arborizations in the neostriatum." The Journal of neuroscience : the official journal of the Society for Neuroscience **29**(2): 444-453.

Matsumoto, M. and M. Takada (2013). "Distinct representations of cognitive and motivational signals in midbrain dopamine neurons." Neuron **79**(5): 1011-1024.

Maylie, J., C. T. Bond, et al. (2004). "Small conductance Ca2+-activated K+ channels and calmodulin." The Journal of physiology **554**(Pt 2): 255-261.

McCutcheon, J. E., K. L. Conrad, et al. (2012). "Dopamine neurons in the ventral tegmental area fire faster in adolescent rats than in adults." Journal of neurophysiology **108**(6): 1620-1630.

Meltzer, L. T., C. L. Christoffersen, et al. (1997). "Modulation of dopamine neuronal activity by glutamate receptor subtypes." Neuroscience and biobehavioral reviews **21**(4): 511-518.

Mena-Segovia, J., P. Winn, et al. (2008). "Cholinergic modulation of midbrain dopaminergic systems." Brain research reviews **58**(2): 265-271.

Mercer, J. N., C. S. Chan, et al. (2007). "Nav1.6 sodium channels are critical to pacemaking and fast spiking in globus pallidus neurons." The Journal of neuroscience : the official journal of the Society for Neuroscience **27**(49): 13552-13566.

Mercuri, N. B., A. Bonci, et al. (1994). "Effects of dihydropyridine calcium antagonists on rat midbrain dopaminergic neurones." British journal of pharmacology **113**(3): 831-838.

Mereu, G., V. Lilliu, et al. (1997). "Spontaneous bursting activity of dopaminergic neurons in midbrain slices from immature rats: role of N-methyl-D-aspartate receptors." Neuroscience **77**(4): 1029-1036.

Messier, C., C. Mourre, et al. (1991). "Effect of apamin, a toxin that inhibits Ca(2+)-dependent K+ channels, on learning and memory processes." Brain research **551**(1-2): 322-326.

Moss, F., L. M. Ward, et al. (2004). "Stochastic resonance and sensory information processing: a tutorial and review of application." Clinical neurophysiology : official journal of the International Federation of Clinical Neurophysiology **115**(2): 267-281.

Mrejeru, A., A. Wei, et al. (2011). "Calcium-activated non-selective cation currents are involved in generation of tonic and bursting activity in dopamine neurons of the substantia nigra pars compacta." The Journal of physiology **589**(Pt 10): 2497-2514.

Murase, S., J. Grenhoff, et al. (1993). "Prefrontal cortex regulates burst firing and transmitter release in rat mesolimbic dopamine neurons studied in vivo." Neuroscience letters **157**(1): 53-56.

Nanou, E., M. H. Alpert, et al. (2013). "Differential regulation of synaptic transmission by pre- and postsynaptic SK channels in the spinal locomotor network." Journal of neurophysiology **109**(12): 3051-3059.

Nedergaard, S. (1999). "Regulation of action potential size and excitability in substantia nigra compacta neurons: sensitivity to 4-aminopyridine." Journal of neurophysiology **82**(6): 2903-2913.

Nedergaard, S., J. A. Flatman, et al. (1993). "Nifedipine- and omega-conotoxin-sensitive Ca2+ conductances in guinea-pig substantia nigra pars compacta neurones." The Journal of physiology **466**: 727-747.

Nedergaard, S. and S. A. Greenfield (1992). "Sub-populations of pars compacta neurons in the substantia nigra: the significance of qualitatively and quantitatively distinct conductances." Neuroscience **48**(2): 423-437.

Neher, E. and B. Sakmann (1976). "Noise analysis of drug induced voltage clamp currents in denervated frog muscle fibres." The Journal of physiology **258**(3): 705-729.

Neher, E. and B. Sakmann (1976). "Single-channel currents recorded from membrane of denervated frog muscle fibres." Nature **260**(5554): 799-802.

Neuhoff, H., A. Neu, et al. (2002). "I(h) channels contribute to the different functional properties of identified dopaminergic subpopulations in the midbrain." The Journal of neuroscience : the official journal of the Society for Neuroscience **22**(4): 1290-1302.

Ngo-Anh, T. J., B. L. Bloodgood, et al. (2005). "SK channels and NMDA receptors form a Ca2+-mediated feedback loop in dendritic spines." Nature neuroscience **8**(5): 642-649.

Nieoullon, A. (2002). "Dopamine and the regulation of cognition and attention." Progress in neurobiology **67**(1): 53-83.

Oster, A. M. and B. S. Gutkin (2011). "A reduced model of DA neuronal dynamics that displays quiescence, tonic firing and bursting." Journal of physiology, Paris **105**(1-3): 53-58.

Overton, P. and D. Clark (1992). "Iontophoretically administered drugs acting at the N-methyl-D-aspartate receptor modulate burst firing in A9 dopamine neurons in the rat." Synapse **10**(2): 131-140.

Overton, P. G. and D. Clark (1997). "Burst firing in midbrain dopaminergic neurons." Brain research. Brain research reviews **25**(3): 312-334.

Paladini, C. A., Y. Iribe, et al. (1999). "GABAA receptor stimulation blocks NMDA-induced bursting of dopaminergic neurons in vitro by decreasing input resistance." Brain research **832**(1-2): 145-151.

Paladini, C. A. and J. M. Tepper (1999). "GABA(A) and GABA(B) antagonists differentially affect the firing pattern of substantia nigra dopaminergic neurons in vivo." Synapse **32**(3): 165-176.

Patlak, J. (1991). "Molecular kinetics of voltage-dependent Na+ channels." Physiological reviews **71**(4): 1047-1080.

Paul, K., D. J. Keith, et al. (2003). "Modulation of calcium-activated potassium small conductance (SK) current in rat dopamine neurons of the ventral tegmental area." Neuroscience letters **348**(3): 180-184.

Penney, M. S. and N. F. Britton (2002). "Modelling natural burst firing in nigral dopamine neurons." Journal of theoretical biology **219**(2): 207-223.

Ping, H. X. and P. D. Shepard (1996). "Apamin-sensitive Ca(2+)-activated K+ channels regulate pacemaker activity in nigral dopamine neurons." Neuroreport **7**(3): 809-814.

Platkiewicz, J. and R. Brette (2011). "Impact of fast sodium channel inactivation on spike threshold dynamics and synaptic integration." PLoS computational biology **7**(5): e1001129.

Prasad, B. M. and S. G. Amara (2001). "The dopamine transporter in mesencephalic cultures is refractory to physiological changes in membrane voltage." The Journal of neuroscience : the official journal of the Society for Neuroscience **21**(19): 7561-7567.

Prisco, S., S. Natoli, et al. (2002). "Group I metabotropic glutamate receptors activate burst firing in rat midbrain dopaminergic neurons." Neuropharmacology **42**(3): 289-296.

Puopolo, M., E. Raviola, et al. (2007). "Roles of subthreshold calcium current and sodium current in spontaneous firing of mouse midbrain dopamine neurons." The Journal of neuroscience : the official journal of the Society for Neuroscience **27**(3): 645-656.

Putzier, I., P. H. Kullmann, et al. (2009). "Cav1.3 channel voltage dependence, not Ca2+ selectivity, drives pacemaker activity and amplifies bursts in nigral dopamine neurons." The Journal of neuroscience : the official journal of the Society for Neuroscience **29**(49): 15414-15419.

Qian, K., N. Yu, et al. (2014). "Mathematical analysis of depolarization block mediated by slow inactivation of fast sodium channels in midbrain dopamine neurons." Journal of neurophysiology **112**(11): 2779-2790.

Reynolds, J. N. and J. R. Wickens (2002). "Dopamine-dependent plasticity of corticostriatal synapses." Neural networks : the official journal of the International Neural Network Society **15**(4-6): 507-521.

Rice, M. E., J. C. Patel, et al. (2011). "Dopamine release in the basal ganglia." Neuroscience **198**: 112-137.

Richards, C. D., T. Shiroyama, et al. (1997). "Electrophysiological and immunocytochemical characterization of GABA and dopamine neurons in the substantia nigra of the rat." Neuroscience **80**(2): 545-557.

Robinson, R. B. and S. A. Siegelbaum (2003). "Hyperpolarization-activated cation currents: from molecules to physiological function." Annual review of physiology **65**: 453-480.

Robinson, S., D. M. Smith, et al. (2004). "Firing properties of dopamine neurons in freely moving dopamine-deficient mice: effects of dopamine receptor activation and anesthesia." Proceedings of the National Academy of Sciences of the United States of America **101**(36): 13329-13334.

Sah, P. (1992). "Role of calcium influx and buffering in the kinetics of Ca(2+)-activated K+ current in rat vagal motoneurons." Journal of neurophysiology **68**(6): 2237-2247.

Sah, P. (1996). "Ca(2+)-activated K+ currents in neurones: types, physiological roles and modulation." Trends in neurosciences **19**(4): 150-154.

Salamone, J. D. and M. Correa (2012). "The mysterious motivational functions of mesolimbic dopamine." Neuron **76**(3): 470-485.

Sanghera, M. K., M. E. Trulson, et al. (1984). "Electrophysiological properties of mouse dopamine neurons: in vivo and in vitro studies." Neuroscience **12**(3): 793-801.

Schiemann, J., F. Schlaudraff, et al. (2012). "K-ATP channels in dopamine substantia nigra neurons control bursting and novelty-induced exploration." Nature neuroscience **15**(9): 1272-1280.

Schneidman, E., B. Freedman, et al. (1998). "Ion channel stochasticity may be critical in determining the reliability and precision of spike timing." Neural computation **10**(7): 1679-1703.

Schultz, W. (1998). "Predictive reward signal of dopamine neurons." Journal of neurophysiology **80**(1): 1-27.

Schultz, W., P. Apicella, et al. (1993). "Responses of monkey dopamine neurons to reward and conditioned stimuli during successive steps of learning a delayed

response task." The Journal of neuroscience : the official journal of the Society for Neuroscience **13**(3): 900-913.

Segev, D. and A. Korngreen (2007). "Kinetics of two voltage-gated K+ conductances in substantia nigra dopaminergic neurons." Brain research **1173**: 27-35.

Sekerli, M., C. A. Del Negro, et al. (2004). "Estimating action potential thresholds from neuronal time-series: new metrics and evaluation of methodologies." IEEE transactions on bio-medical engineering **51**(9): 1665-1672.

Seutin, V., S. W. Johnson, et al. (1993). "Apamin increases NMDA-induced burst-firing of rat mesencephalic dopamine neurons." Brain research **630**(1-2): 341-344.

Shao, L. R., R. Halvorsrud, et al. (1999). "The role of BK-type Ca2+-dependent K+ channels in spike broadening during repetitive firing in rat hippocampal pyramidal cells." The Journal of physiology **521 Pt 1**: 135-146.

Sharp, A. A., M. B. O'Neil, et al. (1993). "Dynamic clamp: computer-generated conductances in real neurons." Journal of neurophysiology **69**(3): 992-995.

Shepard, P. D. and B. S. Bunney (1988). "Effects of apamin on the discharge properties of putative dopamine-containing neurons in vitro." Brain research **463**(2): 380-384.

Shepard, P. D. and B. S. Bunney (1991). "Repetitive firing properties of putative dopamine-containing neurons in vitro: regulation by an apamin-sensitive Ca(2+)-activated K+ conductance." Experimental brain research **86**(1): 141-150.

Shepard, P. D. and B. S. Bunney (1991). "Repetitive firing properties of putative dopamine-containing neurons in vitro: regulation by an apamin-sensitive Ca(2+)-activated K+ conductance." Experimental brain research. Experimentelle Hirnforschung. Experimentation cerebrale **86**(1): 141-150.

Shepard, P. D. and D. Stump (1999). "Nifedipine blocks apamin-induced bursting activity in nigral dopamine-containing neurons." Brain research **817**(1-2): 104-109.

Shi, W. X., P. L. Smith, et al. (1997). "D1-D2 interaction in feedback control of midbrain dopamine neurons." The Journal of neuroscience : the official journal of the Society for Neuroscience **17**(20): 7988-7994.

Shibata, R., K. Nakahira, et al. (2000). "A-type K+ current mediated by the Kv4 channel regulates the generation of action potential in developing cerebellar granule cells." The Journal of neuroscience : the official journal of the Society for Neuroscience **20**(11): 4145-4155.

Sigworth, F. J. and E. Neher (1980). "Single Na+ channel currents observed in cultured rat muscle cells." Nature **287**(5781): 447-449.

Silva, N. L. and B. S. Bunney (1988). "Intracellular studies of dopamine neurons in vitro: pacemakers modulated by dopamine." European journal of pharmacology **149**(3): 307-315.

Silva, N. L., C. M. Pechura, et al. (1990). "Postnatal rat nigrostriatal dopaminergic neurons exhibit five types of potassium conductances." Journal of neurophysiology **64**(1): 262-272.

Skaugen, E. and L. Walloe (1979). "Firing behaviour in a stochastic nerve membrane model based upon the Hodgkin-Huxley equations." Acta physiologica Scandinavica **107**(4): 343-363.

Smith, I. D. and A. A. Grace (1992). "Role of the subthalamic nucleus in the regulation of nigral dopamine neuron activity." Synapse **12**(4): 287-303.

Staff, N. P., H. Y. Jung, et al. (2000). "Resting and active properties of pyramidal neurons in subiculum and CA1 of rat hippocampus." Journal of neurophysiology **84**(5): 2398-2408.

Stanley, D. A., B. L. Bardakjian, et al. (2011). "Stochastic amplification of calcium-activated potassium currents in Ca2+ microdomains." Journal of computational neuroscience **31**(3): 647-666.

Steketee, J. D. and P. W. Kalivas (1990). "Effect of microinjections of apamin into the A10 dopamine region of rats: a behavioral and neurochemical analysis." The Journal of pharmacology and experimental therapeutics **254**(2): 711-719.

Stemmler, M. and C. Koch (1999). "How voltage-dependent conductances can adapt to maximize the information encoded by neuronal firing rate." Nature neuroscience **2**(6): 521-527.

Stocker, M., M. Krause, et al. (1999). "An apamin-sensitive Ca2+-activated K+ current in hippocampal pyramidal neurons." Proceedings of the National Academy of Sciences of the United States of America **96**(8): 4662-4667.

Stocker, M. and P. Pedarzani (2000). "Differential distribution of three Ca(2+)-activated K(+) channel subunits, SK1, SK2, and SK3, in the adult rat central nervous system." Molecular and cellular neurosciences **15**(5): 476-493.

Storm, J. F. (1987). "Action potential repolarization and a fast after-hyperpolarization in rat hippocampal pyramidal cells." The Journal of physiology **385**: 733-759.

Su, W., X. Song, et al. (2010). "Functional expression of a large-conductance Ca2+-activated K+ channel in mouse substantia nigra pars compacta dopaminergic neurons." Neuroscience letters **471**(1): 1-5.

Svensson, T. H. and C. S. Tung (1989). "Local cooling of pre-frontal cortex induces pacemaker-like firing of dopamine neurons in rat ventral tegmental area in vivo." Acta physiologica Scandinavica **136**(1): 135-136.

Swensen, A. M. and B. P. Bean (2003). "Ionic mechanisms of burst firing in dissociated Purkinje neurons." The Journal of neuroscience : the official journal of the Society for Neuroscience **23**(29): 9650-9663.

Tateno, T. (2010). "A small-conductance Ca2+-dependent K+ current regulates dopamine neuron activity: a combined approach of dynamic current clamping and intracellular imaging of calcium signals." Neuroreport **21**(10): 667-674.

Tepper, J. M. and C. R. Lee (2007). "GABAergic control of substantia nigra dopaminergic neurons." Progress in brain research **160**: 189-208.

Tepper, J. M., L. P. Martin, et al. (1995). "GABAA receptor-mediated inhibition of rat substantia nigra dopaminergic neurons by pars reticulata projection neurons." The Journal of neuroscience : the official journal of the Society for Neuroscience **15**(4): 3092-3103.

Tong, Z. Y., P. G. Overton, et al. (1996). "Antagonism of NMDA receptors but not AMPA/kainate receptors blocks bursting in dopaminergic neurons induced by electrical stimulation of the prefrontal cortex." Journal of neural transmission **103**(8-9): 889-904.

Tucker, K. R., M. A. Huertas, et al. (2012). "Pacemaker rate and depolarization block in nigral dopamine neurons: a somatic sodium channel balancing act." The Journal of neuroscience : the official journal of the Society for Neuroscience **32**(42): 14519-14531.

Ungerstedt, U. (1971). "Stereotaxic mapping of the monoamine pathways in the rat brain." Acta physiologica Scandinavica. Supplementum **367**: 1-48.

Ungless, M. A., E. Argilli, et al. (2010). "Effects of stress and aversion on dopamine neurons: implications for addiction." Neuroscience and biobehavioral reviews **35**(2): 151-156.

Ungless, M. A. and A. A. Grace (2012). "Are you or aren't you? Challenges associated with physiologically identifying dopamine neurons." Trends in neurosciences **35**(7): 422-430.

Ungless, M. A., P. J. Magill, et al. (2004). "Uniform inhibition of dopamine neurons in the ventral tegmental area by aversive stimuli." Science **303**(5666): 2040-2042.

van der Staay, F. J., R. J. Fanelli, et al. (1999). "Behavioral effects of apamin, a selective inhibitor of the SK(Ca)-channel, in mice and rats." Neuroscience and biobehavioral reviews **23**(8): 1087-1110.

van Rossum, M. C., B. J. O'Brien, et al. (2003). "Effects of noise on the spike timing precision of retinal ganglion cells." Journal of neurophysiology **89**(5): 2406-2419.

VanDongen, M. L. B. a. A. M. J. (2009). Activation Mechanisms of the NMDA Receptor. Biology of the NMDA Receptor. V. D. A. M, CRC Press.

von Wegner, F., N. Wieder, et al. (2012). "Simulation strategies for calcium microdomains and calcium-regulated calcium channels." Advances in experimental medicine and biology **740**: 553-567.

Walter, J. T., K. Alvina, et al. (2006). "Decreases in the precision of Purkinje cell pacemaking cause cerebellar dysfunction and ataxia." Nature neuroscience **9**(3): 389-397.

Wang, L. P., F. Li, et al. (2011). "NMDA receptors in dopaminergic neurons are crucial for habit learning." Neuron **72**(6): 1055-1066.

Waroux, O., L. Massotte, et al. (2005). "SK channels control the firing pattern of midbrain dopaminergic neurons in vivo." The European journal of neuroscience **22**(12): 3111-3121.

White, J. A., J. T. Rubinstein, et al. (2000). "Channel noise in neurons." Trends in neurosciences **23**(3): 131-137.

Wilent, W. B. and D. Contreras (2005). "Stimulus-dependent changes in spike threshold enhance feature selectivity in rat barrel cortex neurons." The Journal of neuroscience : the official journal of the Society for Neuroscience **25**(11): 2983-2991.

Wilson, C. J. and J. C. Callaway (2000). "Coupled oscillator model of the dopaminergic neuron of the substantia nigra." Journal of neurophysiology **83**(5): 3084-3100.

Wise, R. A. (2004). "Dopamine, learning and motivation." Nature reviews. Neuroscience **5**(6): 483-494.

Wolfart, J., H. Neuhoff, et al. (2001). "Differential expression of the small-conductance, calcium-activated potassium channel SK3 is critical for pacemaker control in dopaminergic midbrain neurons." The Journal of neuroscience : the official journal of the Society for Neuroscience **21**(10): 3443-3456.

Wolfart, J. and J. Roeper (2002). "Selective coupling of T-type calcium channels to SK potassium channels prevents intrinsic bursting in dopaminergic midbrain

neurons." The Journal of neuroscience : the official journal of the Society for Neuroscience **22**(9): 3404-3413.

Womack, M. D. and K. Khodakhah (2003). "Somatic and dendritic small-conductance calcium-activated potassium channels regulate the output of cerebellar Purkinje neurons." The Journal of neuroscience : the official journal of the Society for Neuroscience **23**(7): 2600-2607.

Xia, X. M., B. Fakler, et al. (1998). "Mechanism of calcium gating in small-conductance calcium-activated potassium channels." Nature **395**(6701): 503-507.

Xu, J. and C. E. Clancy (2008). "Ionic mechanisms of endogenous bursting in CA3 hippocampal pyramidal neurons: a model study." PloS one **3**(4): e2056.

Yamada, T., P. L. McGeer, et al. (1990). "Relative sparing in Parkinson's disease of substantia nigra dopamine neurons containing calbindin-D28K." Brain research **526**(2): 303-307.

Yamada, W. M. K., C.; Adams, P.R. (1989). Multiple channels and calcium dynamics. Methods in neuronal modeling: From synapses to networks table of contents 97-133.

Yu, N. and C. C. Canavier (2015). "A Mathematical Model of a Midbrain Dopamine Neuron Identifies Two Slow Variables Likely Responsible for Bursts Evoked by SK Channel Antagonists and Terminated by Depolarization Block." Journal of mathematical neuroscience **5**: 5.

Yung, W. H., M. A. Hausser, et al. (1991). "Electrophysiology of dopaminergic and non-dopaminergic neurones of the guinea-pig substantia nigra pars compacta in vitro." The Journal of physiology **436**: 643-667.

Zhang, J., L. A. Chiodo, et al. (1994). "Influence of excitatory amino acid receptor subtypes on the electrophysiological activity of dopaminergic and nondopaminergic neurons in rat substantia nigra." The Journal of pharmacology and experimental therapeutics **269**(1): 313-321.

Zhang, L. and C. J. McBain (1995). "Potassium conductances underlying repolarization and after-hyperpolarization in rat CA1 hippocampal interneurones." The Journal of physiology **488 (Pt 3)**: 661-672.

Zweifel, L. S., J. G. Parker, et al. (2009). "Disruption of NMDAR-dependent burst firing by dopamine neurons provides selective assessment of phasic dopamine-dependent behavior." Proceedings of the National Academy of Sciences of the United States of America **106**(18): 7281-7288.

Appendix

Permission for reproduction of Figure 3.1 C, D

26 October 2015 17:32
Dear Rajeshwari,

You have my permission

Thank you for your interest in my work

Vincent Seutin

De : Iyer, Rajeshwari [mailto:r.iyer09@csc.mrc.ac.uk]
Envoyé : lundi 26 octobre 2015 17:57
À : v.seutin@ulg.ac.be
Objet : Permission to reproduce figure